THE UNIVERSITY *of* EDINBURGH

Demand-side Flexibility Integration into Virtual Power Plant models

Marcelo Salgado Bravo

THE UNIVERSITY *of* EDINBURGH

Doctor of Philosophy

THE UNIVERSITY OF EDINBURGH

2026

Gratefully to my parents, who made me the person that I am.
To my siblings, which offers their love and energy.

Abstract

The present work explores the capacity to estimate and offer demand-side flexibility through centralized management agents such as virtual power plants and demand aggregators, considering a bottom-up approach to characterise flexible loads and the evaluation of the available flexibility individually and under an aggregate approach. In addition, the influence of external factors on the available flexibility is evaluated, considering price scenarios, weather scenarios, market requirements, appliance operating and user comfort constraints when flexibility is estimated. To reach the main objective, four specific objectives were defined, related to: the development of models to characterize flexible loads and their flexibility; the development of a demand aggregation model for flexibility estimation; the development of forecasting models for temperature and solar irradiation; and finally, the economic evaluation of flexibility and its response capacity to flexibility prices under a virtual power plant approach, considering meteorological and stochastic price scenarios. This thesis is composed of 5 chapters, of which three chapters correspond to published or submitted scientific articles, which comprise this thesis.

Methodologically, this work is divided into three stages, following the four specific objectives. The first stage (Chapter 2) focuses on the modelling of flexible loads and demand aggregation models. By exploring residential loads, their properties, and operating constraints, it is possible to establish operative models for each flexible load and subsequently extend them to evaluate the flexibility of each load. Subsequently, a demand aggregation model was developed for the joint evaluation of flexible loads and their capacity to offer flexibility over time, artificially extending the temporal flexibility capacity of the loads compared to the flexibility of each load individually. The second stage (Chapter 3) focuses on the development of forecasting models for meteorological conditions, focusing on solar irradiation and ambient temperature. Considering cloudiness as an element correlated with both evaluated elements, a neural network model (LSTM, long short-term memory) was developed. Using this approach, a methodology to determine the probabilities of different cloudiness conditions was developed using Markov models, representing the probability of occurrence of each scenario. In the third stage (Chapter 4), the flexibility models presented in Chapter 2 and the stochastic scenarios introduced in Chapter 3 were added to a virtual power plant model. The purpose was to evaluate the flexibility's responsiveness to different external variables and the flexibility prices. The flexibility model was extended to include new flexible loads and the evaluation of the rebound effect, as a counterweight to the benefits obtained by providing flexibility to the system, making the offered flexibility sensitive to the costs produced by time-shifted energy requirements.

The results of this work permit to use the of flexibility on the demand side when scheduling flexible loads and purchasing energy in day-ahead markets. The Flexibility is evaluated with an adaptive framework, which allows an efficient calculation of the available flexibility and evaluation of different flexibility offers. It requires a single calculation of both aggregate demand and flexibility over the entire evaluation period, rather than an individual estimation for each time interval. The influence of weather conditions on flexibility as a consequence of thermal energy losses requires an in-depth analysis of temperature conditions. Consequently, a scenario generation model was formulated based on cloudiness index, using an LSTM model to predict solar irradiance and temperature, characterizing the San Diego climate and generating correlated scenarios. These scenarios were evaluated under a simple virtual power plant model, reducing operational costs compared to a naive forecast, decreasing the number of days with high costs due to unexpected changes in weather conditions. The integration of flexibility estimation, stochastic weather scenarios, and the flexibility rebound effect produces a model sensitive to flexibility prices, offering a flexibility response similar to a sum of four cumulative normal distribution functions (normCDF). Two means from the normCDF were related to a sudden change in flexibility: the first mean is linked to the action of flexible loads with minimum and low flexibility costs, while the second mean corresponds to the penalty for discharging electric batteries. The duration of the flexibility rebound time directly affects the available flexibility, increasing flexibility by 30% when doubling the rebound time, while halving it decreases flexibility by 25%.

Lay Summary

Electric power systems are undergoing a major transformation due to the growing adoption of renewable energy sources, helping to reduce CO2 emissions. However, the variability and uncertainty from solar and wind energy sources make it challenging to maintain a balance between generation and demand. One promising solution is demand-side flexibility, which utilises distributed energy resources and flexible appliances to adjust their energy use in response to grid needs.

This thesis investigates how demand-side flexibility can be estimated and coordinated by aggregation entities (virtual power plants and demand aggregators). Rather than treating consumers as passive energy users, this work examines the aggregated response of flexible devices, including household appliances, heating systems, and electric vehicles, to support the power system.

The research develops models to describe how individual flexible loads can provide flexibility, respecting technical limits and user comfort. These models are incorporated into an aggregation framework, providing more flexibility over time than treating each device separately. The proposed aggregation approach facilitates a more efficient assessment of the flexibility available.

As the flexibility depends on external conditions, the role of weather and electricity prices needs to be evaluated. In particular, temperature and solar radiation influence the generation and thermal comfort in buildings. To address this, a weather scenario generator based on machine learning and cloud conditions was developed to produce realistic forecasts of temperature and solar radiation, as well as to capture their associated uncertainty.

Finally, all these elements are integrated into a virtual power plant model to evaluate how flexibility responds to price signals and operating conditions. The results show that flexibility increases in stages: appliances with no penalties for their usage are activated first, while appliances with degradation associated with their usage are activated at higher flexibility prices or under specific conditions. This study also enhances the importance of the rebound effect, where shifted energy use in form of flexibility must be recovered. The duration of the rebound period has a significant impact on the amount of flexibility that can be offered.

Overall, this thesis presents a unified framework that combines demand aggregation, weather uncertainty, and rebound effects to evaluate demand-side flexibility. The results demonstrate that improved forecasting and coordinated flexibility management reduce operational costs, facilitate decision-making for energy management systems and support more efficient and sustainable participation in electricity markets.

Publications

- **Salgado-Bravo, M.**, Negrete-Pincetic, M., & Kiprakis, A. (2023). Demand-side energy flexibility estimation for day-ahead models. Applied Energy, 347, 121502. The content of this publication is included in Chapter 2.
- **Salgado-Bravo, M.**, Kirli, D., Negrete-Pincetic, M., & Kiprakis, A. Solar and Temperature Scenario Generator Based on Cloud Conditions, Markov Models and LSTM Networks. Under evaluation at IEEE Transactions on Sustainable Energy. The content of this publication is included in Chapter 3.
- **Salgado-Bravo, M.**, Negrete-Pincetic, M., & Kiprakis, A. Price-responsive Demand-side Flexibility Estimation Model with Time-limited Rebound Effect. Under evaluation at Applied Energy. The content of this publication is included in Chapter 4.

Acknowledgements

This work is the consequence of the sum of coincidences. Each coincidence can change your future if you are strong enough to follow the opportunities.

First, I want to thank my parents and aunt for raising me and supporting me in my life decisions, offering their advice and challenging me to explore new horizons. Their vision of life and their hard work to provide for my siblings and me were among the main reasons for me to grow and follow the researcher's path. A special thanks to my grandmother, who would have loved to see her grandchildren achieve their goals.

I sincerely thank Professors Matías Negrete-Pincetic and Aristides Kiprakis for offering me this opportunity to develop as a researcher and for their support in the dual PhD program. I appreciate the trust they have placed in me and the opportunity to explore different approaches and ideas during my studies.

I want to thank the Agile Energy Systems Research Group and OCM (Optimisation, Control and Market) group for being an essential part of my research path and offering help in adapting to the city of Edinburgh and to a different university in Santiago, respectively. In both groups, there are outstanding individuals who deserve the best in their lives and in achieving their academic/industry goals.

The journey to this point has been arduous and satisfying. However, everything that begins must come to an end.

Thank you to each person who shared some steps with me in the last years, and my best wishes to all of them.

Declaration

I declare that this thesis has been composed by myself, that the work contained herein is my own except where explicitly stated otherwise in the text, and that this work has not been submitted for any other degree or professional qualification except as specified.

Marcelo Salgado
January 2026

Contents

Figures and Tables

Figures

Tables

Nomenclature

Acronyms

AFS	Alternative flexibility scenario
ANN	Artificial neural networks
ARIMA	Autoregressive integrated moving average
ARMA	Autoregressive moving average
AS	Ancillary services
AVHRR	Advanced very high resolution radiometer
BRP	Balance responsible party
CAISO	California ISO
CDF	Cumulative density function
CIMSS	Cooperative institute for meteorological satellite studies
CLAVR-x	Clouds from AVHRR Extended System
CNN	Convolutional neural network
DA	Demand aggregator
DAM	Day ahead market
DER	Distributed energy resources
DHI	Direct horizontal irradiance
DNI	Diffuse normal irradiance
DR	Demand response
DSO	Distributed system operator
EMS	Energy management system
ERCOT	Electric reliability council of Texas
ESS	Energy storage systems
EV	Electric vehicles
EWH	Electric Water Heater
GAP	Difference between the best known bound and the objective value
GFS	Global forecast system
GHI	Global horizontal irradiance
GRU	Gated recurrent unit
HASP	Hour-ahead scheduling process
HEMS	Home energy management system
HMM	Hidden markov models
HVAC	Heating, ventilation and air conditioning
ISO	Independent system operator
KSAN	San Diego international airport

LCIS	Low-carbon inertia services
LCOE	Levelised cost of energy
LEM	Local energy markets
LSE	Load serving entities
LSTM	Long short-term memory
MAE	Mean average error
MILP	Mixed integer linear programming
MIP	Mixed integer programming
ML	Machine learning
MLP	Multilayer perceptron
MPC	Model Predictive Control
NCEI	National centers for environmentaliInformation
NOAA	National oceanic and atmospheric administration
NOCT	Nominal operating cell temperature
NREL	National renewable energy laboratory
NSRDB	National solar radiation database
NWP	Numerical weather prediction
OASIS	Open accesss same-time information system, from CAISO
PATMOS-x	Pathfinder atmospheres extended
PDF	Probability density function
PoA	Plane of array
PP	pool pump
PV	Photovoltaics - solar panels
RAM	Random access memory
RMSE	Root mean square error
RTE	Réseau de Transport d'Électricité
RTM	Real time market
SARIMA	Seasonal autoregressive integrated moving average
SVM	Support vector machine
VPP	Virtual power plant
WRF	Weather research and forecasting

Sets and Indexes

$dam \in DAM$	Set of day-ahead market price scenarios
$ev \in EV$	Set of EV appliances
$ewh \in EWH$	Set of EWH appliances
$hvac \in HVAC$	Set of HVAC appliances
$k \in K$	Time set for the alternative flexibility scenario, chapter 3
$k' \in K'$	Time set for the rebound evaluation, used together with K
$n \in N$	Time set for the alternative flexibility scenario, chapter 1

$pp \in PP$	Set of PP appliances
$pr \in Pros$	Set of prosumers
$pv \in PV$	Set of PV appliances
$rtm \in RTM$	Set of real-time market price scenarios
$t \in T$	Time set
$t^{ev}_{out} \in T^{ev}_{out}$	Departure time set per ev appliance
$w \in W$	Set of weather scenarios

Parameters

α_{hvac}	Constant parameter related to energy losses between external and internal air temperature
$\beta_{hvac,[C,H]}$	Constant parameter related to the energy required to increase $1^{circ}C$ the air temperature [K/W]
Δt	Number of hours during the day. Can be adapted if the model evaluates less than 24 hours. [h]
η	Fraction of the expected total daily energy, as an allowed band deviation
$\eta^{elec,PV}_{w,t}$	PV cell efficiency under weather w scenario at time t.
η^{ev}	EV charging efficiency
η^{hvac}_{eff}	Efficiency of the hvac appliance to transform electrical energy into thermal energy
$\eta^{ref,pv}$	Reference efficiency of a solar panel
λ^{dam}_t	Energy price in dam scenario, at time t.
λ^{rtm}_t	Energy price in rtm scenario, at time t.
λ^{FlexDn}_t	Downward flexibility price at time t
λ^{FlexUp}_t	Upward flexibility price at time t
π^{w}	Probability of scenario w [%]
π^{dam}	Probability of scenario dam [%]
π^{rtm}	Probability of scenario rtm [%]
π_{Occ}	Probability of occurrence of flexibility requirement [%]
ρ_{water}	Water density [Kg/m^3]
$\theta^{air,hvac}_{max}$	Maximum air temperature for appliance hvac [K]
$\theta^{air,hvac}_{min}$	Minimum air temperature for appliance hvac [K]
$\theta^{cell,PV}_{w,t}$	Cell temperature of solar panels [K]
$\theta^{e,hvac}_{w,t}$	External air temperature forecast for hvac appliance [K]
θ^{ewh}_{max}	Maximum water temperature for appliance ewh [K]
θ^{ewh}_{min}	Minimum water temperature for appliance ewh [K]
$\theta^{e}_{w,t}$	External air temperature forecast [K]
θ^{input}_{water}	Expected water temp. from external sources [K]
θ^{ref}	PV cell temperature reference [K]
$\theta^{sup,hvac}_{w,t}$	Supplied air temperature, related to hvac appliance [K]

θ_{max}^{hvac}	Maximum air temperature for appliance hvac [K]
θ_{min}^{hvac}	Minimum air temperature for appliance hvac [K]
θ_{room}	Expected room temperature, related to ewh appliance [K]
A^{pv}	Area of the solar panel cells [M^2]
$Av_t^{ev,flex}$	Availability of the ev appliance under flexibility/rebound evaluation
Av_t^{ev}	Availability of the ev appliance
Av_t^{pp}	Availability of the pp appliance
$Band_{pen}$	Expected band penalisation per W.
C_t^E	Energy cost at time t [$/W]
C_t^{DF}	Downward flexibility price at time t [$/W]
C_t^{UF}	Upward flexibility price at time t [$/W]
C_m^{hvac}	Effective heat capacity of a conditioned space, associated to hvac appliance [J/K]
Cp_{water}	Water specific heat capacity [J/(kg K)]
Dch_{usage}^{ev}	Expected battery discharge for ev usage [W]
E^{pp}	Total daily energy required by a PP appliance [W]
$E_{w,t}^{pv}$	Energy provided from pv appliances [W]
E_a	Expected total daily energy required by the appliances for one day. [W]
Fdn_t^{offer}	Downward flexibility contract. Binary variable or parameter
Fup_t^{offer}	Upward flexibility contract. Binary variable or parameter
$G_{w,t}^{PoA}$	Solar irradiance in the plane of array. [W/M]
$H_{tr,[1,2,3]}^{hvac}$	Heat transfer coefficient defined by iso 13790:2008 [W/K]
$H_{tr,[em,is,ms,w]}^{hvac}$	Heat transfer coefficient from external-mass, internal-surface, mass-surface and windows [W/K]
H_{ve}^{hvac}	Heat transfer from ventilation [W/K]
N^{Offers}	maximum number of flexibility contracts per day
n^{pv}	Number of PV solar panels
$N^{T,pv}$	PV Power-temperature coefficient [%/K]
$P_{max}^{[ev,ewh,hvac,pp,pv]}$	Maximum allowed demand for the indicated appliance [W]
P_{max}^{cont}	Maximum power allowed as the sum of distribution contracts per prosumer [W]
$Pmax_{pr}^{cont}$	Maximum power allowed in each prosumer contract [W]
$R_{[1,2,3,4,5,6]}$	Simplified expressions from ISO 13790 thermal model, presented in annexe 2
$SoE^{ev,ExDep}$	Expected state of energy at departure time [W]
$SoE^{ev,start}$	State of energy at the start of the day [W]
$SoE_{[min,max]}^{ev}$	minimum/maximum state of energy allowed to ev appliance [W]
$T_{[min,max]}^{ewh}$	Minimum/maximum water temperature for appliance ewh [K]
$T_{[min,max]}^{hvac}$	Minimum/maximum air temperature for appliance hvac [K]

T_{start}^{hvac}	Building air temperature influenced by hvac at start of the day. [K]
T_{end}^{pp}	Time where the pp appliance is not available
T_{start}^{pp}	Time where the pp appliance start to be available
T_{room}	Expected room temperature [K]
$T_t^{hvac,Forecast}$	External air temperature forecast for hvac appliance at time t [K]
T_{water}^{input}	Expected water temp. from external sources [W]
V_{tank}	Water tank volume [M^3]
W_{tank}	Thermal transmittance of the water tank [$W/(m^2K)$]
$Wuse_t$	Expected hot water usage at time t [M^3]

Variables

$\alpha_{w,rtm,t}^{ev}$	Defines EV charge or discharge process. Binary variable.
$\Phi_{w,t}^{ia,hvac}$	Heat flow rate from internal appliances to air, in scenario w at time t. [W]
$\Phi_{w,t}^{m,hvac}$	Heat flow to internal node m, in scenario w at time t. [W]
$\Phi_{w,rtm,t}^{mtot,hvac}$	Total heat flow rate to wall, in scenario w and price scenario rtm at time t. [W]
$\Phi_{w,t}^{st,hvac}$	Heat flow rateto internal node s, in scenario w at time t. [W]
$\phi_{w,rtm,t}^{+}$	Demand deviation from upper limit in scenario w and price scenario rtm at time t.
$\phi_{w,rtm,t}^{-}$	Demand deviation from lower limit in scenario w and price scenario rtm at time t.
$\theta_{w,rtm,t,k}^{air,hvac,[Up,Dn]}$	Air temperature of appliance hvac, under upward/downward flexibility rebound time [K]
$\theta_{w,rtm,t,k}^{air,hvac,DnEval}$	Air temperature of appliance hvac, under downward flexibility evaluation [K]
$\theta_{w,rtm,t,k}^{air,hvac,UpEval}$	Air temperature of appliance hvac, under upward flexibility evaluation [K]
$\theta_{w,rtm,t}^{air,hvac}$	Air temperature of appliance hvac [K]
$\theta_{w,rtm,t,k}^{ewh,[Up,Dn]}$	Water temperature of appliance ewh, under upward/downward flexibility rebound time [K]
$\theta_{w,rtm,t,k}^{ewh,DnEval}$	Water temperature of appliance ewh, under downward flexibility evaluation [K]
$\theta_{w,rtm,t,k}^{ewh,UpEval}$	Water temperature of appliance ewh, under upward flexibility evaluation [K]
$\theta_{w,rtm,t}^{ewh}$	Water temperature of appliance ewh [K]
$\theta_{w,rtm,t}^{m,hvac}$	Temperature of internal node m under the Crank-Nicholson scheme, related to appliance hvac [K]
$\theta_{w,rtm,t,k}^{mt,hvac,[Up,Dn]}$	Temperature of internal node m, related to appliance hvac, under upward/downward flexibility rebound time [K]
$\theta_{w,rtm,t,k}^{mt,hvac,DnEval}$	Temperature of internal node m, related to appliance hvac, under downward flexibility evaluation [K]

$\theta^{mt,hvac,UpEval}_{w,rtm,t,k}$	Temperature of internal node m, related to appliance hvac, under upward flexibility evaluation [K]
$\theta^{mt,hvac}_{w,rtm,t}$	Temperature of internal node m, related to appliance hvac [K]
$\theta^{s,hvac}_{w,rtm,t}$	Temperature of internal node s (wall surface), related to appliance hvac [K]
B_{pen}	Sum of the band deviation penalisations. [$]
$bP^{hvac,[C,H]}_{t}$	Binary variable associated to cooling/heating operation of the hvac appliance at time t
$D^{alt,[Up,Dn]}_{w,rtm,t,k}$	Demand during the flexibility rebound evaluation in time k which start at time t [W]
D_t	Energy demand at time t [W]
$D_{w,rtm,t}$	Demand in scenario w and price scenario rtm at time t. [W]
Dev_{cost}	Sum of the deviation costs [$/W]
DF_t	Downward flexibility available at time t [W]
$DF^{[ewh,pp,hvac]}_{t,n}$	Downward flexibility from the selected appliance at AFS time n, from time t. [W]
$DF^{hvac,[C,H]}_{t,n}$	Downward flexibility from the HVAC appliance under cooling or heating process at AFS time n, from time t. [W]
$E^{dam,buy}_{t}$	Energy bought in dam at time t [W]
$E^{dam,sell}_{t}$	Energy sold in dam at time t [W]
$E^{pv,[Up,Dn]}_{w,rtm,t,k}$	Energy provided from pv appliances during upward/downward flexibility evaluation. [W]
$E^{rtm,buy}_{w,rtm,t}$	Energy bought in rtm, in scenario w and price scenario rtm at time t. [W]
$E^{rtm,sell}_{w,rtm,t}$	Energy sold in rtm, in scenario w and price scenario rtm at time t. [W]
$eP^{ev}_{w,rtm,t}$	Binary variable associated to charging/discharging operation of the ev appliance
eP^{ewh}_{t}	Emergency heating operation if the water surpass minimum temp. limit.
EV_{pen}	Associated cost to discharge battery operation in ev appliances [$/W]
F_{profit}	Profits obtained from offering flexibility to the grid. [$/W]
Fdn_t	Downward flexibility available at time t [W]
$Fdn^{[cool,heat],hvac}_{w,rtm,t,k}$	Downward flexibility from appliance hvac from heating/cooling process [W]
$Fdn^{[ewh,pp,pv]}_{w,rtm,t,k}$	Downward flexibility for ewh, pp or pv appliances [W]
$Fdn^{ev,[ch,dch]}_{w,rtm,t,k}$	Downward flexibility from ev appliances from charge/discharge process [W]
Fup_t	Upward flexibility available at time t [W]
$Fup^{[cool,heat],hvac}_{w,rtm,t,k}$	Upward flexibility from appliance hvac from heating/cooling process [W]
$Fup^{[ewh,pp,pv]}_{w,rtm,t,k}$	Downward flexibility for ewh, pp or pv appliances [W]
$Fup^{ev,[ch,dch]}_{w,rtm,t,k}$	Upward flexibility from ev appliances from charge/discharge process [W]

$P_{w,rtm,t,k}^{ev,[ch,dch],[Up,Dn]}$	Demand for ev appliance under charge/discharge process in upward/downward flexibility evaluation [W]
$P_{w,rtm,t}^{ev,[ch,dch]}$	Demand for ev appliance under charge/discharge process [W]
$P_{w,rtm,t,k}^{ewh,[Up,Dn]}$	Demand for ewh appliance under upward/downward flexibility evaluation [W]
$P_{w,rtm,t}^{ewh}$	Demand for ewh appliance [W]
$P_{w,rtm,t,k}^{hvac,[heat,cool],[Up,Dn]}$	Demand for ev appliance under heating/cooling process in upward/downward flexibility evaluation [W]
$P_{w,rtm,t}^{hvac,[heat,cool]}$	Demand for ev appliance under heating/cooling process [W]
$P_{w,rtm,t,k}^{pp,[Up,Dn]}$	Demand for pp appliance under upward/downward flexibility evaluation [W]
$P_{w,rtm,t}^{pp}$	Demand for pp appliance [W]
$P_{w,rtm,t,k}^{pv,[Up,Dn]}$	Power generated by pv appliance under upward/downward flexibility evaluation [W]
$P_{w,rtm,t}^{pv}$	Power generated by pv appliance [W]
$P_{t}^{[ewh,pp]}$	Energy demand by the indicated appliance at time t [W]
$P_{t}^{hvac,[C,H]}$	Energy demand by HVAC appliance under cooling and heating process at time t [W]
$PC_{w,rtm,t,k}^{pv,[Up,Dn]}$	Power curtailed by pv appliance under upward/downward flexibility evaluation [W]
$PC_{w,rtm,t}^{pv}$	Power curtailed by pv appliance [W]
RT_{cost}	Sum of the cost in real-time market [$/W]
$SoE_{w,rtm,t,k}^{ev,[Up,Dn]}$	Ev state of energy appliance under upward/downward flexibility rebound [W]
$SoE_{w,rtm,t,k}^{ev,[Upeval,Dneval]}$	Ev state of energy appliance under upward/downward flexibility evaluation [W]
$SoE_{w,rtm,t}^{ev,out}$	Projection of the state of energy at departure time [W]
$SoE_{w,rtm,t}^{ev}$	Ev state of energy appliance [W]
$SoE_{w,rtm,t,k}^{pp,[Up,Dn]}$	Pool pump state of energy under upward/downward flexibility evaluation [W]
$SoE_{w,rtm,t}^{pp}$	Pool pump state of energy [W]
SoH^{pen}	Penalisation associated to ev state of health [$/W]
$T_{t,n}^{[UF,DF],ewh}$	Water temperature under upward/downward flexibility evaluation at time n, from time t [K]
$T_{t,n}^{[UF,DF],hvac}$	Building air temperature under upward/downward flexibility evaluation at time n, from time t [K]
T_{t}^{ewh}	Water temperature at appliance ewh at time t [K]
$T_{w,rtm,t}^{ewh}$	Water temperature for appliance ewh [K]
T_{t}^{hvac}	Building air temperature influenced by hvac appliance at time t [K]

Tr_t	Demand trajectory defined by the optimisation model [W]
UF_t	Upward flexibility available at time t [W]
$UF_{t,n}^{[ewh,pp,hvac]}$	Upward flexibility from the selected appliance at AFS time n, from time t. [W]
$UF_{t,n}^{hvac,[C,H]}$	Upward flexibility from the HVAC appliance under cooling or heating process at AFS time n, from time t. [W]

Chapter 1

Introduction

1.1 Context

1.1.1 The role of Renewable Generation in flexibility

In recent years, the rapid expansion of renewable generation from solar and wind sources has fundamentally transformed power systems worldwide. This transition is primarily driven by a significant reduction in the levelised cost of energy (LCOE) for these technologies, leading to their overwhelming presence in modern generation portfolios Ember (2023); “IRENA renewable power generation costs in 2022” (2023). However, the shift toward a high penetration of non-synchronous renewables has changed how power systems respond to contingencies.

In a traditional generation pool, the generation side responds and modifies its operation to adjust to changes in demand or grid contingencies. The capacity of the system to adapt its operational points is referred to as flexibility, defined as the power system’s ability to balance supply and demand Cruz, Fitiwi, Santos, and Catalão (2018). However, the inherent uncertainty and variability of solar and wind sources introduce new dimensions of operational difficulty Ringkjøb et al. (2020); Russo, Carvalho, Martins, and Monteiro (2023). The uncertainty is associated with the error margin between solar and wind forecasting of the generated energy, and the variability is due to generation fluctuations on the time scale (hours, days, months), mainly associated with wind power plants Ela, Diakov, Ibanez, and Heaney (2013); Ueckerdt, Brecha, and Luderer (2015). To respond to the variability of renewable generation, thermal power plants traditionally provide the required flexibility. However, as decarbonisation reduces the number of controllable generators while wind and solar penetration increase its participation, numerous research projects are evaluating the flexibility challenges for the coming years Evans, Bono, and Wang (2022); Gaeta, Nsangwe Businge, and Gelmini (2022).

International efforts to reach net-zero CO2 emissions by 2050, as reaffirmed in the Paris Agreement and subsequent COP summits on Climate Change) (2023), necessitate a massive scale-up of renewable energy, plus the electrification of transport and industry, which is expected to increase electricity demand by 70% to 100% to 2050 in different scenarios Bloomberg (2025); Enerdata (2025). Most major economies have introduced long-term strategies to achieve 100% clean energy generation and greenhouse gas neutrality within the next few

decades Fam and Fam (2024); Flachsland and Levi (2021); Ministerio del medio ambient (2021). As decarbonisation initiatives lead to the retirement of traditional, controllable fuel-based power plants, the pool of conventional flexibility providers is diminishing, creating an urgent need for alternative flexibility sources to maintain grid stability Evans et al. (2022); Gaeta et al. (2022).

By 2050, it is expected that renewable energy will account for the vast majority of global electricity generation, with wind and solar alone potentially reaching 70% Bouckaert et al. (2021). This scenario presents enormous technical and control challenges for both transmission and distribution networks. While hydro-pumped storage, hydrogen, and batteries are essential measures to increase system flexibility Chyong, Pollitt, Reiner, and Li (2024), the demand-side must also play a critical role. The coordination of flexible appliances, such as heat pumps and electric vehicles, can significantly increase local self-consumption and reduce peak power stress on the grid Rinaldi, Yilmaz, Patel, and Parra (2022).

In conclusion, as wind and solar generation become dominant actors in future energy systems, the resulting decrease in controllable generation will increase the flexibility demanded. To ensure a secure grid operation, each possible flexibility source must be leveraged. The demand-side flexibility, defined as the capacity of customers to adjust their operational points and total demand in response to external requests, is proposed as a vital solution to support the secure integration of high-penetration renewable energy.

The following section introduces flexibility sources in the power grid and the relevance of flexibility evaluation to exploit demand-side flexibility.

1.1.2 Demand-side flexibility overview

In section 1.1, flexibility is introduced as the capacity of power systems to maintain the balance between generation and demand, corresponding to a general definition. Focusing on the demand-side, we can redefine flexibility as the capacity to modify energy patterns under request without affecting power systems stability and end-user satisfaction. This definition enables the generation and demand sides to provide flexibility by incorporating consumer satisfaction and flexibility requests into the flexibility procedures, which could artificially limit the available flexibility. Customer satisfaction is not always considered in flexibility estimation models (Data-driven models estimate flexibility from aggregated demand variations without considering consumer satisfaction in their formulation), while flexibility requests are defined by the ISO/DSO and the energy market when they apply.

In the literature, the demand-side flexibility has been presented as an alternative to prevent imbalances between generation and demand Earl and Fell (2019); Heffron, Körner, Wagner, Weibelzahl, and Fridgen (2020) and offer ancillary services with thermal appliances Kohlhepp, Gröll, and Hagenmeyer (2021); Tina, Aneli, and Gagliano (2022), electric vehicles Clair-

and (2020); Wenzel, Negrete-Pincetic, Olivares, MacDonald, and Callaway (2018) or multiple home appliances under an aggregator approach J. Iria, Scott, Attarha, Gordon, and Franklin (2022); J. P. Iria, Soares, and Matos (2018). Different proposed models aim to exploit the capacity of residential and industrial users to change their consumption patterns in response to direct requirements, economic incentives, peak demand penalties, or price signals. Consequently, a central part of demand-side flexibility comes from aggregation schemes rather than specific technologies, such as demand aggregation (DA) and virtual power plants (VPP). Both schemes work as a decentralised set of flexible appliances (DA) and/or distributed generation resources (VPP) in a city or neighbourhood, which follows a centralised Energy Management System (EMS) as an intermediary to buy/sell energy and offer flexibility services to the power grid, following the ISO/DSO requirements and indications.

Despite the advancements in VPP modeling, a literature gap remains regarding the integration of the rebound effect in aggregated flexibility estimation. While models effectively quantify the immediate load reduction or increase, they often overlook the subsequent energy recovery phase required to return devices—such as HVAC systems or EVs—to their baseline state. Failing to model this 'trajectory' leads to inaccuracies in multi-period flexibility bidding and can create secondary imbalances in the distribution network upon the conclusion of the flexibility event.

Under a VPP scheme, the coordination of distributed energy resources (DER) such as solar plants and ESS is evaluated to offer flexibility by using temporal coupling of DERs and polytope projections to evaluate aggregated flexibility S. Wang and Wu (2021), or by the definition of five metrics related to active and reactive power to simplify decision-making under uncertainty scenarios Sarmiento-Vintimilla, Marene Larruskain, Torres, and Abarrategi (2024). From a DA view, the aggregation and segmentation of flexible appliances simplify their flexibility evaluation, as seen in Diaz-Londono et al. (2019), which defines and compares two strategies for electric charging under the minimisation of operational costs and the maximisation of flexibility capabilities. A similar approach focuses on residential buildings, where the flexibility capacity of thermal appliances (air conditioners, heat pumps, electric water heaters) takes priority due to their significant contribution to total demand Z. Luo et al. (2022). In contrast, electric vehicles have been included in last year's EMS Moura, Yu, and Mohammadi (2020) as a local flexibility provider for large building operations.

Both VPP and DA rely on a superior abstraction layer to provide flexibility to the grid and make energy bids when required. The energy market operates as the upper layer, enabling multiple agents to interact with each other or provide services to the power grid. The flexibility directly depends on the energy market, which defines the type of services, flexibility requirements and goals to fulfil Villar, Bessa, and Matos (2018). Consequently, each modification in the

ruling can create, affect or remove flexibility providers and services. The reserve capacity in generation can be defined as a flexibility service requested by the ISO/DSO, where each agent with power plants can offer its reserve capacity through an auction/bidding scheme, or under direct request from the ISO Bothwell and Hobbs (2017); Just and Weber (2008).

On the demand-side, DA and VPP must fulfil the ISO requirements and obligations to offer services. These frameworks have moved beyond theoretical research into real-life international pilots and trials. An example can be seen in the load serving entity (LSE) definition by CAISO in the United States: any entity that serves or sells energy to end-users, allowing the entity to bid and offer non-spinning reserve and demand reduction in real-time markets through a scheduling coordinator. Responsibilities and obligations are defined in the 'Participating Load Agreement' between CAISO and the LSE Corporation (2013). Similarly, European initiatives such as the Horizon 2020 'FlexCommunity' project or trials conducted by RTE in France have demonstrated the viability of using residential clusters for frequency regulation. Both DA and VPP agents can respond to direct flexibility requests instead of participating in energy/flexibility markets, with the demand response (DR) programs widely studied to provide emergency contingency support and ancillary services O'Connell, Pinson, Madsen, and O'Malley (2014) with the power and energy request defined by the ISO/BRP using energy and availability information from the DR provider.

The Local Energy Markets (LEM) introduced a more decentralised approach for an electricity and flexibility trading platform between buyers, sellers and retailers in a geographically limited area, such as microgrids, neighbourhoods and small cities Jin, Wu, and Jia (2020). The LEM and energy transactions operate over the distribution network. They can communicate with the DSO for load flow analysis and the BRP for imbalance predictions. The LEM can receive flexibility requirements from DSO, BRP, or other participants in the LEM to initiate a flexibility auction, where aggregators and consumers can submit flexibility offers. The LEM makes the market clearing and provides the requested flexibility services Mengelkamp et al. (2018). The flexibility products can be defined according to the DSO/microgrid/community necessities, such as voltage regulation, frequency regulation Couraud et al. (2023) or capacity reserve Lei et al. (2024).

In conclusion, demand-side flexibility shows potential to offer flexibility services and increase the potential penetration of renewable energy, supported by flexible appliances such as electric vehicles and thermal appliances, as well as coordination schemes like virtual power plants and demand aggregators, which centralise the capacity response to offer to the grid. The electrification process will increase the pool of flexible appliances, which could provide flexibility to the grid. However, the flexibility depends on numerous factors: appliance types and properties, users' demand patterns, response time, and market requirements and definitions, making it challenging to estimate demand-side flexibility, especially when considering the temporal coupling of energy recovery, which will be evaluated in the following section.

In conclusion, demand-side flexibility shows potential to offer flexibility services and increase the potential penetration of renewable energy, supported by flexible appliances such as electric vehicles and thermal appliances, as well as coordination schemes like virtual power plants and demand aggregators, which centralise the capacity response to offer to the grid. The electrification process will increase the pool of flexible appliances, which could provide flexibility to the grid. However, the flexibility depends on numerous factors: appliance types and properties, users' demand patterns, response time, and market requirements and definitions, making it challenging to estimate demand-side flexibility, *especially when considering the temporal coupling of energy recovery phases,* which will be evaluated in the following section.

1.1.3 Demand-side flexibility estimation

The available flexibility depends on the set of flexible appliances that can modify their scheduling upon request, the defined market requirements (direction, power, time duration), the flexibility pricing mechanism, network constraints, and weather conditions. Those multiple factors make it challenging to provide a precise and reliable flexibility estimation. In the literature, the primary focus for flexibility evaluation relies on the flexibility properties to be evaluated, such as flexible energy, rebound energy, energy efficiency, maximum flexibility power, flexibility cost, and storage flexibility, among others. Depending on the approach presented in each research publication, the following flexibility indicators can be used to quantify the flexibility H. Li, Wang, Hong, and Piette (2021):

1. Peak power: Reduced power during peak hours from normal operation
2. Self-consumption: Percentage of on-site generation consumed from the total generation.
3. Demand response capacity: Reduction in energy consumption during a demand response event.
4. Demand response efficiency: comparison between energy deviation in prebound time, demand response event and rebound time divided by the energy deviation during the demand response event.
5. Flexibility index: Fraction of the operation cost under flexible and baseline operation.
6. Flexibility factor: Comparison between demand in high-load hours and low-load hours

There is no standardisation of flexibility indicators in the literature, with previously enumerated flexibility indicators being the most used. Other flexibility indicators could depend on units of power/energy, ramping, emissions, and economic indicators. The difficulty in comparing flexibility indicators arises from the fact that the availability of total flexibility depends on the estimation approach used. Furthermore, the adaptability of flexibility indicators to be modified according to the publication's aims complicates the definition of common indicators.

Flexibility estimation approaches can be categorised according to the methodology explored in the literature, depending on the expected goals, available demand data, quantity, and type of flexible appliance, or expected flexibility usage H. Li et al. (2021). The first differentiation between estimation approaches depends on the view of the flexibility available: top-down and bottom-up De Coninck and Helsen (2016). First, the top-down approach evaluates the flexibility estimation problem from a macro perspective to estimate flexibility (i.e., data-driven models that evaluate flexibility from aggregated demand profiles and demand elasticity as a function of electricity prices). Second, bottom-up approaches individualise the flexibility sources and estimate aggregated flexibility as the aggregated effect of each flexible appliance. Both definitions are extended in section 2.1.1.

The second differentiator between estimation models is the proposed methodology to estimate flexibility, divided into three main approaches:

Data-driven approach: corresponds to approaches which rely on aggregated energy data to estimate flexibility by evaluating changes in demand patterns to estimate aggregated flexibility. Under this approach, three main techniques can be individualised:

- Clustering: The clustering approach aims to aggregate flexibility providers with similar attributes in their flexibility responses or demand patterns to estimate their flexibility capacity as an aggregate value, thereby diminishing computational complexity compared to evaluating each flexibility provider individually. The clustering enables the differentiation of flexibility providers, as seen in the work of Andrews and Jain (2022), which establishes flexibility and energy efficiency indicators for building benchmarking and utilises K-medoids to cluster buildings. Focused on residential air conditioners to provide demand response, Qi et al. (2020) uses load level clustering to distinguish power consumption levels and a second two-stage clustering for usage patterns and customer classification.
- Regression: The relationship between a dependent variable (demand response, demand, flexibility) could be the effect of various independent variables. The relationship between variables and identifying patterns in data is known as regression analysis, or more specifically, regression models. This approach is applied in Dyson, Borgeson, Tabone, and Callaway (2014) to model the demand response capacity relationship of thermal models with the cooling state indicator variable and the outdoor temperature. An indirect flexibility estimation can be performed based on the consumer's disposition to participate in demand response programs, an approach explored in A. Srivastava, Van Passel, and Laes (2019) to characterise demographic and geographical disposition to offer flexibility using survey data with 40 predictor variables, employing quantile regression models.

- Machine learning (ML): Similar to regression models, ML is used as a black-box model by assuming a causal relation between input and output data. The input data comprises sensitive signals, such as energy prices, expected renewable generation, or any other variable (e.g., weather data, network constraints), while the ML model assesses their impact on the output data. The estimation of flexibility envelopes for a building is evaluated using Support Vector Machines, K-Nearest Neighbours, and AdaBoost regressors in Hekmat, Cai, Zufferey, Hug, and Heer (2023). Short-term EV demand response prediction under ARIMA and LSTM models is evaluated in Lu et al. (2021). In contrast, convolutional neural network (CNN) models are implemented in Henych, Mamula, Sovka, and Šůcha (2023) to predict automatic frequency restoration reserve. The performance of CNN is compared with that of ARIMA, LSTM, and gated recurrent unit networks.

Optimisation approach: relies on the mathematical formulation of the proposed problem by defining the set of decisions as variables, the constraints that limit the space of solutions and the objective function, aiming to reach the best possible solution. The flexibility sources are modelled to evaluate their behaviour according to their objective, such as minimise operational cost in a real-time market, maximise profitability, increase energy self-consumption, maximise demand response capacity in a time window, penalise peak demand, among others, and include constraints related to network capacity, weather conditions, consumer satisfaction and market limitations. The malleability of optimisation models allows for the modelling of generation, transmission, and demand side in energy problems as the complexity increases and constraints and requirements are included in the model.

Numerous flexibility models have been proposed under optimisation models. In J. Iria, Soares, and Matos (2019), a two-stage bidding model for a demand aggregator was proposed to participate in the energy and secondary reserve market, estimating flexibility per flexible appliance by introducing additional constraints in their operation. A different approach is presented in Harder, Qussous, and Weidlich (2020a), where an optimal baseline demand is first calculated from a set of flexible appliances and a demand response requirement is introduced as an increase/decrease in demand from the baseline. The difference in operational cost will be defined as the flexibility cost to the provider. This approach is similar to that presented in De Coninck and Helsen (2016), which evaluates the flexibility available and its cost in a building by running three optimisation models. The first optimisation model estimates the reference demand for space heating, while the second and third define a target consumption as zero and a high number to assess the flexibility available in a limited time window. The difference from the target consumption is penalised, and the increased operational cost compared with the reference case is the flexibility cost of the building. Energy demand and flexibility estimation models are implemented in sections 2, 3 and 4.

Experimental or simulation approach: Not exclusively but mainly used in building thermal appliances, the simulation approach creates white-box models to characterise the thermal properties of buildings and uses or defines a flexibility quantification framework instead of including flexibility expressions in the model. Similar to the data-driven approach, the flexibility quantification depends on characterising demand variations resulting from flexibility actions in the thermal models, such as pre-heating/pre-cooling of spaces, changing the set-point building temperature, dimming lights, unplugging low-priority appliances, and ramp limitations in demand, among others N. Luo, Langevin, Chandra-Putra, and Lee (2022). The thermal properties are characterised using specialised and highly detailed simulation software, such as EnergyPlus Bampoulas, Saffari, Pallonetto, Mangina, and Finn (2021), TRNSYS S. e. a. Klein (2017), and Modelica K. Klein, Herkel, Henning, and Felsmann (2017), which follow physical and first-principles models.

The difference in flexibility approaches, numerous flexibility indicators, the flexibility properties under evaluation and the possible services that can be served by using flexibility loads come to a singular conclusion: The flexibility estimation problem can not be standardised, depends on the type of service to offer and can not be possible to compare unless the flexibility indicator is normalised from the flexibility attributes and the flexibility framework is the same or at least maintains a minimum set of procedures to have a fair comparison. Even if the methods and indicators are the same, the end-user energy behaviour and the difference in demand patterns between users will change the results on the flexibility available.

As an additional problem related to flexibility estimation, the cost of offering flexibility and the aggregated response to flexibility prices have been a challenging problem to tackle. Some flexibility indicators related to demand response efficiency and flexibility index can provide information about the demand difference when flexibility is provided. Still, under dynamic tariff schemes, the price differences could surpass and exploit the energy inefficiencies to reduce the flexibility cost. In the literature, one approach to obtain the flexibility cost involves evaluating the reference demand for an EMS and the additional operational cost when a demand response requirement is provided, as seen in Harder et al. (2020a), where both problems are solved sequentially. This approach requires the re-optimisation of the EMS operation problem after each flexibility requirement, whether we desire to respond to more flexibility requirements during the day. Another approach is introduced in Zade, Incedag, El-Baz, Tzscheutschler, and Wagner (2018), where the HEMS operation is evaluated, and the flexibility price is calculated based on the energy cost differences between day-ahead and intra-day markets. This approach reduces computational time but offers limited flexibility.

Alternative methodologies include reference demand and flexibility under one optimisation model, as illustrated in J. P. Iria, Soares, and Matos (2019). This approach provides both upward and downward flexibility, governed by a binary parameter related to the tertiary reserve direction, which constrains flexibility estimation and responsibility from flexible appliances. Un-

der a demand response approach Nojavan and Maghouli (2024), the deviation from expected demand is considered in the model formulation, linking the total daily upward deviation with the total daily downward deviation. Both methodologies facilitate upward or downward flexibility per time-step; however, their models do not explicitly account for the rebound effect of the flexibility offered. This gap in the literature highlights a crucial aspect of the research idea: energy management, flexibility response estimation, and rebound effect considerations need to be integrated into a single optimisation process. However, flexibility estimation must be independent of the energy management problem if no flexibility requests exist. This thesis explores this opportunity by including the flexibility estimation problem in the virtual power plant formulation for numerous flexible appliances, providing an aggregated flexibility response that could not be possible by evaluating each flexible appliance separately.

The following sections in chapter 1 introduce the objectives, hypothesis and methodology proposed to tackle this problem. As a summary of the thesis, the main results obtained from the proposed research are introduced in section 1.5. Finally, the scientific contributions made from the proposed study are presented in section 1.6.

1.2 Thesis objectives

General Objective: To develop a robust framework for estimating and offering demand-side flexibility through aggregation agents (Virtual Power Plants and Demand Aggregators), by integrating bottom-up load modeling with stochastic scenarios. The properties of flexible appliances, flexibility market requirements, and uncertainty from weather and price sources are considered elements that could modify the available flexibility.

To achieve this, four specific objectives are pursued in a sequence of increasing complexity:

1. Load Modeling: Develop operational models to characterise flexible appliances (Chapter 2).
2. Demand Aggregation: Formulate a model for continuous-time aggregated flexibility estimation (Chapter 2).
3. Forecasting: Integrate LSTM-based weather forecasting, based on correlated weather parameters with cloud information(Chapter 3).
4. Economic Evaluation: Assess VPP economic performance and flexibility response to price signals under stochastic conditions and rebound effects for numerous appliances (Chapter 4).

1.3 Hypothesis

The central hypothesis of this thesis is to explore how the available demand-side flexibility is influenced by weather conditions, the control approach, appliance limitations and operational constraints related to energy and flexibility markets. Including the factors that modify the available flexibility with an energy management system model such as VPP and DA that considers weather uncertainty and price scenarios, the flexibility from demand-side can be managed and provided to the power grid, improving the response capacity of the grid to face generation variability, transmission congestion and increasing local consumption. In particular, the following specific hypothesis can be formulated:

1. Flexibility depends on the flexibility duration requirement and the rebound time. The nature of the flexible appliance limits the flexibility duration, while the rebound time directly increases or reduces the flexibility.
2. The integration and coordinated operation of heterogeneous flexible appliances improve aggregated demand-side flexibility. Various flexible appliances can offer short-term flexibility coordinated to provide flexibility for a longer time window.
3. Including operational features from the flexible appliances and weather variability into VPP models can improve the VPP bidding in energy and flexibility markets.

1.3.1 Hypothesis Validation

The hypothesis will be assessed by comparing the VPP's operational costs and flexibility response under various conditions (comparison between stochastic and naive scenarios, seasonal pricing difference, and flexibility requirement duration). The coordination capabilities can be demonstrated by comparing the flexibility response to unexpected conditions during the flexibility evaluation. Success is defined by a measurable reduction in unexpected high-cost days and minor differences with 'perfect information' benchmarks.

1.4 Research Approach

To reach the proposed objectives presented in section 1.2, the following steps were proposed to estimate aggregated flexibility and to understand how the operational constraints can affect its availability

1. A review of data available, focusing on weather irradiance and energy pricing.
2. Selection of flexible appliances and the development of operation models under an MILP approach.
3. Flexibility estimation approach for aggregated flexibility and extended time intervals (maximum flexibility to offer)

4. Weather scenario generator for virtual power plants and demand aggregator, exploring the correlation between cloud conditions, solar irradiance and temperature
5. Stochastic virtual power plant model with flexibility sensitivity to prices.

The first two steps are relevant at each stage of the proposed research, forming the basis for the subsequent steps. The third step addresses the central problem proposed, defining how flexibility is evaluated and offered in day-ahead markets, and developing a framework to coordinate flexible appliances and provide flexibility. The fourth step focused on the influence of uncertainty in flexible appliances, which depends on weather conditions, by establishing a weather scenario generator using local weather conditions. Finally, the fifth step consolidates the advances presented in each step into a day-ahead VPP model capable of providing day-ahead flexibility estimations based on weather and price scenarios.

As the first step, evaluating meteorological and energy pricing data from multiple sources was required for viability purposes. The correlation between weather conditions and energy pricing was under research, with the first aim being to obtain a set of data sources from different locations that offer both databases in the same time window. The second limitation is the availability of flexibility prices in day-ahead and real-time markets. The selected place was San Diego, California, USA. The Open Access Same-Time Information System (OASIS) platform *California Independent System Operator. Open access same time information system* (2022) provides reliable information about the California ISO (CAISO), including day-ahead and real-time energy markets, ancillary services prices and various forecasts. The solar irradiance database selected is the National Solar Radiation Database from NREL Sengupta et al. (2018) due to the cloud information provided, along with various weather parameters. Finally, historical outdoor air temperature data from NOAA NCEI Climate Normals Arguez et al. (2010) were selected due to their high-quality data compared to other sources. Each source stores the required data between January 2017 and December 2019.

The next step defines the approach used to select the flexible appliances under research and develop basic operational models. The state-of-the-art on demand-side flexibility identifies different appliances under evaluation, which were separated according to their attributes:

- Deferrable appliances: Appliances that can be shifted from their expected operation.
- Interruptible appliances: Can restart operation after a pause with minimal or without demand losses.
- Adjustable appliances: The level of demand can be adjusted according to some parameters.
- Storage appliances: Can store energy in an electric or physical medium.

The described attributes can be associated with mathematical expressions in a MILP formulation, where each appliance could represent one or various flexibility attributes. As a conclusion of the review of state-of-the-art, five appliances were selected to be studied:

- Pool pumps: Deferrable, interruptible and adjustable load with high presence in buildings. The pump operation is representative of other appliances that rely on electric motors.
- Electric vehicles: shows all the indicated attributes. The EV was selected due to its high demand and expected increase in the following years as part of the decarbonisation process.
- Air conditioners: High-demand load and relevant presence in literature. The central difficulty for HVAC appliances is the formulation of the building thermal model.
- Electric water heaters: Huge presence in buildings and apartments with high energy demand, more manageable to model than air conditioners.
- Photovoltaic plants: considered a distributed energy resource rather than an appliance, the PV was selected as an adjustable but not deferrable and interruptible appliance.

There are other appliances, such as washing machines, lighting, and dishwashers, among others. However, their impact on energy demand in households and buildings is lower than the selected appliances. A new database revision was made for the selected appliances to reflect their physical and demand properties. The webpage ev-database.org *Electric Vehicle Database* (n.d.) lists electric vehicles available in Europe, along with their properties. The 30 most sold EVs in Europe until 2021 were chosen as the set of EV appliances. The case of air conditioners is different; during the flexibility estimation model introduced in chapter 2 a 5-floor building with 10 apartments per floor was designed following indications from EnergyPlus software DoE (2010), while in the Flexibility integration into VPP shown in chapter 4, the thermal model was developed by following the ISO 13790:2008(E) specifications ISO 13790:2008(E) (2008) and the building properties were selected from the TABULA project Loga, Stein, and Diefenbach (2016). For pool pumps and electric water heaters, numerous appliances were selected from commercial pages and their properties were extracted from datasheets. For the PV appliance, rather than choosing between multiple solar panels, the number of panels, orientation and slope angle were associated with a random number between $\pm 10^{\circ}$ from the latitude and longitude of the selected place. Finally, basic flexible appliance operational models were developed for each appliance by following the flexibility attributes and special considerations indicated in the literature.

The third step involves formulating the aggregated flexibility estimation model, which is proposed to address high-duration flexibility requirements with a short-flexibility appliance. The flexibility estimation approach is bottom-up, defining the flexibility available per appliance as a variable that depends on the load's expected demand, maximum demand, and additional constraints related to the rebound effect. Those constraints aim to identify upward and downward flexibility from their capacity to deviate their demand in the first stage. In contrast to other flexibility methods that evaluate the flexibility envelope or require more than one stage to assess reference demand and flexibility requests, a novel flexibility estimation model was proposed that defines reference demand and flexibility available in a single step. An alternative

time-window with the same duration as the flexibility requirement was proposed to achieve this goal. Both time units coexist in the same model, where the scheduled appliances at time t (main time window) influence the demand plus demand deviation at time k (alternative time window). The model evaluates flexibility for more than one time window, allowing it to respond to extended flexibility requirements. Still, an additional operational constraint needs to be included: The flexibility offered at time t will be lower than each flexibility estimation during time $k \in K$. To evaluate the aggregate flexibility estimation model, five case scenarios were proposed to observe the flexibility response: Flexibility response without energy prices, ToU pricing scheme, dynamic pricing, response to 1-hour flexibility requirement with variable time granularity and flexibility response for a 4-block flexibility duration, with expected scheduling from 1-block to 3-block flexibility duration. This work is detailed in chapter 2.

In the fourth step, the variability of weather conditions is introduced under a weather scenario generator. The cloud index from the CLAVR-x satellite model was selected to differentiate cloud conditions and their influence on solar irradiance. Solar irradiance and ambient temperature are correlated to cloud conditions, which can be exploited by using LSTM models as black-box models. The solar irradiance forecast was trained using the cloud index and expected extraterrestrial irradiance, along with other variables, while the ambient temperature was trained using the solar irradiance and the cloud index. The model was trained to forecast the next 24 hours on both variables using 2 years of meteorological data. The second stage considers formulating the possible cloud conditions for the next day by defining a framework to generate scenarios. The framework utilises hidden Markov models with cloud conditions indicators to estimate cloud transitions between different states, which are categorised into two levels: sunny conditions and cloudy conditions. Each cloud index is clustered into clear-sky or cloudy clusters by calculating the Euclidean distance of the density probability function of the solar irradiance divided by the extraterrestrial solar irradiance. The HMM defines a set of eight scenarios with different cloud conditions and probabilities of occurrence per month. According to the observed cloud conditions the day before, these scenarios are used as inputs in the trained LSTM models to generate solar irradiance and temperature scenarios. The scenarios were compared with naive and perfect forecast information in a basic stochastic VPP formulation for 500 flexible appliances. This work is detailed in chapter 3.

In the final step, the previously developed flexibility models and weather scenario generator are used to develop a stochastic virtual power plant which can estimate and offer demand-side flexibility. The VPP model can estimate and offer demand-side flexibility using flexibility prices, because the rebound effect to the flexibility provided was explicitly included in the model formulation, assuming an additional operational cost in the flexibility offered and the subsequent rebound effect, which needs to be lower than the flexibility price multiplied by the total flexibility provided in each time interval. Using alternative flexibility scenarios introduced in chapter 2 is mandatory to calculate the reference demand, the flexibility offered and the expected

rebound effect. A relaxation of the thermal model is implemented to reduce its computational complexity, allowing for an initial operation estimation with dual heating/cooling operations, which forces the HVAC operation to follow the higher demand in the next iteration. The model is tested by using 500 flexible appliances under different cases: A comparison of the relaxed HVAC operation against usual binary models, flexibility evaluation under fixed energy prices, stochastic DAM and RTM prices, a stepwise flexibility price, a comparison between stochastic and naive forecast, variable rebound time and deterministic primary frequency regulation prices for flexibility. This work and the obtained results are detailed in chapter 4.

In figure 1.1, a flow diagram illustrates the proposed thesis, starting with the relevance of the problem, proposed solution, alternative flexibility scenario plus weather scenario generator and their integration into a stochastic VPP.

1.5 Main results

The present section summarises the most relevant results obtained in steps three to five, presented in chapters 2, 3 and 4.

1.5.1 Demand-side energy flexibility estimation for day-ahead models

The chapter 2 explored the demand-side flexibility problem, which involves the aggregated capacity of numerous flexible appliances. Under a centralised coordination model, this capacity could fulfil flexibility duration requirements longer than each appliance's individual flexibility capacity. To reach the proposed goal, a novel demand-side flexibility estimation model named 'Alternative flexibility scenario' was developed to quantify available flexibility in each time-step with a customisable flexibility duration.

The developed model relies on the evaluation of the aggregated demand deviation during the flexibility requirement, where the model evaluates the reference demand in $t \in T$ and the aggregated demand deviation during $k \in K$ for each $t \in T$, where K duration is equal to the flexibility duration. The calculation of both reference demand and demand deviation in the model enables the proposed model to deliver numerous flexibility offers in a single iteration, thereby reducing the computational power required compared to other models that evaluate each flexibility requirement individually. The reference demand was responsible for price cases; however, the method used to estimate flexibility does not directly respond to flexibility prices. The energy prices have a minor impact on the upward and downward flexibility available. Still, the model formulation estimates the maximum flexibility capacity that can be delivered from the appliances without surpassing the rebound and operational constraints defined in the model. The capacity of the model to provide flexibility for a longer duration than the selected time interval was confirmed by the evaluation of a 4-block flexibility duration

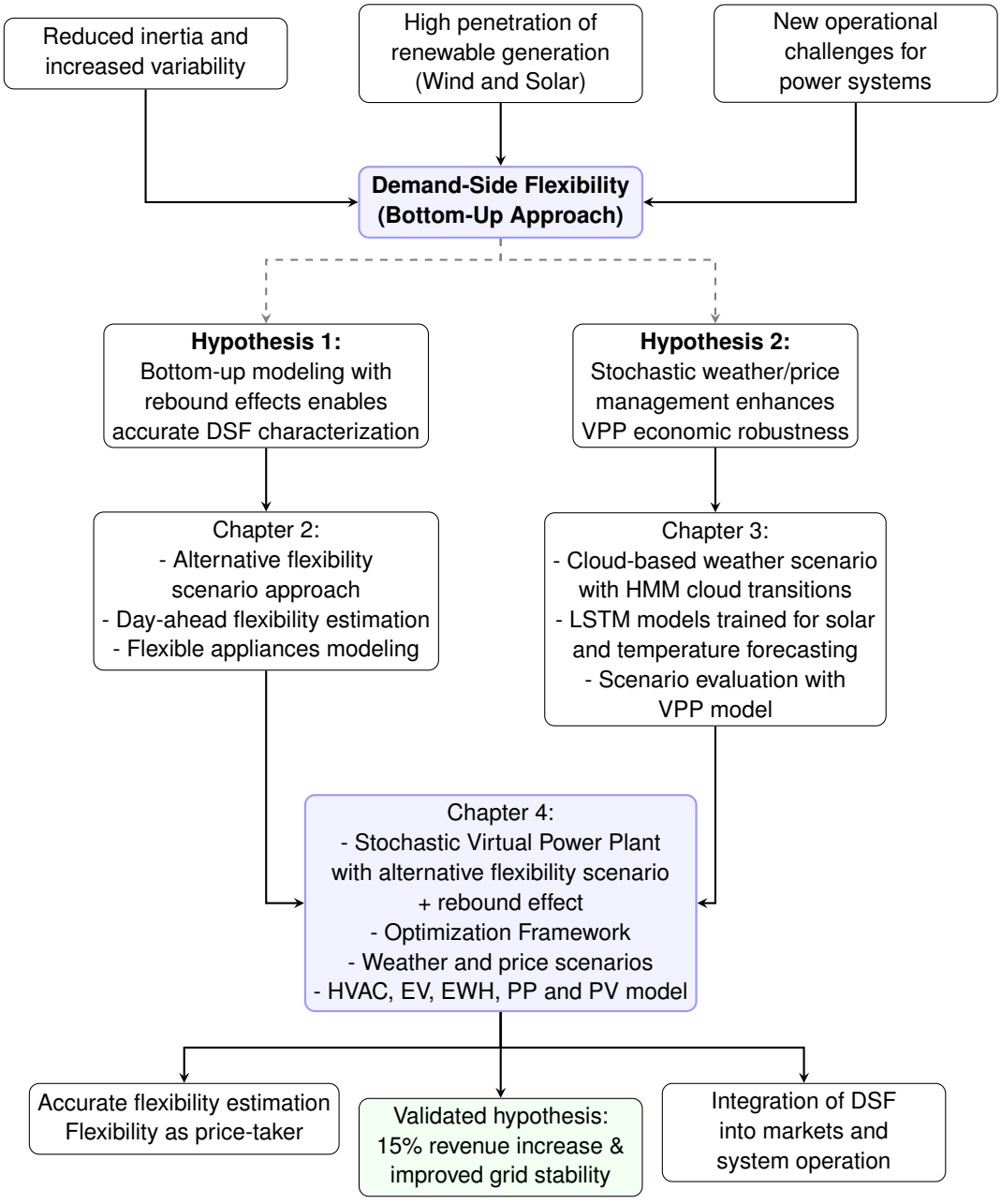

Figure 1.1: Flow diagram illustrating the develop of the flexibility estimation framework, weather scenario generation and their integration into the VPP optimisation model.

requirement using the proposed scheduling from cases with a lower duration, where even if the flexibility required was lower than the estimated values in the cases with lower duration, the requirement to maintain the flexibility for a longer time was not provided in some cases, being the 1-block case the worst case, because of their aggressive scheduling to minimise demand increases changes on demand. In contrast, the 3-block case got similar flexibility responses to the 4-block case with lower deviations, except at 17:00 hrs. reaching a deviation peak of 60%.

1.5.2 Solar and Temperature Scenario Generator Based on Cloud Conditions, Markov Models and LSTM Networks

In chapter 3, a weather scenario generator of solar irradiance and temperature is developed as input data for stochastic virtual power plant models. To reach this goal, a forecasting model based on Long Short-Term Memory neural networks is proposed. This architecture is specifically selected for its ability to handle the non-linearities and long-term temporal dependencies inherent in meteorological data, which traditional regression models often fail to capture.

The model focuses on pattern identification and generation associated with cloud conditions, where the cloud index parameter from the CLAVR-x software provides information on cloud conditions for a particular location. Using the cloud index as input in the model training allows for associating the changes in solar irradiance and temperature behaviour with each index. Each cloud type has its own probability density function related to solar irradiance versus extraterrestrial irradiance. Changes in cloud conditions were evaluated using Markov models for the transition index. A set of eight possible cloud conditions was defined to assess weather for the next 24 hours, based on the possible index transitions in specific time windows.

The proposed weather generator was tested under a basic stochastic virtual power plant, which aims to minimise total cost of operation in a day-ahead market. The energy price forecast was obtained from the DeepVAR model, which compares the influence of both weather and price scenarios on VPP operation against a naive forecast. The Markov transition probabilities for each one of the eight possible weather conditions were used as the probability occurrence of each scenario in the VPP model. It was found that the proposed weather forecast model reduces the total operational cost of the models compared to the naive weather forecast, being significantly lower than the influence of stochastic prices against naive pricing. The main contribution of the weather scenarios is the reduction of days with high operational costs. In contrast, the average cost of the other days increases due to considering more scenarios in the formulation.

1.5.3 Price-responsive Demand-side Flexibility Estimation Model with Time-limited Rebound Effect

In chapter 4, the flexibility estimation model developed in chapter 2 and the weather scenario generator from chapter 3 were applied to a stochastic virtual power plant with flexible appliances and distributed solar generation to evaluate the available flexibility to offer in a day-ahead market. The flexibility evaluation model was rethought to include and reinforce the rebound effect within a limited timeframe, addressing one of the weaknesses of the flexibility estimation problem: the need for a price-sensitive model.

First, the increase in computational complexity of the model necessitated a change in the thermal model's operation, removing the binary variables related to heating and cooling. This two-step approach enables both operations to be performed simultaneously in the first step, while allowing only heating or cooling in the second step. The differences in the objective function between the binary and two-step approaches compared to the relaxed model were 4.34% and 4.55%, respectively, for the case with 10 thermal appliances. In contrast, the case with 10 flexible appliances from each type reaches 0.28% and 0.3%, where the EV and PV plants gain more relevance than thermal appliances. The obtained results were similar. Nevertheless, the value in this approach relies on the required time to solve the problem, limited to 15 minutes in the binary case (exceeding this limit in over 80% of the cases), to less than one minute for the two-step approach.

The flexibility estimation approach becomes price-sensitive by introducing the time-limited rebound effect after providing flexibility. The proposed stochastic VPP was tested under different price schemes. Under fixed energy prices in DAM and RTP, the flexibility response exhibits a normal cumulative density function (normCDF) to the energy prices, revealing two mean values that can be attributed to the action of pool pumps. The second mean value depends on the price penalty for discharging EV batteries to offer flexibility. Both mean values were confirmed under stochastic pricing schemes, with higher variability in the mean values and the standard deviation associated mainly with price variations, and a minimal contribution from weather conditions to the variability in the standard deviation. Finally, the influence of the rebound duration on the estimated flexibility was evaluated, showing how duplicating the rebound time increases flexibility by approximately 30% while reducing rebound time by half reduces the flexibility available between 21% and 25%. These results facilitate flexibility estimation and bidding in a real-time market, with no time to re-estimate flexibility.

1.6 Scientific contribution of the thesis

First, a novel method for estimating flexibility was proposed to evaluate aggregated flexibility. The 'alternative flexibility scenario' allows for the inclusion of the reference demand and the capacity of the flexible appliances to deviate from the proposed demand in a single formulation. The inclusion of both stages of flexibility estimation reduces the number of iterations required to estimate flexibility, offering the available upward and downward flexibility in each time window for the defined flexibility duration requirement, in comparison with other models in literature which require estimating flexibility in each time window individually or offering multiple flexibility estimations during the day but using the differences between upward and downward flexibility to obfuscate the rebound effect on the offered flexibility.

Second, flexibility constraints were designed to be incorporated into the operational model of each type of flexible appliance, which can be adapted to numerous appliance models, including constraints related to the rebound effects in the offered flexibility if required.

Third, a weather scenario generator that depends on cloud conditions will be developed to determine solar irradiance and temperature conditions for the next 24 hours. The plasticity of using cloud conditions allows for the evaluation of weather conditions under controlled conditions according to the user's needs, such as evaluating clear sky conditions during the morning and both clear sky and cloudy conditions during the afternoon. In addition, the scenario generator uses a hidden Markov model to evaluate cloud transitions, which can be used to calculate the probability of each scenario during the day or for a defined time window. The obtained probabilities can be used in stochastic optimisation models. The model was trained using solar and cloud data from the National Solar Radiation Database (NSRDB) by NREL, which utilises multiple satellite data sources covering the entire northern hemisphere, from latitude 60° north, and the whole southern hemisphere, except Antarctica. Consequently, the model can be trained to evaluate weather conditions on more than 90% of the Earth's surface.

Finally, a stochastic virtual power plant model capable of estimating demand-side flexibility. The model has two differential factors compared with other models in the literature.

1. The estimation approach is price-sensitive: Including the time-limited rebound effect as a constraint changes the flexibility estimation approach to offer the maximum flexibility in each scenario, with flexibility profitability higher than or equal to the additional cost or losses produced due to the rebound effect.

2. The estimated flexibility considers the aggregated response of the appliance and the weather influence: the offered flexibility is the aggregated response of the flexible appliances, which offers the minimal-cost flexible appliances at the defined price, providing flexibility from non-scheduled appliances if a scheduled appliance is unavailable. The estimated flexibility can be satisfied in each weather scenario evaluated, thereby diminishing the consequences of non-optimal appliance scheduling and potential penalisation for not providing flexibility.

Those two differential factors and the inclusion of the 'alternative flexibility scenario' adapted to numerous weather and price scenarios make the stochastic VPP flexibility estimation model a relevant and unexplored approach for flexibility bidding in day-ahead markets.

Chapter 2

Demand-side energy flexibility estimation for day-ahead models

2.1 Introduction

Two key trends have gained relevance in power systems in recent years. First, the rise of renewable generation (solar and wind power plants) introduces challenges associated with the uncertainty and high variability in their generation Bessa, Moreira, Silva, and Matos (2014). Second, decarbonisation plans reduce the pool of power plants that can provide inertia to the grid. Consequently, power systems have reduced their response capacity to unexpected generation changes or transmission contingencies Verastegui, Lorca, Olivares, and Negrete-pincetic (2021), thereby increasing the flexibility requirements in the power system. In this new scenario, demand-side flexibility can be an option to maintain grid security and balance between generation and demand Shaughnessy, Shah, Parra, and Ardani (2022); Strbac et al. (2019).

Numerous studies propose the use of flexibility from demand-side appliances to prevent unbalances between generation and demand Aduda, Labeodan, Zeiler, Boxem, and Zhao (2016); Earl and Fell (2019); Heffron et al. (2020), offer ancillary services using Air conditioning appliances Kohlhepp et al. (2021); Qureshi and Jones (2018); Tina et al. (2022); H. Wang, Wang, and Tang (2019), electric vehicles Alipour, Mohammadi-Ivatloo, Moradi-Dalvand, and Zare (2017); Clairand (2020); Wenzel et al. (2018) or multiple home appliances under an aggregator approach J. Iria et al. (2022, 2019); J. P. Iria et al. (2018). However, to provide flexibility from the demand-side, the evaluation of the appliance's properties to shift its demand over continuous time intervals has not been extensively studied. This publication addresses the flexibility estimation problem, considering that the flexibility duration requirement may vary, ranging from 15-minute requests to 4-hour flexibility requirements, in accordance with the flexibility and ancillary services market requirements.

2.1.1 Flexibility literature

For power systems, flexibility can be defined as the power systems capacity to balance supply with demand Cruz et al. (2018), while demand-side response can be defined as the regulation of the consumer energy patterns A. Dixon (2019), usually under financial incentives. To account for the demand-side effect, flexibility can be redefined as the device's ability to adjust its operation to maintain a balance between supply and demand without compromising power system stability or user satisfaction.

The flexibility quantification can be explored under two approaches: top-down and bottom-up. The top-down approach examines the demand profiles of users and buildings to identify patrons associated with demand flexibility. Data-driven models to evaluate EV flexibility according to their changing behaviour Sadeghianpourhamami, Refa, Strobbe, and Develder (2018), users occupancy behaviour to model buildings in cluster buildings A. Wang, Li, and You (2018), Long Short-Term Memory and Gated Recurrent Unit methods to predict flexibility in heat pumps Brusokas, Pedersen, Šikšnys, Zhang, and Chen (2021) and ARMA models to evaluate Demand Response in HVAC appliances Kara, Tabone, MacDonald, Callaway, and Kiliccote (2014) can be considered under the top-down approach. In contrast, the bottom-up approach evaluates the appliance's properties to shift its demand under an optimal control model and optimise its consumption according to price signals, CO2 minimisation, or other incentives.

Under the bottom-up approach, two methodologies have been identified in the literature to evaluate flexibility:

- Ex-ante flexibility: Evaluate flexibility and appliance operation under the same model.
- Ex-post flexibility: Evaluate the flexibility as the difference between a demand curve that offers flexibility and a reference demand trajectory.

The ex-ante approach is used to evaluate changes in the control strategies considering one or various attributes (minimise CO2 emissions, energy prices, demand response requests) and how the flexibility can help to achieve these objectives Reynders et al. (2018). This approach compares innovative control strategies with flexibility indicators to evaluate their performance, as seen in the work of Six Six, Desmedt, Vanhoudt, and Van Bael (2011), which introduces the "Delayed Flexibility" and "Forced Flexibility" indicators to estimate the time that a residential heat pump can be delayed or anticipated, similar to D'hulst D'hulst et al. (2015) considering the delayed flexibility, and the increased and decreased power consumption as flexibility indicators. Stinner Stinner, Huchtemann, and Müller (2016) proposes the "Energy Flexibility" and "Power Flexibility" indicators to quantify the flexibility available for a water storage tank, while Klein K. Klein et al. (2017); K. Klein, Langner, Kalz, Herkel, and Henning (2016) proposes the Grid Support Coefficients indicator to quantify the energy used from non-renewable sources. Marotta Marotta, Guarino, Cellura, and Longo (2021) presents a comprehensive review of flexibility indicators, analysing 27 indicators and utilising the flexibility

factor to compare the energy used in high- and low-penalty hours. Other ex-ante flexibility models do not need to use flexibility indicators, as seen in Wen Wen, Hu, You, and Duan (2022), which evaluates the flexibility of various appliances to offer an aggregated feasible region, using the Fourier-Motzkin Elimination process to reduce constraint redundancy. Iria J. Iria et al. (2019); J. P. Iria et al. (2018) formulates a demand aggregator model that includes flexibility constraints in the appliance formulation, offering flexibility according to price markets and testing its performance using an Model Predictive Control (MPC).

The ex-post approach requires a direct quantification of the flexibility based on the difference between a predefined demand profile and the appliance's response if a flexibility requirement is received. This approach is explored by De Coninck De Coninck and Helsen (2016), to calculate a flexibility cost curve in proportion to the energy required by the flexibility request, related to the Oldewurtel Oldewurtel, Sturzenegger, Andersson, Morari, and Smith (2013) approach, using price signals to evaluate the power shifting efficiency and potential. An alternative approach is explored by Junker Junker et al. (2018), who proposes a dynamic flexibility function based on the impulse response function for thermal systems, tested with two flexibility indicators, and a flexibility indicator comparison for energy and carbon dioxide emissions reduction using the energy shifting, prebound and rebound effect to quantify flexibility Kathirgamanathan et al. (2020). Other ex-post publications evaluate the flexibility costs including the cost of unplanned use of batteries and EV's Harder, Qussous, and Weidlich (2020b), considering the flexibility as a virtual energy storage system to determine the available storage capacity, the storage efficiency, and the power shifting capability in HVAC systems Reynders et al. (2018), or evaluates the savings on the operation cost using flexible appliances in a microgrid Gottwalt, Gärttner, Schmeck, and Weinhardt (2016).

2.1.2 Contributions

Based on the previously indicated approaches, the flexibility models in demand response scenarios can evaluate the available flexibility for each time interval or the demand deviation if a demand response request is received. A gap in the flexibility literature appears whether the frequency reserve problem is evaluated: a flexibility request duration can vary between 15 minutes and 2 hours, requiring the evaluation of various time blocks to offer flexibility. The state-of-art flexibility models can solve this problem when the flexibility requirement is known in advance. Still, whether the flexibility can be requested and dispatched with a 15-minute notice, a day-ahead model cannot offer an adequate response when the flexibility requirement is longer than the time interval used. The MPC models for microgrids Kathirgamanathan, De Rosa, Mangina, and Finn (2021); Mao, Jin, Hatziargyriou, and Chang (2014) can tackle this problem in real-time. However, a day-ahead flexibility model designed for frequency reserve markets presents a research opportunity if the flexibility can be offered for continuous time intervals.

This publication focused on developing an Aggregated Flexibility Estimation model with a defined flexibility request duration. The flexibility duration is the number of time blocks to offer the estimated flexibility to the grid. For example, a flexibility request with a three blocks duration in a 15-minute time interval case is equivalent to a 45 minutes flexibility request. To offer flexibility for a defined duration, an alternative flexibility scenario is proposed to estimate the flexibility. The alternative scenario evaluates how the offered flexibility by the appliances affects the next time blocks. The model quantifies and maximises the flexibility in the alternative scenario, where the minimum flexibility value from the alternative time blocks will be offered as the appliance's aggregated flexibility, ensuring a constant flexibility offer for the expected flexibility duration. The main contributions of this paper are:

- A flexibility estimation model for centralised energy management systems that considers the flexibility effects on the appliance's properties.
- A new set of constraints is presented to quantify the flexibility of the considered flexible appliances.
- The flexibility rebound effect is integrated into the appliance's constraint.
- The model estimates the flexibility as the maximum value offered for continuous time blocks.

2.1.3 Document structure

The publication is organised as follows: Section 2.2 presents the proposed flexibility approach and introduces the mathematical formulation for the aggregated flexibility estimation model. Section 2.3 presents the results and discussion of various study cases related to aggregated flexibility estimation model. Finally, section 2.4 provides the concluding remarks.

2.2 Aggregated Flexibility Estimation Methodology

2.2.1 Flexibility estimation

The proposed aggregated flexibility estimation model aims to minimise the operation cost and estimate the available flexibility from a set of appliances, assuming that the flexibility offered must be available for a defined flexibility service duration. This model introduces an alternative flexibility scenario to evaluate whether the expected flexibility can be provided over continuous time intervals. In simple terms, the appliance's scheduling in the alternative scenario considers the flexibility delivered in each time-step to guarantee that the flexibility offered can be provided during the flexibility duration service.

The model is introduced as an aggregated flexibility approach because it considers the coordinated response of the evaluated appliances for the continuous time-steps. For example, if two appliances are respond to a 30-minute flexibility request, the appliance 1 provides 2 kW of flexibility for the first 15 minutes and the appliance 2 offers 2kW of flexibility in the last

15 minutes. As a result, the aggregated flexibility response considers that the appliances have provided 2kW of flexibility for 30 minutes. This approach allows short-term, flexible appliances to offer services for a longer period of flexibility. The mathematical formulation for this approach is presented in expression 2.1, where the flexibility estimated for the time step t must be lower or equal to the sum of the flexibility offered in each time block from the alternative scenario.

In the model formulation, the index n represents the time steps for the alternative scenario. In this notation, the appliance's properties are evaluated assuming that the flexibility estimated in $n = 0$ only considers the scheduling for t, as shown in the figure 2.1. If $n > 0$ the flexibility estimated is evaluated according to the scheduling decisions in $t + n$ and the flexibility offered in $n - 1$.

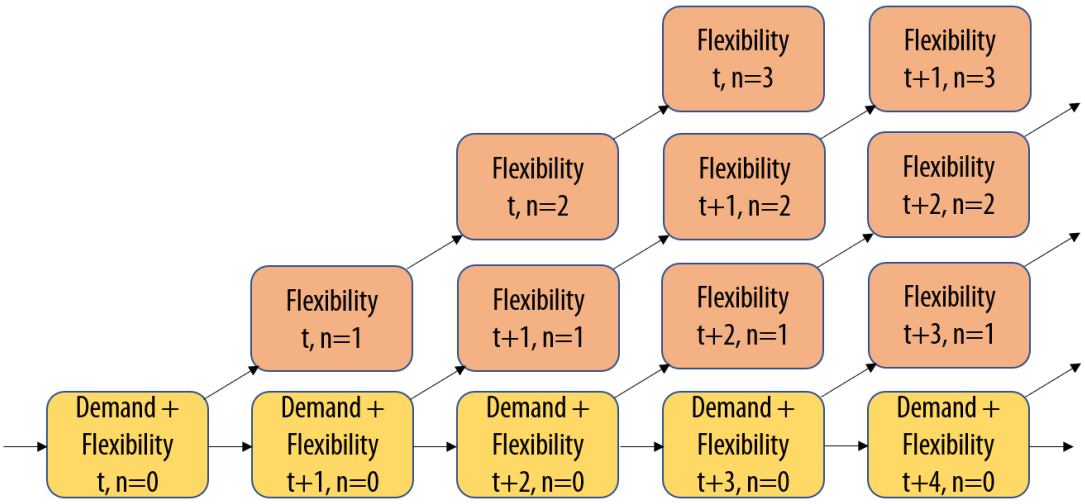

Figure 2.1: Graphical representation of the alternative flexibility scenario. The index t represents the time-steps for the proposed time, including the appliance scheduling, expected demand, and estimated flexibility according to the expected demand, while n represents the time-steps in the alternative flexibility scenario starting at time t, using $n - 1$ demand, flexibility, and appliance scheduling to estimate the flexibility in n. The flexibility offered in t corresponds to the minimal flexibility value found in the n time-steps.

Time blocks

The proposed model can be used with different time intervals according to the EMS preferences. The constraints expressed have been tested using three approaches: a 15-minute approach (96 time blocks per day), a 30-minute approach (48 time blocks), and a 1-hour approach (24 time blocks). The flexibility estimation uses the notation "1-block" to indicate for how many time blocks the aggregated flexibility response is evaluated. For example, a 30-minute approach with a 2-block flexibility estimation evaluates the flexibility for 1 hour in each time block, while a 1-hour approach with a 3-block estimation considers the flexibility response for 3 hours.

2.2.2 Flexibility model formulation

The flexibility estimation model schedules a set of flexible appliances, such as Pool Pumps, Electric Water Heaters, and Air Conditioning, considering operational and comfort constraints for each appliance. The flexibility model formulation aims to provide flexibility for continuous time-steps, while considering a variable time-step (24, 48, and 96 time-steps per day). The proposed model considers energy and flexibility prices to minimise its operation, offer flexibility services, and evaluate how flexibility changes in response to price signals. The presented flexibility approach can be considered a deterministic model, and there is no penalisation if a demand deviation occurs.

Objective function and Flexibility estimation

The proposed objective function minimises the operational cost, considering energy and flexibility prices for daily operation. The model optimises the appliance's scheduling and the available flexibility for each time-step, where the flexibility must be provided for an N number of time-steps defined by the flexibility service duration, according to the expression 2.1.

$$\min \sum_{t} \left(C_t^E * D_t - C_t^{UF} * UF_t - C_t^{DF} * DF_t \right) \tag{2.1a}$$

$$\text{s.t. } D_t = \sum_{EWH} P_t^{ewh} + \sum_{PP} P_t^{pp} \tag{2.1b}$$
$$+ \sum_{HVAC} \left(P_t^{hvac,H} + P_t^{hvac,C} \right) \qquad \forall t \in T$$

$$UF_t \leq \sum_{EWH} UF_{t,n}^{ewh} + \sum_{PP} UF_{t,n}^{pp} \tag{2.1c}$$
$$+ \sum_{HVAC} \left(UF_{t,n}^{hvac,H} + UF_{t,n}^{hvac,C} \right) \qquad \forall t \in T, n \in N$$

$$DF_t \leq \sum_{EWH} DF_{t,n}^{ewh} + \sum_{PP} DF_{t,n}^{pp} \tag{2.1d}$$
$$+ \sum_{HVAC} \left(DF_{t,n}^{hvac,H} + DF_{t,n}^{hvac,C} \right) \qquad \forall t \in T, n \in N$$

Expression (2.1b) introduces the total energy consumption at time t as the sum of the flexible appliances. The expressions (2.1c,2.1d) introduce the flexibility estimation for continuous time-steps for upward and downward flexibility. The flexibility estimated for t time-step must be lower than the flexibility provided by the flexible appliances for the n time-steps associated with the alternative flexibility scenario, maximising the UF_t and DF_t values that are limited by the lowest aggregated flexibility in n time-steps.

Pool Pumps - Deferrable appliances

The deferrable appliances are electrical loads that can be stopped or shifted without incurring any penalties related to their operation, and they require a certain amount of energy within a given period. The pool pump can be considered the appliance most closely related to the definition of a deferrable appliance. Numerous publications Barooah, Buic, and Meyn (2015); Gazafroudi et al. (2017); Hao and Chen (2014) promote the active usage of the pool pumps as a flexibility provider in power systems.

The flexibility estimation constraints has been introduced into the pool pump operational model. The expression (2.2) presents the pool pump operational constraints, including the total energy required per day as the sum of the supplied energy per time-step (2.2a), the maximum power and the pool pump availability are included in (2.2b,2.2c).

$$\sum_{t} P_t^{pp} = E^{pp} \tag{2.2a}$$

$$0 \leq P_t^{pp} \leq P_{max}^{pp} \quad \forall t \in T \tag{2.2b}$$

$$P_t^{pp} = 0 \qquad if\, t \notin [T_{start}^{pp}, T_{end}^{pp}] \tag{2.2c}$$

In expression (2.3) are shown the required constraints to estimate the Pool Pump flexibility per time-step. Constraint (2.3a) limits the flexibility to the time-steps when the pool pump is available. Expressions (2.3b) and (2.3c) limit the upward and downward flexibility in time-step t and alternative time-step n to the maximum displacement from the scheduled demand. The previous expressions need additional constraints to ensure that the pool pump can offer flexibility without breaking the constraints presented in (2.2). Therefore, to reinforce constraint (2.2a), the expression (2.3d) evaluates in each time-step n if the upward flexibility offered does not exceed the pool pump's daily power. Also, the expression (2.3e) verifies if the pool pump has enough upward flexibility in the next time-steps to compensate for the downward flexibility to provide at time-step t. Both expressions estimate the rebound effect in the pool pump model, allowing to the appliance to provide flexibility that can be compensated in the future.

$$UF_{t,n}^{pp} = DF_{t,n}^{pp} = 0 \qquad if\, t+n \notin [T_{start}^{pp}, T_{end}^{pp}] \tag{2.3a}$$

$$UF_{t,n}^{pp} \leq P_{max}^{pp} - P_{t+n}^{pp} \qquad \forall t \in T, \forall n \in N \tag{2.3b}$$

$$DF_{t,n}^{pp} \leq P_{t+n}^{pp} \qquad \forall t \in T, \forall n \in N \tag{2.3c}$$

$$\sum_{l=0}^{t+n} P_l^{pp} + \sum_{s=0}^{n} UF_{t,s}^{pp} \leq E^{pp} \quad \forall t \in T, \forall n \in N \tag{2.3d}$$

$$\sum_{s=0}^{n} DF_{t,s}^{pp} \leq \sum_{l=t+1+s}^{T} UF_{l,0}^{pp} \quad \forall t \in T, \forall n \in N \tag{2.3e}$$

Heating, Ventilation, and Air Conditioning appliances

The high energy consumption of Heating, Ventilation, and Air Conditioning (HVAC) appliances, combined with the thermal inertia associated with the building's heat capacity, allows the HVAC system to shift its consumption, modifying its demand curve. The HVAC appliances and their flexibility have been extensively studied Chen, Xu, Gu, Schmidt, and Li (2018); Faqiry, Wang, and Wu (2019); Gazafroudi et al. (2017) and incorporated into various Energy Management System approaches, such as Virtual Power Plants, Demand Aggregators, and Home Energy Management Systems.

The HVAC appliances depend on the room temperature, the building thermal inertia, and the ambient temperature to schedule their operation without exceeding the comfort temperature chosen by the users. The base HVAC formulation is presented in expression (2.4). The equations (2.4a) and (2.4b) evaluate the room temperature as a function of its previous state, the forecasted ambient temperature, and the power used to heat or cool the room. In both expressions, the terms α and β are used as constant values related to the effect of the relevant variables (room temperature in the previous time-step, ambient temperature, heating, and cooling power) on the room temperature. The different approaches to estimate α and β are presented on .1. Expressions (2.4c) and (2.4d) introduce the room temperature constraints and the HVAC maximum power consumption.

$$T_t^{hvac} = T_{start}^{hvac} + \alpha_{hvac} * (T_{t-1}^{hvac,Forecast} - T_{start}^{hvac}) + \beta_{hvac,H} * P_t^{hvac,H} - \beta_{hvac,C} * P_t^{hvac,C} \quad t = 0, \forall hvac \in HVAC \tag{2.4a}$$

$$T_t^{hvac} = T_{t-1}^{hvac} + \alpha_{hvac} * (T_{t-1}^{hvac,Forecast} - T_{t-1}^{hvac}) + \beta_{hvac,H} * P_t^{hvac,H} - \beta_{hvac,C} * P_t^{hvac,C} \quad t \neq 0, \forall hvac \in HVAC \tag{2.4b}$$

$$T_{min}^{hvac} \leq T_t^{hvac} \leq T_{max}^{hvac} \qquad \forall t \in T \tag{2.4c}$$

$$0 \leq P_t^{hvac,H} + P_t^{hvac,C} \leq P_{max}^{hvac} \qquad \forall t \in T, \forall hvac \in HVAC \tag{2.4d}$$

To calculate the demand and flexibility provided by an HVAC appliance in a unique scenario, the expression (2.5) determines whether the room temperature exceeds the room temperature constraints while offering flexibility to the power system. The expressions (2.5a) and (2.5b) calculate the room temperature if the flexibility increases the expected consumption, while expressions (2.5c) and (2.5d) estimate the downward flexibility effects on the room temperature for the n time-steps. The expression (2.5e) limits the temperature for the room temperature under flexibility requirements.

HVAC temperature variation under upward and downward flexibility [eq. 2.5]:

$$T_{t,n}^{UF,hvac} = T_{t-1}^{hvac} + \alpha_{hvac} * (T_{t-1}^{Forecast} - T_{t-1}^{hvac}) + \beta_{hvac,H} * (P_t^{hvac,H} + UF_{t,n}^{hvac,H}) - \beta_{hvac,C} * (P_t^{hvac,C} + UF_{t,n}^{hvac,C}) \quad n = 0, \forall hvac \in HVAC \tag{2.5a}$$

$$T_{t,n}^{UF,hvac} = T_{t,n-1}^{UF,hvac} + \alpha_{hvac} * (T_{t-1+n}^{Forecast} - T_{t,n-1}^{UF,hvac}) + \beta_{hvac,H} * (P_{t+n}^{hvac,H} + UF_{t,n}^{hvac,H}) - \beta_{hvac,C} * (P_{t+n}^{hvac,C} + UF_{t,n}^{hvac,C}) \quad n \neq 0, \forall hvac \in HVAC \tag{2.5b}$$

$$T_{t,n}^{DF,hvac} = T_{t-1}^{hvac} + \alpha_{hvac} * (T_{t-1}^{Forecast} - T_{t-1}^{hvac}) + \beta_{hvac,H} * (P_t^{hvac,H} - DF_{t,n}^{hvac,H}) \tag{2.5c}$$

$$- \beta_{hvac,C} * (P_t^{hvac,C} - DF_{t,n}^{hvac,C}) \quad n = 0, \forall hvac \in HVAC$$

$$T_{t,n}^{DF,hvac} = T_{t,n-1}^{DF,hvac} + \alpha_{hvac} * (T_{t-1+n}^{Forecast} - T_{t,n-1}^{DF,hvac}) + \beta_{hvac,H} * (P_{t+n}^{hvac,H} - DF_{t,n}^{hvac,H}) \tag{2.5d}$$
$$- \beta_{hvac,C} * (P_{t+n}^{hvac,C} - DF_{t,n}^{hvac,C}) \quad n \neq 0, \forall hvac \in HVAC$$

$$T_{min} \leq (T_{t,n}^{UF}, T_{t,n}^{DF}) \leq T_{max} \quad \forall n \in N \tag{2.5e}$$

(2.5f)

The HVAC appliances can provide flexibility independently of their operational mode (heat or cooling), but having two or more variables to quantify the flexibility can produce some discrepancies in the appliance scheduling. To avoid this problem, the expression (2.6) unifies the flexibility variables per operational mode into one variable for upward flexibility and another for downward flexibility. The expressions (2.6a) and (2.6b) limit the downward flexibility according to the expected power for the heating and cooling process, while the expression (2.6c) limits the upward flexibility according to the HVAC maximum power consumption. Finally, expressions (2.6d) and (2.6e) sum the flexibility from both operational modes on a single variable.

HVAC upward and downward flexibility constraints [eq. 2.6]:

$$DF_{t,n}^{hvac,H} \leq P_{t+n}^{hvac,H} \quad \forall t \in T, \forall n \in N, \forall hvac \in HVAC \tag{2.6a}$$

$$DF_{t,n}^{hvac,C} \leq P_{t+n}^{hvac,C} \quad \forall t \in T, \forall n \in N, \forall hvac \in HVAC \tag{2.6b}$$

$$P_{t+n}^{hvac,H} + P_{t+n}^{hvac,C} + UF_{t,n}^{hvac,H} + UF_{t,n}^{hvac,C} \leq P_{max} \quad \forall t \in T, \forall n \in N, \forall hvac \in HVAC \tag{2.6c}$$

$$UF_{t,n}^{hvac} = UF_{t,n}^{hvac,H} + UF_{t,n}^{hvac,C} \quad \forall t \in T, \forall n \in N, \forall hvac \in HVAC \tag{2.6d}$$

$$DF_{t,n}^{hvac} = DF_{t,n}^{hvac,H} + DF_{t,n}^{hvac,C} \quad \forall t \in T, \forall n \in N, \forall hvac \in HVAC \tag{2.6e}$$

The expression (2.6) consider the flexibility for heating and cooling in the same equations [(2.6c), (2.6d), and (2.6e)], but the HVAC appliances cannot heat and cool simultaneously. Hence, the HVAC heating and cooling operation are limited by the expression (2.7) using a BigM notation to couple the expected demand to a heating or cooling binary variable.

$$P_t^{hvac,H} \leq P_{max} * bP_t^{hvac,H} \quad \forall t \in T, \forall hvac \in HVAC \tag{2.7a}$$

$$P_t^{hvac,C} \leq P_{max} * bP_t^{hvac,C} \quad \forall t \in T, \forall hvac \in HVAC \tag{2.7b}$$

The inclusion of binary variables associated with the HVAC operational modes requires deciding between a free binary model (first approach) or artificially limiting the binary decisions (second approach). The first approach (expression (2.8)) allows the HVAC to select between both operation modes without limitations, an approach that has two weaknesses. First, allowing the model to choose between heat and cool in each time-step increases the computational power required to solve the scheduling problem. Second, the scheduling model can alternate between heat and cooling to artificially increase the flexibility. The additional energy cost can diminish the artificial flexibility increase if that scheduling strategy is used. However, systems with low or zero energy cost will increase their energy consumption unnecessarily. This approach is helpful in models with a longer time-step (1-hour), but it can be unfeasible

for daily appliance scheduling using a 15-minute or a 30-minute time-step.

First Approach

$$bP_t^{hvac,H} + bP_t^{hvac,C} \leq 1 \quad \forall t \in T, \forall hvac \in HVAC \tag{2.8a}$$

Consequently, the operational decision mode employed in this work is the second approach (expression (2.9)), which limits the heating or cooling operation based on the ambient temperature forecast. For example, the HVAC cannot heat the room if the predicted outside temperature is $28°C$ and the maximum room temperature is $24°C$. The appliance can choose its operational mode without limitations when the forecast temperature does not surpass the temperature comfort range (expression (2.9c)). The temperature limits in expressions (2.9a) and (2.9b) can be adjusted according to the requirements.

Second Approach

$$bP_t^{hvac,H} = 0, if\ T_t^{Forecast} \geq T_{max} \quad \forall t \in T, \forall hvac \in HVAC \tag{2.9a}$$

$$bP_t^{hvac,C} = 0, if\ T_t^{Forecast} \leq T_{min} \quad \forall t \in T, \forall hvac \in HVAC \tag{2.9b}$$

$$bP_t^{hvac,H} + bP_t^{hvac,C} \leq 1$$
$$if\ T_t^{Forecast} \in [T_{min}, T_{max}] \quad \forall t \in T, \forall hvac \in HVAC \tag{2.9c}$$

Finally, the expression (2.10) limits the HVAC flexibility according to the operational mode selected by the model.

$$UF_{t,n}^{hvac,H} \leq P_{max} * bP_{t+n}^{hvac,H} \quad \forall t \in T, \forall n \in N, \forall hvac \in HVAC \tag{2.10a}$$

$$UF_{t,n}^{hvac,C} \leq P_{max} * bP_{t+n}^{hvac,C} \quad \forall t \in T, \forall n \in N, \forall hvac \in HVAC \tag{2.10b}$$

$$DF_{t,n}^{hvac,H} \leq P_{max} * bP_{t+n}^{hvac,H} \quad \forall t \in T, \forall n \in N, \forall hvac \in HVAC \tag{2.10c}$$

$$DF_{t,n}^{hvac,C} \leq P_{max} * bP_{t+n}^{hvac,C} \quad \forall t \in T, \forall n \in N, \forall hvac \in HVAC \tag{2.10d}$$

Electric Water Heater (EWH)

The Electric Water Heater has a relevant presence in households and buildings. The EWH penetration in US households reaches 39% Ryan, Long, Lauf, Ledbetter, and Reeves (2013), and their energy consumption can be 30% of the energy bills Diao et al. (2012). The EWH utilises a resistor as a heating element, allowing for flexibility in response to variations in water temperature and user water usage.

The EWH model used is based on the one-node approach, where the water temperature is assumed to be homogeneous throughout the tank. Other approaches consider two or more water compartments with different temperatures Mukherjee, Bhattarai, Hanif, and Pratt (2022). The basic EWH model is presented in the expression (2.11). The temperature evolution per time-step is given in (2.11a), including the user's water usage and thermal losses. Expression (2.11b) introduces the temperature limitation in the model. The term eP_t^{ewh} is used to exceed the minimum temperature constraint if the water temperature is lower than the expected value, forcing the EWH heating at maximum power (expression (2.11a)).

$$T_t^{ewh} = T_{t-1}^{ewh} * \frac{V_{tank} - WU_t}{V_{tank}} + T_{water}^{input} * \frac{WU_t}{V_{tank}} + \frac{P_t^{ewh} + P_{max}^{ewh} * eP_t^{ewh} - W_{tank} * (T_{t-1}^{ewh} - T_{room})}{V_{tank} * \rho_{water} * \frac{Cp_{water}}{3600}} \quad if\, t \neq 0 \tag{2.11a}$$

$$T_{min}^{ewh} - bigM * eP_t^{ewh} \leq T_t^{ewh} \leq T_{max}^{ewh} \quad \forall t \in T \tag{2.11b}$$

$$0 \leq P_t^{ewh} + P_{max}^{ewh} * eP_t^{ewh} \leq P_{max}^{ewh} \quad \forall t \in T \tag{2.11c}$$

The flexibility evaluation uses the same approach presented for the HVAC model. The available flexibility is estimated based on the demand deviation without surpassing the thermal constraints, as shown in expression (2.12). The upward flexibility temperature $T_{t,n}^{UF}$ is introduced in expressions (2.12a) and (2.12b), while the downward flexibility temperature $T_{t,n}^{DF}$ is shown in (2.12c) and (2.12d). Expressions (2.12a) and (2.12c) help the transition between the appliance scheduling and the alternative flexibility scenario, using T_{t-1} as a start point and changes to $T_{t,n-1}^{UF}$ and $T_{t,n-1}^{DF}$ for the alternative time-step. The temperature limits shown in (2.12e) do not evaluates the emergency heating variable, as the appliance lacks flexibility in unexpected scenarios.

EWH Temperature variation under Upward and Downward Flexibility [eq. 2.12]:

$$T_{t,n}^{UF,ewh} = T_{t-1}^{ewh} * \frac{V_{tank} - WU_{t+n}}{V_{tank}} + T_{water}^{input} * \frac{WU_{t+n}}{V_{tank}} + \frac{P_{t+n}^{ewh} + P_{max}^{ewh} * eP_{t+n}^{ewh} + UF_{t,n}^{ewh} - W_{tank} * (T_{t-1}^{ewh} - T_{room})}{V_{tank} * \rho_{water} * \frac{Cp_{water}}{3600}} \quad if\, n = 0 \tag{2.12a}$$

$$T_{t,n}^{UF,ewh} = T_{t,n-1}^{UF,ewh} * \frac{V_{tank} - WU_{t+n}}{V_{tank}} + T_{water}^{input} * \frac{WU_{t+n}}{V_{tank}} + \frac{P_{t+n}^{ewh} + P_{max}^{ewh} * eP_{t+n}^{ewh} + UF_{t,n}^{ewh} - W_{tank} * (T_{t,n-1}^{UF,ewh} - T_{room})}{V_{tank} * \rho_{water} * \frac{Cp_{water}}{3600}} \quad if\, n \neq 0 \tag{2.12b}$$

$$T_{t,n}^{DF,ewh} = T_{t-1}^{ewh} * \frac{V_{tank} - WU_{t+n}}{V_{tank}} + T_{water}^{input} * \frac{WU_{t+n}}{V_{tank}} + \frac{P_{t+n}^{ewh} + P_{max}^{ewh} * eP_{t+n}^{ewh} - DF_{t,n}^{ewh} - W_{tank} * (T_{t-1}^{ewh} - T_{room})}{V_{tank} * \rho_{water} * \frac{Cp_{water}}{3600}} \quad if\, n = 0 \tag{2.12c}$$

$$T_{t,n}^{DF,ewh} = T_{t,n-1}^{DF,ewh} * \frac{V_{tank} - WU_{t+n}}{V_{tank}} + T_{water}^{input} * \frac{WU_{t+n}}{V_{tank}} + \frac{P_{t+n}^{ewh} + P_{max}^{ewh} * eP_{t+n}^{ewh} - DF_{t,n}^{ewh} - W_{tank} * (T_{t,n-1}^{DF,ewh} - T_{room})}{V_{tank} * \rho_{water} * \frac{Cp_{water}}{3600}} \quad if\, n \neq 0 \tag{2.12d}$$

$$T_{min}^{ewh} \leq T_{t,n}^{UF,ewh}, T_{t,n}^{DF,ewh} \leq T_{max}^{ewh} \qquad \forall t \in T, \forall n \in N \tag{2.12e}$$

The expression (2.13) limits the EWH flexibility according to the power. The downward flexibility depends on the power consumption (expression (2.13a)), and its limited by the emergency heating variable (expression (2.13b)). The upward flexibility depends on the difference between the power consumption and the EWH maximum power (expression (2.13c)).

$$DF_{t,n}^{ewh} \leq P_{t+n}^{ewh} \qquad \forall t \in T, \forall n \in N \tag{2.13a}$$

$$DF_{t,n}^{ewh} \leq (1 - eP_{t+n}^{ewh}) * P_{max}^{ewh} \qquad \forall t \in T, \forall n \in N \tag{2.13b}$$

$$P_{t+n}^{ewh} + P_{max}^{ewh} * eP_{t+n}^{ewh} + UF_{t,n}^{ewh} \leq P_{max}^{ewh} \qquad \forall t \in T, \forall n \in N \tag{2.13c}$$

2.2.3 Case study

To validate the proposed model, it is necessary to specify the energy resources, databases, case generation process, and other inputs used in the model formulation. First, two sets of appliances were used to evaluate its flexibility:

- 300 appliances - 100 HVAC, 100 PP, and 100 EWH
- 3000 appliances - 1000 HVAC, 1000 PP, and 1000 EWH

The HVAC formulation considers a building with five floors and ten apartments per floor (50 HVAC appliances per building). The apartment's surface area is 80 square meters. Each apartment has one EWH with a 120L tank and a maximum power consumption of 2200W. The Pool Pumps were randomly selected from a set of 46 different pool pump models, assuming that the pool pump needs to operate for the minimum required time to filter the water at least twice daily.

Second, the flexible appliances information. The hot water consumption profiles for the EWH were generated with the software *Load Profile Generator*Pflugradt (2016). For the temperature forecast, historical outdoor air temperature data from NOAA NCEI Climate Normals Arguez et al. (2010) are used, sourced from the San Francisco International Airport (ID GHCND:USW00023234). Building material properties and wall-building design were extracted from *EnergyPlus* softwareDoE (2010). Energy prices were downloaded from the CAISO OASIS Platform *California Independent System Operator. Open access same time information system* (2022). The Energy Component in the HASP Locational Marginal Prices and the Regulation Up and Down from the Interval AS Clearing Prices were used as Energy and Flexibility prices. The energy and flexibility prices data have a 15-minute granularity, and the mean price value is used for the 30-minute and 1-hour cases.

Finally, to test the flexibility changes in a predefined set of appliances, are presented 5 case studio to evaluate how the flexibility changes according to the duration of the flexibility requirement and the energy prices:

- Case 1: Flexibility estimation without considering energy prices for the different time intervals
- Case 2: Response to a 1-hour flexibility requirement for the different time intervals
- Case 3: Flexibility under different tariff schemes
- Case 4: flexibility response for real-time prices (one per season)
- Case 5: Appliance response for a 4-block flexibility response

The first case evaluates the appliance response for various flexibility requirements with different durations. The objective is to demonstrate how the offered flexibility decreases as the flexibility duration request increases. This case does not consider energy prices, and the flexibility prices are fixed at 1 USD/MWh. The second case examines how the time interval used to estimate flexibility can impact the flexibility itself. The third flexibility case examines how flexibility is affected by the price schemes outlined in Table 2.1, specifically during the peak time between 16:00 and 21:00 hours. The fourth case shows how the appliances modify their flexibility for four distinct real-time price profiles, considering one day per season (and their respective temperature forecast). Finally, the last case validates the usage of extended flexibility estimation models. The flexibility estimated for the 4-block approach is introduced as a flexibility requirement for the 1-block, 2-block, and 3-block appliance scheduling calculated by the model. The objective is to quantify the demand deviation if a lower (in power) flexibility requirement but higher in time is received.

Table 2.1: Energy and flexibility prices for the different tariff schemes.

	Energy $[USD/MWh]$		Upward Flexibility $[USD/MWh]$		Downward Flexibility $[USD/MWh]$	
No price	0		1		1	
Fixed Tariff	80		24		24	
Real-time	CAISO clearance prices at May 10th, 2022					
	Energy		Upward Flexibility		Downward Flexibility	
	non-peak	peak	non-peak	peak	non-peak	peak
Time-of-Use (ToU)	70	100	24	30	24	30
ToU - Case 1	70	100	24	30	24	0
ToU - Case 2	70	100	24	0	24	30

The first four cases used a 300-appliance set, while the last used a 3000-appliance set to evaluate the aggregated response to the flexibility requirements. The first two cases evaluate the proposed three time intervals (15-min, 30-min, and 1-hour), while the last three use a 15-minute approach with a 2-block flexibility requirement to standardise results. Energy prices used in the flexibility estimation were from May 10, 2022, unless otherwise indicated. The case studies were coded in Python using Pyomo Libraries Hart et al. (2017); Hart, Watson,

and Woodruff (2011). The solver GUROBI Gurobi Optimization, LLC (2024) with a 0.02 MIP GAP is chosen to solve the proposed problems. Cases 1 to 4 were run on a Ryzen 9 5900HX processor with 16 GB RAM. The last case was run on an Intel i7 10700 processor with 32 GB RAM. The 15-minute approach with a high number of appliances requires a large amount of RAM, and even more RAM if the model considers more than 4-blocks. In contrast, a commercial laptop can easily calculate the 30-minute and 1-hour approaches with a vast set of appliances.

2.3 Results

The 5 case studies proposed in the section 2.2.3 to evaluate the alternative flexibility scenario and the prices effects on flexibility will be discussed below.

2.3.1 Flexibility under different approaches

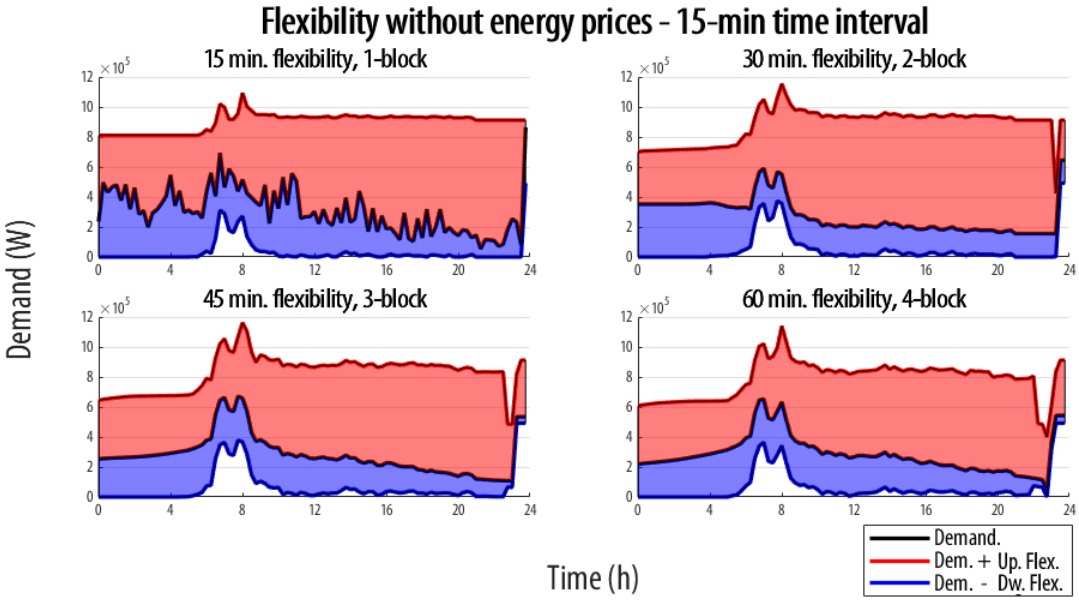

Figure 2.2: Flexibility estimation for various time blocks under a 15-minute time interval. The proposed approach considers an alternative flexibility scenario for a defined number of blocks. For example, if the time interval is 15-minute and the number of blocks is three, the indicated flexibility can be offered for 45 minutes.

Figure 2.2 shows the flexibility estimated for the 15-minute approach considering flexibility requirements from 15 minutes (1-block) until 1 hour (4-block), assuming energy prices equal to zero. The flexibility results for 1-block present higher flexibility and more variability on the scheduled demand compared with the extended flexibility requirements. Table 2.2 are shown the total daily flexibility and the flexibility percentage related to the 1-block case. The flexibility

values indicated are the total response capacity, without consider rebound effects. For the 15-minute approach, the downward flexibility showed at least a 20% decrease if the flexibility requested have more than a 1-block duration, while in the upward flexibility is observed that flexibility for the 2-block requirement in the 15-minute approach is higher than the base case, indicating that the flexibility is restricted by the power limitations and proposed scheduling rather than the thermal storage capacities in the EWH and the HVAC, statement that does not apply for the 30-minute and 1-hour approach, which shows decreases in the upward flexibility as expected.

Table 2.2: Daily aggregated flexibility for the studied time-steps and 1-block to 4-block flexibility requirements. The Flexibility percentage uses the 1-block case as reference

		Requirement duration			
Time-step		1-block	2-block	3-block	4-block
15-minute	Up. Flex. [MWh]	14.27	14.62	13.14	12.06
	% Up. Flex.	100%	102%	92%	84%
	Down. Flex. [MWh]	6.65	5.34	5.23	5.26
	% Down. Flex.	100%	80%	79%	79%
30-minute	Up. Flex. [MWh]	13.93	11.95	10.82	10.17
	% Up. Flex.	100%	86%	78%	73%
	Down. Flex. [MWh]	6.18	5.18	4.64	4.28
	% Down. Flex.	100%	84%	75%	69%
1-hour	Up. Flex. [MWh]	11.22	10.06	9.29	8.50
	% Up. Flex.	100%	90%	83%	76%
	Down. Flex. [MWh]	5.39	3.89	3.16	2.78
	% Down. Flex.	100%	72%	59%	52%

The demand variability observed for the 1-block case in figure 2.2 is repeated in each evaluated time-step. As seen in figure 2.3, the upward and downward flexibility estimated for the 1-block scenario exhibit high temporal variability when is compared with the flexibility for multiple blocks. This behaviour can be explained based on the non-temporal flexibility dependence in the 1-block case. In contrast, the temporal flexibility dependence for the 2-block case and others, forces the model to choose a smooth demand scheduling to maximise the flexibility. For example, if turning on an appliance in $t+1$ reduces the possible flexibility for t (flexibility evaluated with $n=1$ for the time-step t), the model will prefer to postpone the appliance activation.

Figure 2.3 compares the flexibility proposed for the different time interval approaches with different flexibility requirements (from 1 to 4-block requirements). In each hour, the estimated flexibility for an n-block flexibility requirement decreases according to the increase in n, if it is considered only the cases where $n \geq 1$. This statement can not be fulfilled if $n=1$ because of the high variability in the flexibility estimated.

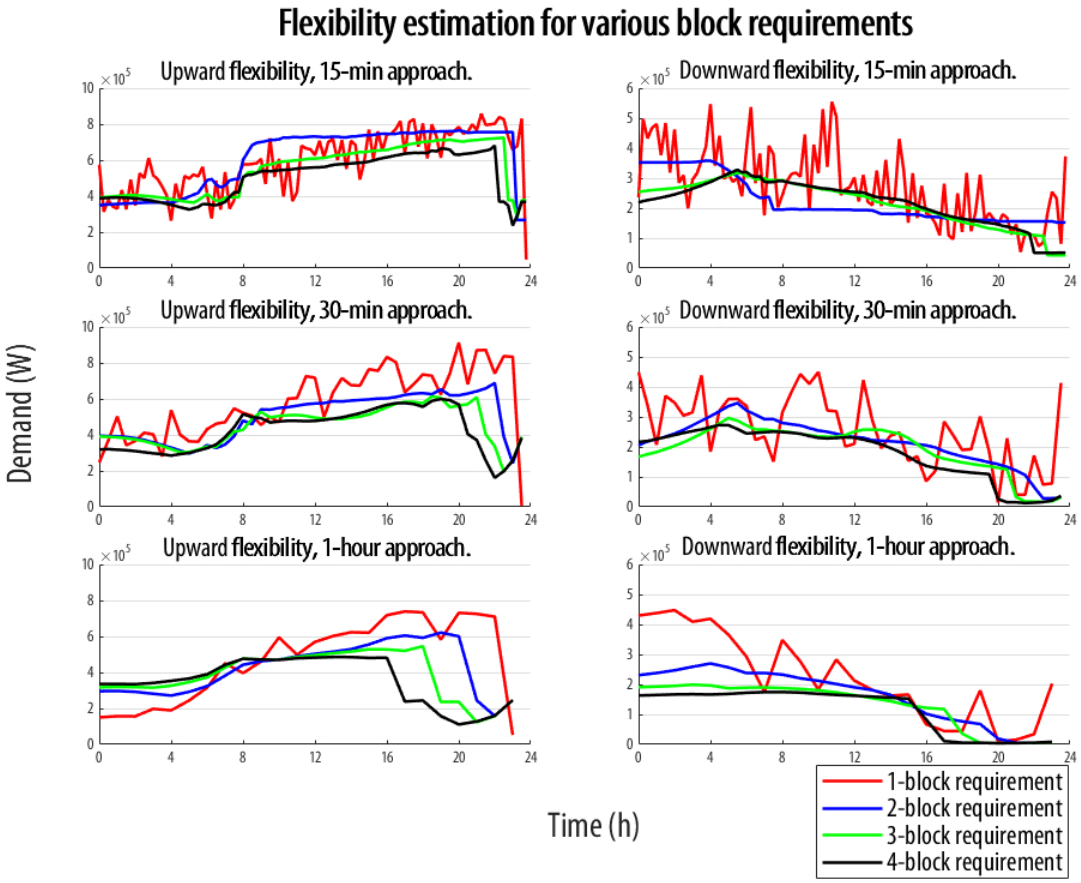

Figure 2.3: Flexibility estimation results for the studied time blocks and time intervals. The upward flexibility results are shown on the left, while the downward flexibility values are exposed on the right.

A reduction in flexibility is observed at the end of the day, which is directly related to the duration of the flexibility requirement. The flexibility reduction can be explained by the energy displaced to increase flexibility when the day starts, and the rebound constraints introduced in the appliances, which offer less flexibility if the displaced flexibility cannot be compensated. Both effects exhibit their maximum observed decrease in the 4-block 1-hour case, where the flexibility reduction starts at hour 16. A rolling horizon approach to estimate flexibility could be helpful for HVAC and EWH appliances, which evaluate their flexibility based on the room and water temperature. However, it can be an issue for the pool pump appliances that need a specific amount of energy daily. If a limited number of hours is evaluated, the proposed flexibility estimation model may not be enough to capture the Pool Pump behaviour.

2.3.2 Aggregated response for a 1-hour flexibility requirement

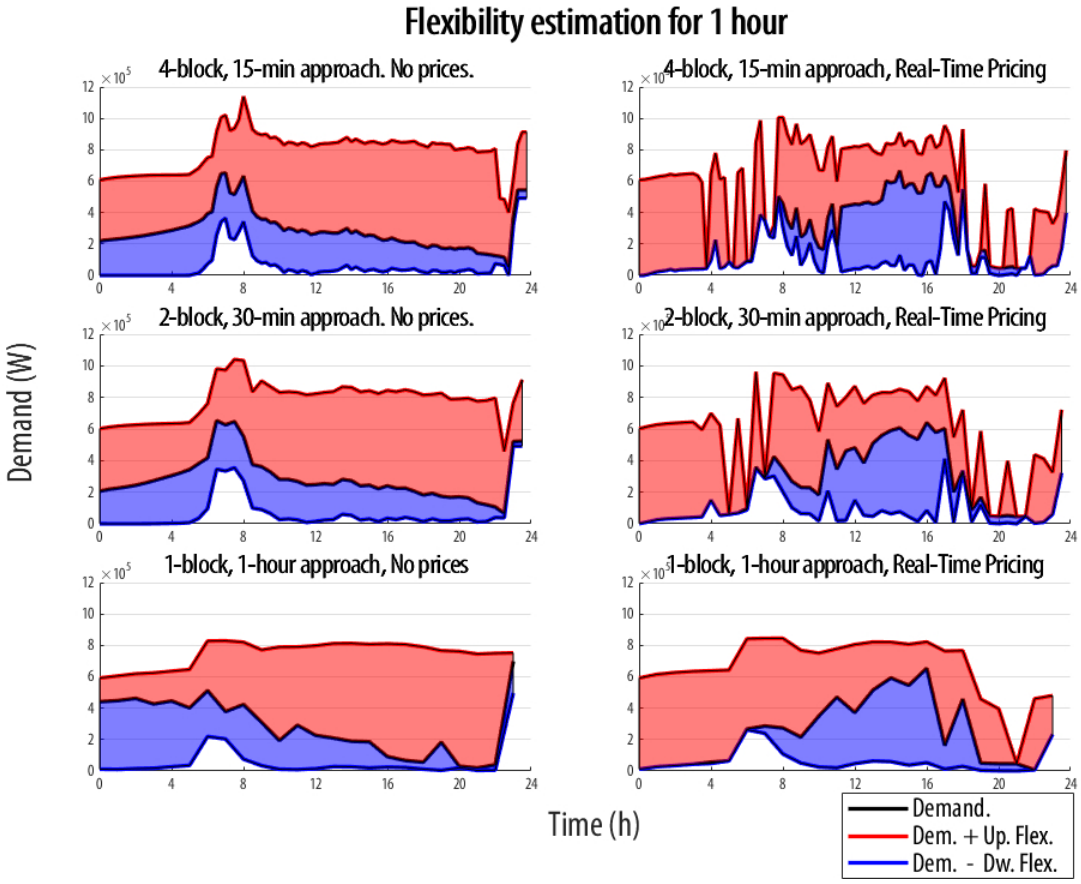

Figure 2.4: Flexibility estimation for 1-hour requirement under various time intervals. The 15-minute flexibility approach shows a high definition in demand and flexibility estimation. In contrast, the 1-hour approach presents smoothed values and reduces the available flexibility.

Table 2.3: Daily aggregated flexibility considering a 1 hour flexibility requirement

	No price		Real-time Pricing	
	Up. Flex. [MWh]	Down. Flex. [MWh]	Up. Flex. [MWh]	Down. Flex. [MWh]
15-minute	12.05	5.26	8.38	3.48
30-minute	11.95	5.18	8.79	3.77
1-hour	11.22	5.39	10.26	4.30

Figure 2.4 shows the estimated flexibility by the three time interval approaches if a 1-hour flexibility requirement is received. On the left side, the estimated flexibility is shown without considering energy prices, while the right side shows the flexibility considering real-time pricing. The first difference between no-price and real-time pricing is the appearance of zero flexibility hours, conditioned by a zero price in specific time intervals. This effect can not be shown in the 1-hour approach because the mean flexibility price diminishes the impact of the 15-minute intervals with zero flexibility prices. A second difference between the two

input signals is the downward flexibility shape. In the no-price signal, downward flexibility is distributed throughout the day with an expected reduction at the end of the day, whereas the real-time price approach concentrates the downward flexibility between 8:00 hrs and 18:00 hrs.

An unexpected result is an increase in upward flexibility in no-price schemes when the time interval is reduced (for example, from 1-hour to 30-min), while in real-time pricing, the flexibility decreases, as shown in table 2.3. The expected result was an increase in flexibility if the time interval considered more time blocks in a day, because specific constraints, such as temperature limitations, are evaluated four times per hour in the 15-minute time interval and once per hour in the 1-hour approach. This result can be an unexpected consequence of the energy price, which concentrates demand and flexibility in specific hours.

2.3.3 Tariff schemes response

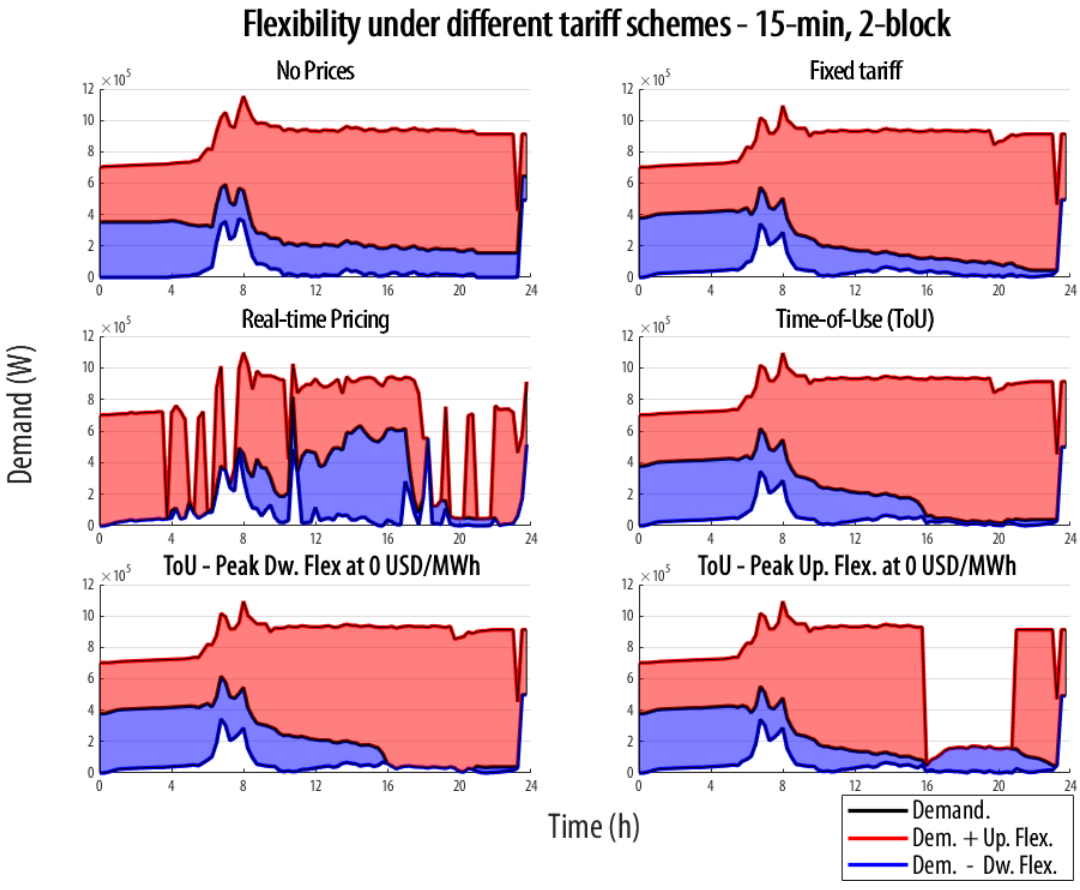

Figure 2.5: Flexibility estimation for 30 minutes under a 15-minute time interval. The energy and flexibility prices are indicated in table 2.1

Figure 2.5 shows the estimated flexibility for the 300 appliances under different tariff schemes. The used tariffs are indicated in table 2.1. The difference between a no-price flexibility estimation and a fixed tariff is the downward flexibility reduction at the end of the day, limited by the lack of demand to shift its consumption. A similar problem occurs with the Time-of-Use (ToU) tariff. In this case, the energy price in the peak hour (16:00 to 21:00 hrs) directly affects the downward flexibility, reducing demand to diminish operational costs. This behaviour, combined with the reduction in flexibility in the last hours of the day, significantly reduces the appliance's capacity to adjust its consumption during critical hours. The Time-of-Use tariff considers that upward and downward flexibility have the same value in the peak hour, generating an artificial incentive to increase upward flexibility because downward flexibility depends on energy consumption, which is penalised during peak hours. To visualise how the input signal can affect flexibility, two additional cases were considered: ToU tariffs with downward flexibility and no value, and ToU tariffs with upward flexibility and no value. The reduction in the flexibility prices is only viewed for peak hours. The first case yields similar results to the ToU case, reducing demand consumption to near zero during peak hours. In contrast, the demand in the second case increases during peak hours because if the downward flexibility prices are higher, the model will increase its demand to offer more flexibility, negatively affecting the ToU peak hours aim, which seeks to decrease energy consumption in power systems.

In comparison, the upward flexibility can increase its capacity during the day regardless of the scheduled demand (and if the flexibility prices are higher than zero), being limited only by the appliance's maximum power and rebound constraints. It should be noted that upward flexibility considers the capacity to increase consumption if a flexibility requirement is received, without considering the energy price in the alternative scenario, to prioritise the maximum energy the appliances can shift in time. The reason for using this approach is because the EMS does not want to increase its consumption without reason, only if an external request is received. A new formulation that considers the EMS cost to provide flexibility in the event of a new request and defines how many energy shifts in time can be explored according to the received signal in the future.

2.3.4 Flexibility estimation per season

The energy and flexibility prices (or other incentives) define the demand consumption and the amount of flexibility that will be offered during the day, based on the scheduled demand. To assess the price effect of flexibility, figure 2.6 shows the proposed demand consumption and the flexibility offered under four scenarios (one scenario per season). Demand consumption on February 15th depends on the HVAC operation because of the low outdoor temperatures (the 10-percentile temperature was used in this case). The constant energy consumption allows to the scheduled appliances to offer downward flexibility throughout the day. In contrast, August 16th shows a prohibitive energy price between 16:00 and 22:00 hrs, limiting the downward

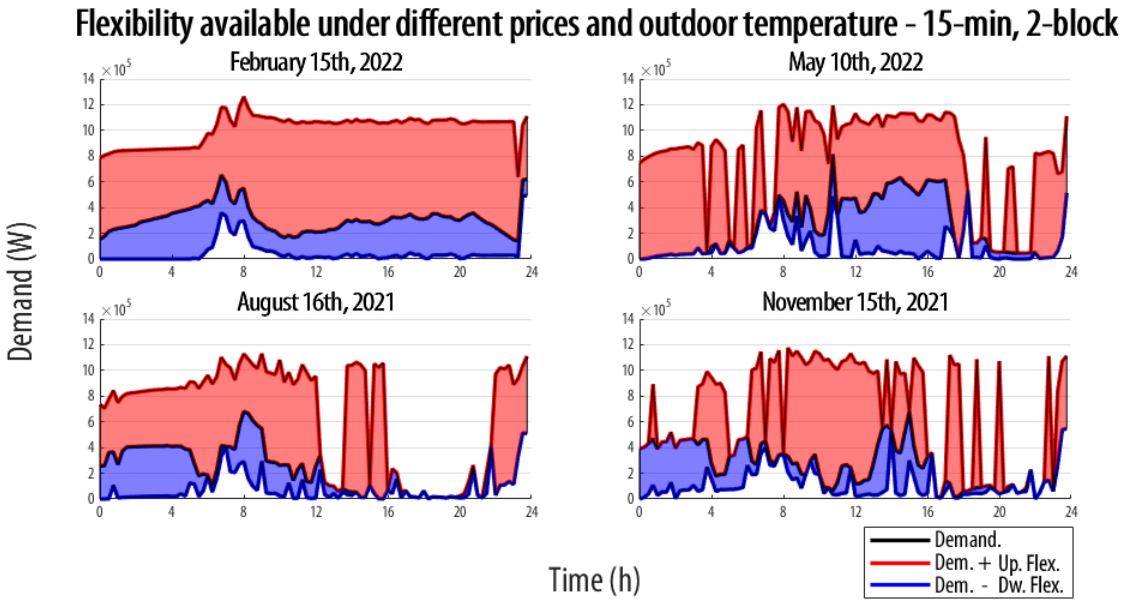

Figure 2.6: Flexibility estimation values for 30 minutes under a 15-minute time interval, considering temperature and price values for one day per season. Temperature values from May and November consider 50-percentile temp., February uses 10-percentile temp. and August, 90-percentile temp.

flexibility to the night and the first hours in the morning, while the upward flexibility price was 0 USD/MWh in the indicated time window. The scheduled demand consumption for May 10th and November 15th presents similar patterns to August demand, a considerable demand decrease in the peak hours and some hours in the day where there are no incentives to offer upward flexibility to the grid. An unexpected conclusion from the results is the lack of downward flexibility in peak hours; unless the day-ahead flexibility incentives surpass the benefits of not consuming energy in peak hours, the flexible appliances prefer to use their flexibility to decrease their total cost instead of offering it to the system.

As a deterministic model, modifying the objective function (expression 2.1a) to return the energy price if a downward flexibility offer is delivered will generate an artificial increase in energy consumption. The downward flexibility will not have a cost, so we can shift all the demand to the hours where the downward flexibility has high prices. To tackle this problem, a stochastic approach must be developed to incorporate the possibility of offering or not offering flexibility, depending on the potential energy prices and non-controllable demand, including the profitability and potential losses if the offered flexibility is inadequate.

2.3.5 Aggregated appliance response for a 4-block flexibility requirement

One of the principal advantages of the proposed model is its ability to consider flexibility requirements that can be extended over multiple time steps. In order to validate the extended flexibility response advantage, the flexibility estimated by the 4-block approach will be introduced as a flexibility requirement for the appliance scheduling proposed by the 1-block, 2-block, and 3-block flexibility approaches. The model assumes that the potential flexibility estimated by the 4-block problem is lower than that offered by the other approaches. However, considering a higher flexibility duration in their estimation is decisive to the energy flexibility provided by the appliances. The model will evaluate if the 1-block to 3-block cases can follow their initial scheduling and offer the same (and lower in power) flexibility as the 4-block case. To clarify, flexibility or response deviation will be considered as the flexibility requirements that the proposed appliance's scheduling can not fulfil.

Figure 2.7 and 2.8 compare the upward and downward flexibility response to the indicated 4-block flexibility requirement. The upward flexibility in figure 2.7 shows the flexibility reduction when the requirement duration increases, except for the flexibility at hour 10, which shows lower flexibility values for the 1-block case. The low energy price can explain the reduction in flexibility between hours 10 and 17 compared to the rest of the day, which increases the demand scheduled within the indicated time window. The mean price difference between the 10 to 17 hours and the rest of the day is over 40 USD/MWh, which is decisive in the appliance scheduling proposed in all cases.

The flexibility requirements are compared per block to evaluate if the observed deviations can be correlated to a specific time block. For the upward case, the flexibility estimated by the 1-block approach presents a difference of up to 60% at hour 10, influenced by the scheduled demand at 10:30 am. The demand scheduled by the 1-block approach surpasses the demand by the 4-block approach by 86%, while the demand peak at 10:45 am generates flexibility deviations at 10:45 (1-block), 10:30 (2-block), and 10:15 (3-block). Flexibility deviations between 12:00 to 16:00 were produced by the high variability in demand scheduled by the 1-block approach.

Flexibility deviations for the 2-block and 3-block approaches are reduced by the decreased demand variability, particularly for the 3-block approach. Flexibility deviations were observed at hour 10 and hour 14, which are associated with an increase in the scheduled demand. If the flexibility deviation obtained is compared with the 1-block deviation, the extended flexibility estimation demonstrates that including temporal dependence in flexibility reduces the demand variability and increases the response capacity to offer flexibility services.

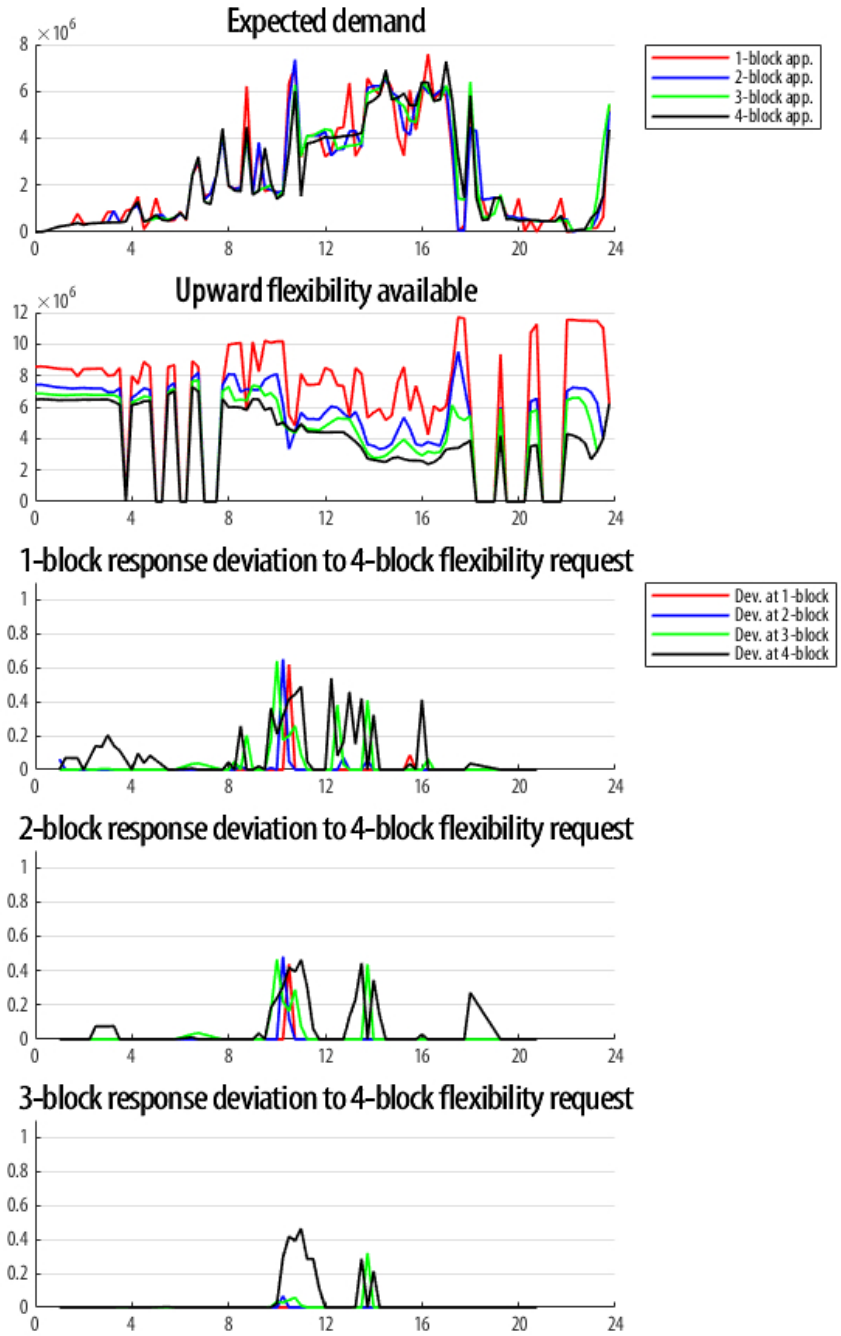

Figure 2.7: 4-block upward flexibility requirement for the 1, 2, and 3-block approach. The flexibility estimated by the 4-block approach is the lowest flexibility (in power) compared to the other methods, but the proposed scheduling allows for offering flexibility for a longer time. The response deviation indicates the percentage of the flexibility requests that the appliances cannot offer per block. The "Dev. at 1-block" line indicates the flexibility deviation in the first block considered in the flexibility requirement, intending to analyse each flexibility block independently of the others.

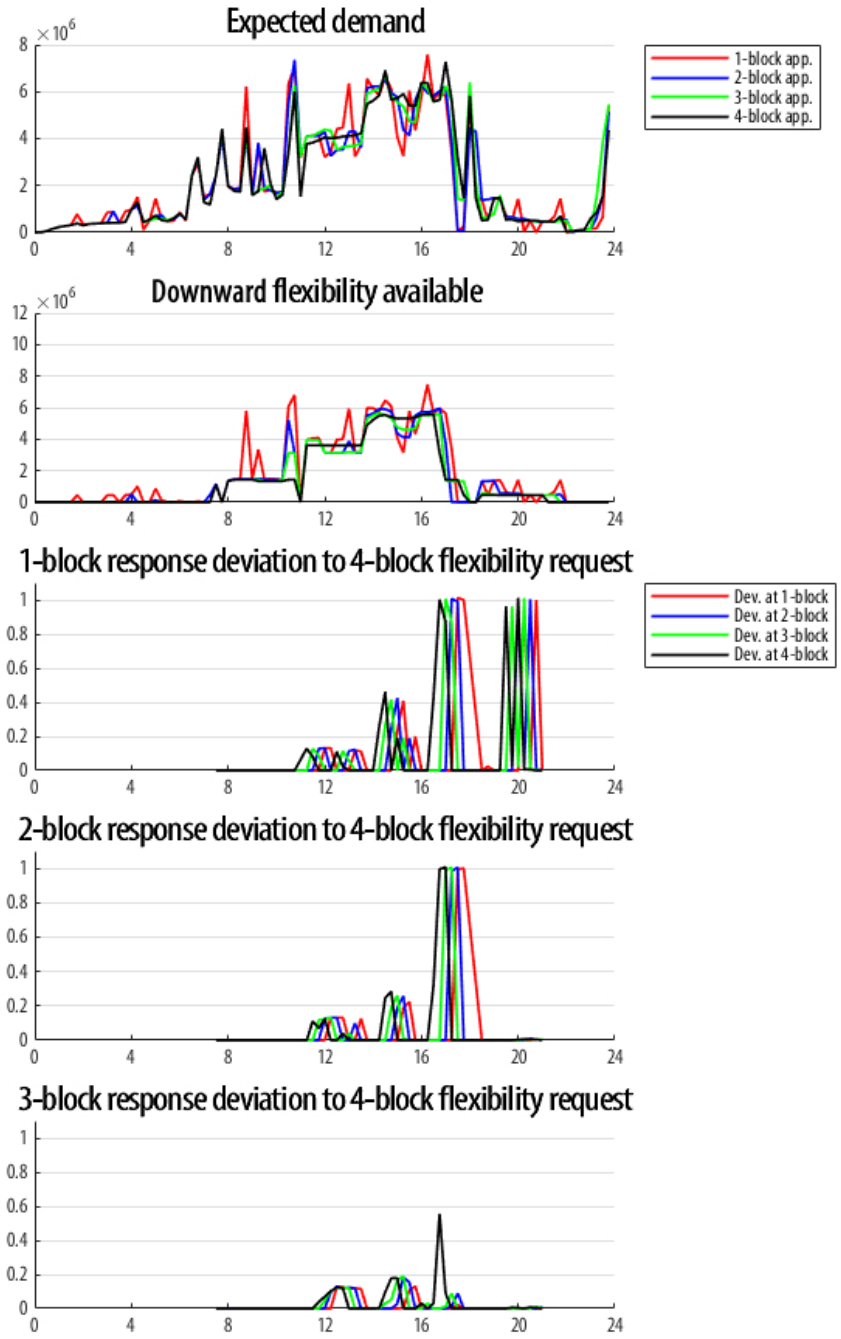

Figure 2.8: 4-block downward flexibility requirement for the 1, 2, and 3 block approach. The response deviation indicates the percentage of the flexibility request that the appliances cannot offer per block.

The downward flexibility case (figure 2.8) shows higher differences between the estimated flexibility per block approach and their final implementation, reaching a 100% flexibility deviation in some hours. For the 1-block case, the high variability in scheduled demand results in energy reductions from 6 MW to 0 MW between 17:00 and 18:00 hours (generated by an energy price increase), which decreases the appliance's response and denies possible flexibility services to the grid. A similar episode occurs between 19:00 and 21:00 hrs, where the demand differences in time diminish the appliance's response. The principal difference between upward and downward flexibility lies in the downward dependence on scheduled demand and energy costs. The proposed model can offer a demand schedule that diminishes or nullifies the possibility of providing flexibility in specific hours if the energy price drastically changes between two successive time-steps. Unless the flexibility prices are high enough to consume energy during low-cost hours, the proposed model will utilise its own flexibility to decrease its cost instead of offering flexibility to the grid.

To conclude, the extended flexibility estimation can ensure the energy offered in comparison with an instantaneous flexibility offer for multiple time-steps, utilising fast flexibility appliances to provide an aggregated and longer-term flexibility response. A negative effect of the proposed approach is the variability reduction on the scheduled demand, which limits its ability to capture price differences if the flexibility price is high enough to generate this effect.

2.4 Conclusions

A flexibility estimation model is proposed to evaluate the aggregated flexibility response from a set of appliances. The proposed model quantifies the appliance's flexibility based on the frequency reserve requirements. The model offers an aggregated response for a defined flexibility duration, which can range from 15 minutes to 4 hours, depending on the time interval and flexibility service duration used to estimate appliance scheduling and flexibility. New flexibility constraints were introduced to evaluate the flexibility and rebound effect of air conditioners, pool pumps, and electric water heaters. The flexibility is estimated based on the maximisation of the minimum flexibility offered by the appliances, using a unique variable for the flexibility estimation in the subsequent n time blocks.

The presented approach was designed to facilitate the flexibility estimation for frequency reserves in accordance with ISO requirements for each country. The model can adapt its operation to the flexibility requirement duration per market or country. As an example, CAISO secondary and tertiary response has a 30 minutes duration (the activation time changes between secondary and tertiary) Colbert (2016), the RTE (*Réseau de Transport d'Électricité*) considers the replacement reserve volume and the manual frequency restoration service with a 90 minutes and 120 minutes duration Le réseau de transport d'électricité (2022). In comparison, the non-spinning reserve in ERCOT requires 30 minutes of interrupted demand

or the capability to sustain demand for 1 hour ERCOT (2021). The CAISO and ERCOT flexibility requests can be accommodated by the 15-minute approach with 2-block and 4-block flexibility durations, while the RTE request can be covered by the 30-minute approach with 3-block and 4-block flexibility durations. A particular case to consider is when the dispatch time interval is lower than 15 minutes. Assuming a 30 minutes flexibility request and a 5-minute dispatch interval, this requirement can be tackle using one of the following two options: use a 15-min approach with a 3-block flexibility duration to cover any possible flexibility requirement or reduce the time interval in the model to a 5-min approach and limits the problem to a 6-hour time horizon instead of 24 hours to do not increase the model's computational complexity. The proposed model can be adapted to offer day-ahead flexibility regardless of the ISO requirements.

The flexibility model was tested under different energy price schemes and scenarios to observe how the flexibility offered changes over time. The appliances depend directly on energy prices to offer downward flexibility. Suppose the energy prices are low; the demand and downward flexibility increase, while the lack of demand increases the upward flexibility. In contrast, the lack of downward flexibility in the hours with high energy costs is counterproductive to the high downward flexibility prices. Unless the flexibility prices can afford the high energy costs, there will be no flexibility to offer, because the model prefers to use its flexibility to reduce operational costs.

The extended flexibility requirement approach was tested considering a flexibility request equal to the values estimated by a 4-block approach. Even if the estimated potential flexibility was lower than in the other cases, the 1-block to 3-block approach could not fulfil the flexibility requirement without showing deviations from the expected demand. If the evaluated flexibility approach considers an extended duration, the observed flexibility deviations will be reduced, and the scheduled demand will exhibit lower variability than in the 1-block case.

Future work includes an extensive formulation of a Virtual Power Plant for flexible appliances, to coordinate local flexibility with renewable generation and non-controllable demand under a stochastic approach. The aim will be to simultaneously offer flexibility services to the grid and mitigate variability in demand and generation. Second, develop a heuristic to determine the number of blocks to consider in the flexibility formulation according to the scheduled demand, energy prices, and historical flexibility duration requirements. Finally, the inclusion of new appliances such as electric vehicles and a new economic approach to quantify the direct benefits offered by the flexibility. The new approach assumes a competitive flexibility market where the agents offer multiple bids for a flexibility requirement or the quantification of the minimal flexibility bid based on the cost of providing flexibility to the power system.

Chapter 3

Solar and Temperature Scenario Generator Based on Cloud Conditions, Markov Models and LSTM Networks

3.1 Introduction

Forecasting and scenario generation of solar irradiance and temperature play a crucial role in energy management, as they are actively required for the operation of solar farms, thermal appliances, peak demand reduction, and congestion in transmission. An inaccurate forecast could schedule operational points for Distributed Energy Resources (DER) that cannot be reached, forcing the energy demand to unfeasible cases that could increase operational costs or surpass the transmission capabilities of the electrical grid. In the literature, multiple approaches to weather forecasting exist, depending on the available data and computational capacity.

Traditional statistical approaches in solar and temperature forecasting have been used for decades, where models from the auto-regressive integrated moving average (ARIMA) and seasonal ARIMA (SARIMA) have been employed for daily temperature Murat, Malinowska, Gos, and Krzyszczak (2018); Ozbek, Sekertekin, Bilgili, and Arslan (2021), solar radiation Chodakowska et al. (2023); Shadab, Ahmad, and Said (2020) and generation Vagropoulos, Chouliaras, Kardakos, Simoglou, and Bakirtzis (2016). Other approaches explore the copula probability model Jiao and Emura (2022); Lazoglou and Anagnostopoulou (2019); Sun, Feng, and Zhang (2020), unsupervised clustering techniques for short-term solar irradiation Feng et al. (2018); Sanhudo, Rodrigues, and Ênio Vasconcelos Filho (2021), and hidden Markov models (HMM) for solar generation scenarios Zargar and Yaghmaee Moghaddam (2020), plus considering cosine similarity Ghasvarian Jahromi, Gharavian, and Mahdiani (2020).

Data-driven approaches derived from artificial neural networks (ANN), such as long short-term memory (LSTM) and convolutional neural networks (CNN), have increased their use in forecasting. LSTM models are used for short-time solar forecasting, where a modified ensemble empirical mode decomposition integrated with a CNN-LSTM network is proposed in Gao, Huang, Shi, Tai, and Zhang (2020). A similar approach is explored in Zang et al. (2020), which suggested a hybrid CNN-LSTM approach where the LSTM network learns the spatial correlation using historical data and the CNN is trained to identify temporal correlation. The inclusion of cloud conditions was previously explored using ground cameras for short-term forecast with LSTM models Zuo, Qiu, Jia, Wang, and Li (2022) and incorporating satellite data to utilise cloud type indicators as an input Yu, Cao, and Zhu (2019). For temperature forecasting, the use of CNN and LSTM models was compared with seasonal auto-regressive integrated moving average approaches Kreuzer, Munz, and Schlüter (2020), and hybrid models between adaptive neuro-fuzzy inference system and LSTM structures Sekertekin et al. (2021) were proposed. Hybrid approaches mixed ARIMA and ANN models to forecast solar irradiation Belmahdi, Louzazni, and Bouardi (2020) or Support Vector Machines (SVM) for solar irradiance Boualit and Mellit (2016) and generation Bouzerdoum, Mellit, and Massi Pavan (2013). For temperature forecast, hybrid SARIMA-LSTM models for air temperature Kumar Dubey, Kumar, García-Díaz, Kumar Sharma, and Kanhaiya (2021); G. Li and Yang (2023) have been under evaluation.

Satellite-based models utilise data from geostationary and polar-orbiting satellites to offer wide spatial coverage and high spatial resolution. The use of numerical weather prediction (NWP) data, satellite images, and radiative transfer calculations can be employed to propose short-term solar irradiance forecasting Miller, Rogers, Haynes, Sengupta, and Heidinger (2018), where cloud properties and their future movement impact the variability of solar generation. Other approaches utilise satellite images combined with convolutional-LSTM models to forecast cloud movement and XGBoost to predict solar irradiance, considering the influence of clouds in the forecast Si, Yang, Yu, and Ding (2021). Alternatively, neighbouring satellite pixels are used for spatial ensemble forecasting using an ANN with Monte Carlo sampling Yagli, Yang, and Srinivasan (2022). For temperature forecasting, Numerical Weather Prediction (NWP) models such as the Global Forecast System (GFS) Center (2003) and the Weather Research and Forecasting (WRF) model Skamarock et al. (2021), solve complex mathematical equations to simulate atmospheric processes for weather forecasting.

The basis of this publication is to explore the relevance of cloud conditions in solar irradiance, as observed in satellite-based models, and the correlation between solar irradiation and air temperature. So, this paper introduces a solar and temperature scenario generator based on the cloud type indicator, determined from satellite images and software developed under the Pathfinder Atmospheres Extended (PATMOS-x) project Heidinger, Foster, Walther, and Zhao (2014). The cloud type is used as a cloud state for an HMM model to determine cloud condition

Table 3.1: Cloud type states defined by the CLAVR-x model.

0 - Clear sky	4 - Supercooled water	8 - Overlapping
1 - Probably Clear Sky	5 - Mixed	9 - Overshooting
2 - Fog	6 - Opaque Ice	
3 - Water	7 - Cirrus clouds	

and the transition matrix. In addition, LSTM models are trained to capture the shapes of solar and temperature data using the cloud state as input for the forecast, generating a set of eight scenarios based on the cloud conditions. To evaluate the proposed weather scenarios, a simple stochastic virtual power plant (VPP) has been used to compare the operational cost of flexible appliances such as electric vehicles (EV), air conditioners (HVAC), electric water heaters (EWH), pool pumps (PP) and photovoltaic (PV) generation plants. The VPP proposes energy bids in the day-ahead (DA) market, allowing it to buy and sell energy in the real-time (RT) market if required. The main contributions of the proposed work are:

- A monthly trained transition matrix to capture seasonal weather variations in the cloud type.
- LSTM-trained models to forecast solar irradiance and air temperature using satellite cloud type indicators.
- Evaluation of the scenarios generated under a stochastic VPP, using weather and pricing stochastic scenarios and a naive forecast

3.2 Weather Scenario Generation Methodology

The modelling procedure and the approaches to generate the weather scenarios are presented below.

3.2.1 Cloud type and solar irradiance

Different cloud types exhibit variations in their optical and physical properties, which affect the absorption, reflection, and transmission of solar irradiance. The Clouds from AVHRR Extended System, also known as CLAVR-x, is a processing system developed by the Cooperative Institute for Meteorological Satellite Studies (CIMSS) from the University of Wisconsin-Madison, which generates quantitative cloud products from satellite images. It is capable of classifying cloud conditions with a resolution of 1km. A list of the cloud-type states is presented in Table 3.1.

Cloud conditions directly influence solar radiation and air temperature throughout the day. The presence of clouds implies a decrease in solar irradiance compared to clear-sky conditions, while the cloud's influence on temperature depends on its insulating role of trapping Earth's long-wave radiation emitted into space, which diminishes the temperature drop over time. The relationship between the solar irradiance and the cloud type is presented in the figure 3.1 for the San Diego International Airport, California.

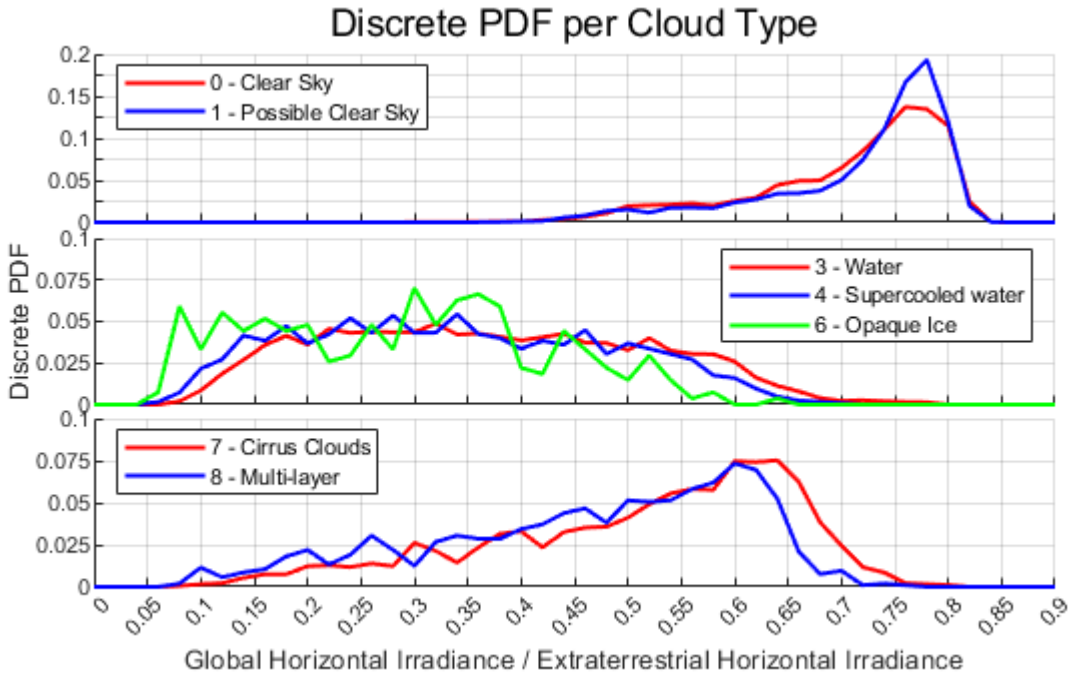

Figure 3.1: Discrete probability distribution function per each cloud type state defined by CLAVR-x at San Diego International Airport, California. The cloud types were separated according to the Euclidean distance.

The cloud type and its discrete probability density function (PDF) in relation to global horizontal irradiance (GHI) and extraterrestrial irradiance (known as the clearness index K_t) offer a distinct approach to distinguishing between clear-sky and cloudy days. The standard approach to separating cloudy and clear-sky conditions is to choose an arbitrary K_t value to differentiate between cloud conditions Yu et al. (2019). Using a cloud state indicator allows different possible K_t values under specific conditions (a thin cloud layer or one-hour cloudy conditions in a clear sky day).

3.2.2 Hidden markov models and cloud conditions

The definition of cloud states based on the AVHRR cloud type provides the opportunity to use HMM as a probabilistic approach to manage cloud conditions. For solar forecasting, the clearness index can be considered as the observation; the cloud types are the model states, the transition matrix describes the state transitions and the discrete PDFs are the output probabilities (figure 3.1).

Cloud states representing less than 0.5% of the total observations were removed to decrease the number of possible scenarios. Figure 3.1 shows the considered cloud states.

The day was divided into five-time windows with specific rules to build a scenario. This division was proposed to reduce the number of combinations and to allocate a probability to each scenario. The developed scenarios are built according to the rules expressed in table 3.2. The states were aggregated into Clear sky conditions (states 0 and 1) and cloudy conditions (states 3,4,6,7,8).

Table 3.2: Definition of the cloud conditions per scenario, based on their capacity to change from clear sky to cloudy only once per time window.

1-Midnight to Sunrise	2-Sunrise to Midday	3-Midday	4-Midday to Sunset	5-Sunset to Midnight
One random transition in time between the midnight index and the sunrise index	Clear sky	Clear sky	Clear sky	The cloud type evolves following the night transition matrix
	Clear sky	Clear sky	Cloudy	
	Clear sky	Cloudy	Clear sky	
	Clear sky	Cloudy	Cloudy	
	Cloudy	Clear sky	Clear sky	
	Cloudy	Clear sky	Cloudy	
	Cloudy	Cloudy	Clear sky	
	Cloudy	Cloudy	Cloudy	

Two different transition matrices were estimated to differentiate cloud transitions during day (time windows 2, 3, and 4) and night (time windows 1 and 5). Between the time windows 1 to 4, only one transition between clear sky and cloudy conditions is allowed. If the state is cloudy, it could be any possible cloudy state, according to the transition matrix, after removing the clear sky conditions.

Each one of the possible scenarios presented in the table 3.2 is associated with a transition probability, which is usually calculated using the Chapman-Kolmogorov equation to evaluate the probability of passing from state i to j at each time interval. However, in this specific case, there is only one transition allowed per time window, forcing the calculation of only the possible combinations and normalising the probabilities to 1.

ML model 1 - Solar irradiance	
Input	- Extraterrestrial horizontal irradiance (next 24 hours). - Cloud type (next 24 hours). - Numerous meteorological variables (1 hour - last measurement).
Output	- Global horizontal irradiance (next 24 hours)

ML model 2 - Temperature	
Input	- Global horizontal irradiance (next 24 hours). - Cloud type (next 24 hours). - Temperature (1 hour - last measurement). - Numerous meteorological variables (1 hour - last measurement).
Output	- Temperature (next 24 hours)

Figure 3.2: LSTM input and output parameters

3.2.3 Long Short-Term Memory

The forecast model utilises the Long Short-Term Memory architecture to train and forecast solar irradiance and temperature using the cloud conditions as model input, replacing the discrete PDF to forecast solar irradiance and temperature. This specific variant of Recurrent Neural Network (RNN) was selected because its gated cell structure (comprising input, forget, and output gates) effectively addresses the vanishing gradient problem, capturing the non-linear, long-term temporal dependencies of weather patterns over the forecast period, which traditional autoregressive models or standard RNNs struggle to maintain. There are no changes in the LSTM structure using the same cell reported in Hochreiter and Schmidhuber (1997). In contrast to the usual LSTM and Bidirectional LSTM formulations, there is no use of the look-back irradiance and temperature (data from the last hours or last day) in the network's input. The cloud type is introduced as a binary indicator using a one-hot encoder, where only one value equals 1. Furthermore, this differentiation in training was implemented to encourage the network to catch the influence of the cloud type in the variables to forecast, instead of replicating the previous day's behaviour

The input data was normalised under the min-max approach to improve the network training convergence. The chosen time interval is one hour. The models were trained using temperature and solar irradiance data between 2017 and 2019. The training data covers two time windows: January 2017 - October 2018 and January - April 2019. The validation data are separated into two blocks: November-December 2018 and May-June 2019, encompassing both winter and summer weather conditions during the validation. The testing data starts in July 2019 and finishes in December 2019.

3.2.4 Weather scenario generation

This section builds upon the basic HMM approach introduced in Section 3.2.2, with specific rules and limitations for calculating cloud condition scenarios per day, which are elaborated below. The scenario generation can be separated into four stages:

1. Estimation of the transition matrix and scenario probability.
2. Training and testing of LSTM models (as described in Section 3.2.3).
3. Generation of specific cloud scenarios with the estimated transition matrix.
4. Generation of solar and temperature scenarios based on cloud scenarios.

The transition matrix was estimated for the month under evaluation, using cloud type data from 2013 to 2020, allowing the model to capture seasonal weather behaviour throughout the year. The training stage of the LSTM and BiLSTM models follows the indications from the section 3.2.3. In Figure 3.2, the data input and expected output of the LSTM models are introduced. The term 'numerous meteorological variables' includes pressure, wind speed and relative humidity. The generation of the cloud scenarios follows the rules indicated in Table 3.2. The probabilities of the eight possible scenarios were calculated as indicated in section 3.2.2, allowing only one transition per time window. Finally, solar and temperature scenarios were created based on the eight cloud scenarios, where the cloud types served as input to the LSTM model. This approach yields eight solar and temperature scenarios corresponding to each cloud condition.

3.3 Test environment

3.3.1 Stochastic virtual power plant formulation

A basic stochastic Virtual Power Plant model has been developed to compare DAM energy buying decisions between the proposed weather scenario generator and naive forecasts in weather and pricing values.

The model presented in expression 3.1 estimate the energy bids in the DAM using forecasted energy prices, temperature and solar irradiance as uncertainty parameters (as the generated weather scenarios). The operational cost of the VPP will be determined as the objective function under perfect information case (real price and weather conditions) with the proposed energy buy/sell from the stochastic case.

VPP formulation [eq. 3.1]:

$$\min \sum_{w}\sum_{dam}\sum_{t}\left[\pi^{w}\pi^{dam}\lambda_{t}^{dam}\left(E_{t}^{dam,buy}-E_{t}^{dam,sell}\right)\right] \tag{3.1a}$$
$$+\sum_{w}\sum_{rtm}\sum_{t}\left[\pi^{w}\pi^{rtm}\lambda_{t}^{rtm}\left(E_{w,rtm,t}^{rtm,buy}-E_{w,rtm,t}^{rtm,sell}\right)\right]$$

$$\text{s.t.} \quad \sum_{pp} P^{pp}_{w,rtm,t} + \sum_{ev} \left(P^{ev,ch}_{w,rtm,t} + P^{ev}_{max} * eP^{ev}_{w,rtm,t} \right) \tag{3.1b}$$
$$\sum_{hvac} \left(P^{hvac,heat}_{w,rtm,t} + P^{hvac,cool}_{w,rtm,t} \right)$$
$$+ \sum_{ewh} \left(P^{ewh}_{w,rtm,t} + P^{ewh}_{max} * eP^{ewh}_{w,rtm,t} \right)$$
$$= \sum_{ev} P^{ev,dch}_{w,rtm,t} + \sum_{pv} E^{pv}_{w,t} + E^{dam,buy}_{t} - E^{dam,sell}_{t}$$
$$+ E^{rtm,buy}_{w,rtm,t} - E^{rtm,sell}_{w,rtm,t} \qquad \forall t \in T, \forall w \in W, \forall rtm \in RTM$$
$$- P^{cont}_{max} \leq E^{dam,buy}_{t} - E^{dam,sell}_{t} + E^{rtm,buy}_{w,rtm,t} \tag{3.1c}$$
$$- E^{rtm,sell}_{w,rtm,t} \leq P^{cont}_{max} \qquad \forall t \in T, \forall w \in W, \forall rtm \in RTM$$
$$\sum_{t} \left[\sum_{pp} P^{pp}_{w,rtm,t} + \sum_{ev} \left(P^{ev,ch}_{w,rtm,t} + P^{ev}_{max} * eP^{ev}_{w,rtm,t} \right) \right. \tag{3.1d}$$
$$\sum_{hvac} \left(P^{hvac,heat}_{w,rtm,t} + P^{hvac,cool}_{w,rtm,t} \right)$$
$$\left. + \sum_{ewh} \left(P^{ewh}_{w,rtm,t} + P^{ewh}_{max} * eP^{ewh}_{w,rtm,t} \right) \right] \geq \sum_{t} \left[E^{dam,buy}_{t} + E^{rtm,buy}_{w,rtm,t} \right]$$
$$\forall w \in W, \forall rtm \in RTM$$

The expression 3.1a introduces the objective function to minimise the energy buy-sell in DAM and RTM markets based on weather scenarios (and their probabilities). Expression 3.1b is the energy balance per hour. On the left side, demand sources (such as electric vehicles and air conditioners) are shown, while on the right side, energy sources (including EV discharge, solar panels, and energy from markets) are displayed.

The introduction of expressions 3.1c and 3.1d comes from the necessity to limit the buying capacity of the model if there is a relevant difference between the DAM and RTM energy pricing. Expression 1c limits energy trading according to the maximum energy transmission per customer ($P^{max}_{cont} = \sum_{prosumers} P^{max}_{prosumer}$). Expression 1d limits the maximum energy bought per day/scenario to the energy required by the appliances plus expected solar generation. The inclusion of solar plants arises from possible cases where the expected energy injected into the grid exceeds the expected demand.

3.3.2 Flexible appliances

The flexible appliances used in the stochastic VPP will be briefly explained, properly cited, and the differences from the cited publication will be explained. The mathematical expressions will be included in the model formulation, but please look at the citations for a detailed explanation.

Electric vehicles

EV appliances are included due to their high energy requirements and government policies aimed at increasing their usage. The EV model presented in expression 3.2 introduces charge, discharge, expected usage and EV availability for charging purposes.

Electric vehicle constraints [eq. 3.2]:

$$SoE^{ev}_{w,rtm,t} = SoE^{ev}_{w,rtm,t-1} + \eta^{ev} * (P^{ev,ch}_{w,rtm,t} + P^{ev}_{max} * eP^{ev}_{w,rtm,t}) - \frac{P^{ev,dch}_{w,rtm,t}}{\eta^{ev}} - (1 - Av^{ev}_{t}) * Dch^{ev}_{usage} \quad \forall t \in T, \forall w \in W, \forall rtm \in RTM \tag{3.2a}$$

$$SoE^{ev}_{min} * (1 - eP^{ev}_{w,rtm,t}) \leq SoE^{ev}_{w,rtm,t} \leq SoE^{ev}_{max} \quad \forall t \in T, \forall w \in W, \forall rtm \in RTM \tag{3.2b}$$

$$0 \leq P^{ev,ch}_{w,rtm,t} + P^{ev}_{max} * eP^{ev}_{w,rtm,t} \leq P^{ev}_{max} * Av^{ev}_{t} * \alpha^{ev}_{w,rtm,t} \quad \forall t \in T, \forall w \in W, \forall rtm \in RTM \tag{3.2c}$$

$$0 \leq P^{ev,dch}_{w,rtm,t} \leq P^{ev}_{max} * Av^{ev}_{t} * (1 - \alpha^{ev}_{w,rtm,t}) \quad \forall t \in T, \forall w \in W, \forall rtm \in RTM \tag{3.2d}$$

$$SoE^{ev,out}_{w,rtm,t} \leq SoE^{ev}_{w,rtm,t} + (t^{ev}_{out} - t) * \eta^{ev} * P^{ev}_{max} \quad if\, t^{ev}_{out} \geq t, \forall t^{ev}_{out} \in T^{ev}_{out}, \forall w \in W, \forall rtm \in RTM \tag{3.2e}$$

$$SoE^{ev}_{w,rtm,t=23} \geq 0.9 * SoE^{ev}_{w,rtm,t=0} * Av^{ev}_{t=23} \quad \forall w \in W, \forall rtm \in RTM \tag{3.2f}$$

In expression 3.2a, $P^{ev}_{w,rtm,t}$ is an emergency charge variable, which in expression 3.2b allows the EV to have a SoE lower than the minimum, forcing the EV to charge at its maximum capacity. The binary variable $\alpha^{ev}_{w,rtm,t}$ defines the charge and discharge process for the EV (as 1 and 0, respectively). The parameter Av^{ev}_{t} is a 1-D array associated with EV availability to charge (1 - can be charged, O - EV not available) and to discharge, assuming everyday use. The EV availability has been explored under a Markov chain approach in Srilakshmi and Singh (2022). The expression 3.2e evaluates a projected charging process at the hour that the EV will leave the charging point. The expression 3.2f forces a similar SoE at the start and end of the time interval if the EV is available at the end of the day.

Heating-cooling models

An HVAC model has been implemented based on the ISO 13790 ISO 13790:2008(E) (2008) hourly thermal model, using a 5R1C (five resistances, one capacitance) lumped parameter network. This model is used due to the availability of real household parameters from the TABULA database. A linearised version of the hourly thermal model can be found in Schütz, Schiffer, Harb, Fuchs, and Müller (2017); Zarrella, Prataviera, Romano, Carnieletto, and Vivian (2020). In expression 3.3, the equations related to the air conditioning operational mode and their influence on the thermal model are included. The parameter η_{eff}^{hvac} is the efficiency of the air conditioning appliance to transform electrical energy into thermal energy. For a detailed description, refer to annexe C in the ISO document ISO 13790:2008(E) (2008) and Mazhar, Zou, Zeng, Shen, and Liu (2022).

HVAC model constraints [eq. 3.3]:

$$\Phi_{w,rtm,t}^{mtot,hvac} = \Phi_{w,t}^{m,hvac} + H_{tr,em}^{hvac} * \theta_{w,t}^{e,hvac} + \frac{H_{tr,3}^{hvac}}{H_{tr,2}^{hvac}} \left\{ \Phi_{w,t}^{st,hvac} + H_{tr,w}^{hvac} * \theta_{w,t}^{e,hvac} + H_{tr,1}^{hvac} * \theta_{w,t}^{sup,hvac} + \frac{H_{tr,1}^{hvac}}{H_{ve}^{hvac}} \left(\Phi_{w,t}^{ia,hvac} + \eta_{eff}^{hvac} * \left[P_{w,rtm,t}^{hvac,heat} + P_{w,rtm,t}^{hvac,cool} \right] \right) \right\} \quad \forall t \in T, \forall w \in W, \forall rtm \in RTM \tag{3.3a}$$

$$\theta_{w,rtm,t}^{mt,hvac} = \frac{\theta_{w,rtm,t-1}^{m,hvac} \left[\frac{C_m^{hvac}}{3600} - 0.5(H_{tr,3}^{hvac} + H_{tr,em}^{hvac}) \right] + \Phi_{w,rtm,t}^{mtot,hvac}}{\frac{C_m^{hvac}}{3600} + 0.5(H_{tr,3}^{hvac} + H_{tr,em}^{hvac})} \quad \forall t \in T, \forall w \in W, \forall rtm \in RTM \tag{3.3b}$$

$$\theta_{w,rtm,t}^{m,hvac} = (\theta_{w,rtm,t}^{mt,hvac} + \theta_{w,rtm,t-1}^{mt,hvac})/2 \quad \forall t \in T, \forall w \in W, \forall rtm \in RTM \tag{3.3c}$$

$$\theta_{w,rtm,t}^{s,hvac} = \frac{H_{tr,ms}^{hvac} * \theta_{w,rtm,t}^{m,hvac} + \Phi_{w,t}^{st,hvac} + H_{tr,w}^{hvac} * \theta_{w,t}^{e,hvac}}{H_{tr,ms}^{hvac} + H_{tr,w}^{hvac} + H_{tr,1}^{hvac}} + \frac{H_{tr,1}^{hvac} * \theta_{w,t}^{sup,hvac} + \frac{H_{tr,1}^{hvac}}{H_{ve}^{hvac}} * \Phi_{w,t}^{ia,hvac}}{H_{tr,ms}^{hvac} + H_{tr,w}^{hvac} + H_{tr,1}^{hvac}} + \frac{\frac{H_{tr,1}^{hvac}}{H_{ve}^{hvac}} * \left(\eta_{eff}^{hvac} * \left[P_{w,rtm,t}^{hvac,heat} + P_{w,rtm,t}^{hvac,cool} \right] \right)}{H_{tr,ms}^{hvac} + H_{tr,w}^{hvac} + H_{tr,1}^{hvac}} \quad \forall t \in T, \forall w \in W, \forall rtm \in RTM \tag{3.3d}$$

$$\theta_{w,rtm,t}^{air,hvac} = \frac{H_{tr,is}^{hvac} * \theta_{w,rtm,t}^{s,hvac} + H_{ve}^{hvac} * \theta_{w,t}^{sup,hvac} + \Phi_{w,t}^{ia,hvac}}{H_{tr,is}^{hvac} + H_{ve}^{hvac}} + \frac{\eta_{eff}^{hvac} * \left[P_{w,rtm,t}^{hvac,heat} + P_{w,rtm,t}^{hvac,cool} \right]}{H_{tr,is}^{hvac} + H_{ve}^{hvac}} \quad \forall t \in T, \forall w \in W, \forall rtm \in RTM \tag{3.3e}$$

$$\theta_{min}^{hvac} \leq \theta_{w,rtm,t}^{air,hvac} \leq \theta_{max}^{hvac} \tag{3.3f}$$

$$\forall t \in T, \forall w \in W, \forall rtm \in RTM$$

$$0 \leq P^{hvac,heat}_{w,rtm,t} + P^{hvac,cool}_{w,rtm,t} \leq P^{hvac}_{max} \quad \forall t \in T, \forall w \in W, \forall rtm \in RTM \tag{3.3g}$$

Electric water heater

The electric water heater (EWH) model is included to reflect the increasing electrification of home appliances. The EWH model presented here builds upon the one-node approach Nel, Booysen, and van der Merwe (2018), which assumes homogeneous water temperatures within the tank. A more complex approach involving two or more nodes can be found in Mukherjee et al. (2022).

The expected operation of the electric water heater is described by expression 3.4. The evolution of water temperature over time, water usage, and additional heat required is captured in equation 3.4a. In this model, the decision variable $eP^{ewh}_{w,rtm,t}$ ensures emergency heating operations are triggered if the water temperature falls below the minimum allowed temperature, effectively removing the constraint on expression 3.4b. The parameters WU_t and T^{input}_{water} represent expected hourly water usage and input water temperatures, respectively.

EWH model constraints [eq. 3.4]:

$$T^{ewh}_{w,rtm,t} = T^{ewh}_{t-1,rtm,t} * \frac{V_{tank} - Wuse_t}{V_{tank}} + T^{input}_{water} * \frac{Wuse_t}{V_{tank}} + \frac{P^{ewh}_{w,rtm,t} + P^{ewh}_{max} * eP_{w,rtm,t} - W_{tank} * (T^{ewh}_{t-1,rtm,t} - T^{ewh}_{room})}{V_{tank} * \rho_{water} * \frac{Cp_{water}}{3600}} \quad if\, t \neq 0, \forall w \in W, \forall rtm \in RTM \tag{3.4a}$$

$$T^{ewh}_{min} - bigM * eP^{ewh}_{w,rtm,t} \leq T^{ewh}_{w,rtm,t} \leq T^{ewh}_{max} \quad \forall t \in T \quad \forall t \in T, \forall w \in W, \forall rtm \in RTM \tag{3.4b}$$

$$0 \leq P^{ewh}_{w,rtm,t} + P^{ewh}_{max} * eP^{ewh}_{w,rtm,t} \leq P^{ewh}_{max} \quad \forall t \in T \quad \forall t \in T, \forall w \in W, \forall rtm \in RTM \tag{3.4c}$$

(3.4d)

Pool pumps

The pool pump is modelled as a deferrable appliance which can be stopped or shifted without penalty to its operation. The basic pump operation is described by the expression 3.5. The expression 3.5a encourage the pool pump to provide the required energy for its expected operation, where $E^{pp} = P^{pp}_{max} * operation hours\, per day$ is the energy required per day for the pool pump's regular operation. Assuming the pool pump aims to operate for a defined number of hours daily.

$$\sum_t P^{pp}_{w,rtm,t} = E^{pp} \quad \forall t \in T, \forall w \in W, \forall rtm \in RTM \tag{3.5a}$$

$$0 \leq P^{pp}_{w,rtm,t} \leq P^{pp}_{max} \quad \forall t \in T, \forall w \in W, \forall rtm \in RTM \tag{3.5b}$$

$$P^{pp}_{w,rtm,t} = 0 \quad if\ t \notin [T_{start}, T_{end}], \forall w \in W, \forall rtm \in RTM \tag{3.5c}$$

PV panels

There are no constraints related to the PV operation in the model. The curtailability of the solar panels was not taken into consideration. The expected PV generation was calculated based on the forecasted solar irradiance, outdoor temperature, PV cell properties, and zenith and azimuth angles. The PVlib library was used to calculate hourly solar of direct horizontal irradiance (DHI) and diffuse normal irradiance (DNI) using the Boland approximation Boland, Scott, and Luther (2001) to estimate the irradiance in the plane of array (PoA) of the solar panels.

$$\theta^{cell,PV}_{w,t} = \theta^{e}_{w,t} + \left[\frac{NOCT - 20}{800}\right] * G^{PoA}_{w,t} \tag{3.6a}$$

$$\eta^{elec,PV}_{w,t} = \eta^{ref,pv}\left(1 - N^{T,pv}(\theta^{cell,PV}_{w,t} - \theta^{ref})\right) \tag{3.6b}$$

$$E^{pv}_{w,t} = n^{pv} * A^{pv} * G^{PoA}_{w,t} * \eta^{elec,PV}_{w,t} \tag{3.6c}$$

3.3.3 Pricing scenarios

The scenarios for DAM and RTM prices have been considered independent of the weather scenario generator. Temperature and solar irradiance can influence the energy prices, as seen in Luoma, Mathiesen, and Kleissl (2014), which evaluates the effect of solar forecasting value in DAM pricing at 63 sites in California. However, we assume that the weather conditions at a specific location have minimal impact on regional energy prices.

The DAM and RTM price values have been formatted with averages as hourly data. The Deep-VAR model Salinas, Bohlke-Schneider, Callot, Medico, and Gasthaus (2019); Salinas, Flunkert, Gasthaus, and Januschowski (2020) was trained using price data from 2017 to 2019, utilising PyTorch Forecasting libraries. The multivariate Gaussian copula process allows the forecast to be run multiple times to estimate the percentiles used as pricing scenarios. A total of 100 iterations were run to calculate five levels of percentile: 10th, 25th, 50th, 75th, and 90th percentiles. The probability of each scenario is [0.175, 0.2, 0.25, 0.2, 0.175], respectively.

3.3.4 Basic VPP test

To validate the weather scenarios proposed by the DAM scenario generator, it is proposed to calculate the operational cost of a basic stochastic virtual power plant model, as presented in expression 3.1. We will assume that the following conditions hold:

1. Estimation of the eight temperature and irradiance scenarios for the next 24 hours.
2. Calculate parameters that do not depend on the decision variables in the model
3. Optimise the objective function in 3.1a, subject to constraints from expressions [3.1, 3.2, 3.3, 3.4, 3.5], according to the weather and pricing scenarios.
4. Extract the DAM energy bought/sold by the stochastic model.
5. Rerun the optimisation model using perfect pricing and weather information, adding the DAM energy values from the stochastic model as a constraint to calculate the operational cost of the DAM energy decision.

The comparison of the objective function from the forecasted case to the perfect information run evaluates a differentiated observation of the uncertainty sources. The weather and pricing scenarios are considered independent sources of uncertainty. The weather and pricing scenarios used as input information for the optimisation model indicated in step 3 is:

- Stochastic pricing and weather scenarios (case stoP-stoW).
- Stochastic pricing scenario and naive weather (case naiveP-naiveW).
- Naive pricing and stochastic weather scenario (case naiveP-stoW).
- Naive pricing and weather scenario (case stoP-naiveW).

The scenario used a code name depending on whether a stochastic or naive scenario was used, plus the first letter of 'weather' and 'pricing'. For example, the optimisation using stochastic pricing and stochastic weather is called stoP-stoW, while naive pricing and stochastic weather are referred to as naiveP-stoW.

In the VPP model, each appliance will have 100 loads for comparison purposes. The four appliance cases are:

- 100 HVAC appliances
- 100 PV appliances
- 100 HVAC, PV, EV, EWH and PP appliances. The EV will not be able to discharge the battery.
- 100 HVAC, PV, EV, EWH and PP appliances.

Each case will be evaluated for a period of 36 days. The selected days are from the 17th to the 25th of each month. The evaluated months are March, June, September and December, including all the year's solstices and equinoxes.

3.3.5 Appliance properties and data sources

The house properties for the HVAC model are extracted from the TABULA and EPISCOPE projects database Loga et al. (2016); *Website of the TABULA and EPISCOPE projects, section Publications/Download* (n.d.), following the ISO 13790 ISO 13790:2008(E) (2008) to process their information and calculate input values. The houses from Spain, Italy, and France were used because of their similarities to households in the southwestern part of the USA. Each EWH used has a 120L tank and a maximum power consumption of 2200W. The hot water consumption profiles were generated with the software *Load Profile Generator* Pflugradt (2016). The Pool Pumps were randomised from a set of 46 commercial pool pump models, assuming that the pool pump needs to operate for the minimum required time to filter the water at least twice daily. The EV properties used are based on the 30 most viewed vehicles from *EV Database Electric Vehicle Database* (n.d.), with random selection for each appliance. PV panel properties come from the module JASolar JAM66S30 500/MR, with peak power randomised between 2 kW and 10 kW, orientation true south $\pm 15^{\circ}$. Angle is $32^{\circ} \pm 5^{\circ}$.

The development of the scenario generator requires specific data from different sources. The cloud type information and solar irradiance were obtained from the National Solar Radiation Database (NSRDB) Sengupta et al. (2018), location San Diego International Airport (KSAN), California (32° 43' 48", -117° 10' 48"). The cloud type and solar irradiance data from 2013 to 2020 were used for HMM, while data from 2017 to 2019 were employed to train LSTM models. Temperature data was obtained from NOAA National Weather Service for the exact location between 2017 and 2019. The case studies were developed in Python 3.9 van Rossum (1995) using additional libraries provided by Tensorflow Abadi et al. (2016). For optimisation, the DAM and RTM prices were downloaded from the CAISO OASIS platform *California Independent System Operator. Open access same time information system* (2022). The case studies were coded in Python using Pyomo libraries Hart et al. (2017, 2011). The Boland approximation and estimation of the plane of array (PoA) in the PV panels utilised the PVlib library Anderson et al. (2023). The solver GUROBI Gurobi Optimization, LLC (2024) with a 0.02 MIP GAP is chosen to solve the proposed problems, with a time limit of 3600 seconds if the GAP is not reached.

3.4 Results and Discussion

The stages presented in section 3.2.4 to generate the weather scenarios and their results are discussed below.

3.4.1 Transition matrix and probability per scenario

Table 3.3 shows the occurrence probability of each proposed scenario. The first column of the table corresponds to the observed cloud conditions at the moment to generate the forecast, while the cloud conditions in columns two, three and four are the expected cloud conditions in the respective time window.

Table 3.3: Scenario probabilities according to cloud conditions

Cloud start	Sunrise to Mid.	Midday	Midday to Sunset	March [%]	June [%]	Sept. [%]	Dec, [%]
Clear sky	Clear	Clear	Clear	16.29	21.28	48.95	19.36
	Clear	Clear	Cloudy	9.54	3.56	4.29	6.17
	Clear	Cloudy	Clear	9.88	23.34	9.24	2.95
	Clear	Cloudy	Cloudy	7.06	14.12	5.01	5.61
	Cloudy	Clear	Clear	17.62	10.38	15.82	26.70
	Cloudy	Clear	Cloudy	10.32	1.74	1.39	8.51
	Cloudy	Cloudy	Clear	17.07	15.93	9.93	10.60
	Cloudy	Cloudy	Cloudy	12.21	9.64	5.38	20.11
Cloudy	Clear	Clear	Clear	15.48	14.75	44.05	17.45
	Clear	Clear	Cloudy	9.07	2.47	3.86	5.56
	Clear	Cloudy	Clear	9.39	16.18	8.31	2.66
	Clear	Cloudy	Cloudy	6.71	9.79	4.50	5.05
	Cloudy	Clear	Clear	18.27	15.65	19.11	28.06
	Cloudy	Clear	Cloudy	10.71	2.62	1.68	8.94
	Cloudy	Cloudy	Clear	17.70	24.01	11.99	11.14
	Cloudy	Cloudy	Cloudy	12.66	14.53	6.50	21.13

As we explore the transition matrix, it becomes clear that the cloud conditions at midnight impact the probability of our predictions for the next few hours. There is a slight increase in the occurrence probability if the cloud condition at midnight coincides with the condition in the second interval. For example, the probability of having a clear-sky day in June changes from 14.75% to 21.28% if the cloud conditions at midnight were clear sky instead of cloudy.

The seasonal behaviour of the cloud conditions is reflected in the occurrence probabilities, where the probability of having a clear-sky day in September surpasses 40% under both cloudy and clear-sky conditions, while in December, there is a predominant position of cloudy conditions.

Table 3.4: LSTM indicator results and comparison.

Solar forecast							
Case	Horizon	Layers	Hidden cells	Drop	MAE $[W/m^2]$	RMSE $[W/m^2]$	R^2
Proposed LSTM	24h	2	512	0.15	16.45	33.94	0.988
MLP Alfadda, Rahman, and Pipattanasomporn (2018)	1h	2	7 - 5	-	-	32.75	-
Satellite LSTM S. Srivastava and Lessmann (2018)	24h	2	10 to 150	0.2	15.67 to 27.94	23.6 to 59.2	-
CNN-LSTM Zang et al. (2020)	1h	-	-	-	37.2 to 52	69.26 to 86.33	-
Temperature forecast							
Case	Horizon	Layers	Hidden cells	Drop	MAE $[°C]$	RMSE $[°C]$	R^2
Proposed BiLSTM	24h	2	100	0.5	1.11	1.57	0.852
LSTM Sekertekin et al. (2021)	1h	-	250	-	0.4597	0.6436	-
CNN-LSTM Jingwei Hou and Tian (2022)	1h	-	-	-	1.02	1.97	-
GRU-LSTM Haque, Tabassum, and Hossain (2021)	6h	-	-	-	1.37	1.90	0.9

3.4.2 LSTM training

Table 3.4 shows the obtained values for the indicators MAE, RMSE and R^2 for the proposed approach and other publications from the literature. The obtained MAE and RMSE values are located in the lower range compared to those obtained by other models in the literature, which limits the use of look-back data and instead relies on cloud conditions as a replacement.

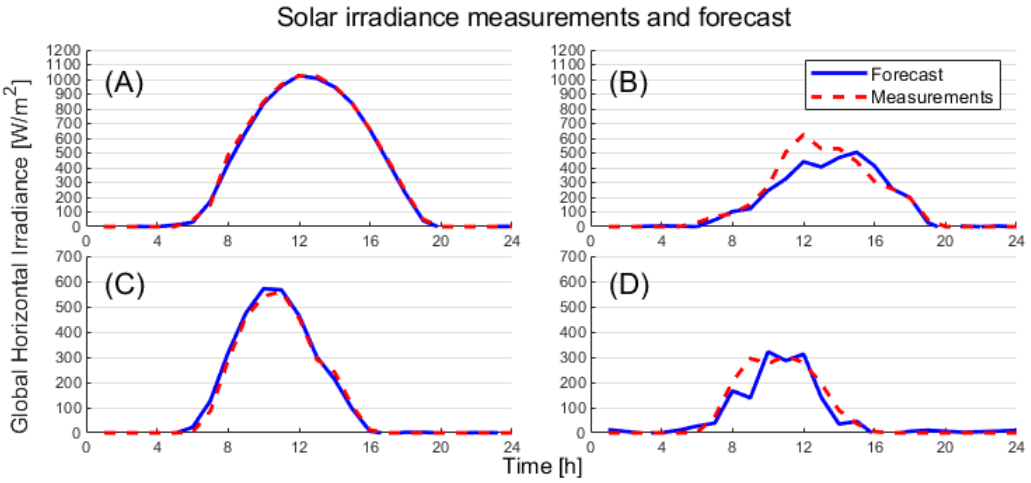

Figure 3.3: Four representative days were used to evaluate the proposed forecast and observed GHI from the test data. Plots A and B correspond to the clear sky and cloudy conditions from 2 days in July 2019, while figures C and D are their counterparts from December 2019.

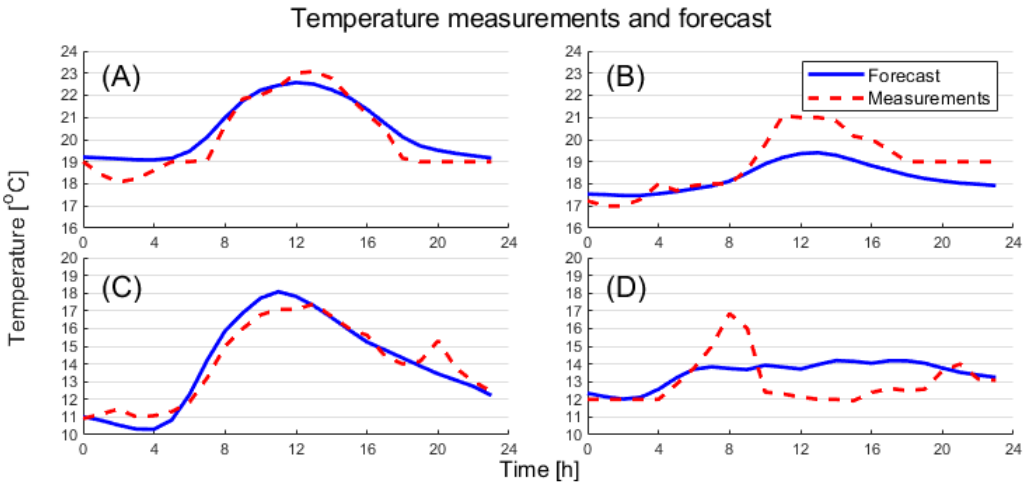

Figure 3.4: Four representative days were used to evaluate the proposed forecast and observed temperature from the test data. Plots A and B correspond to the clear sky and cloudy conditions from 2 days in July 2019, while figures C and D are their counterparts from December 2019.

Figure 3.3 shows the proposed forecast for a clear sky and cloudy days in July and December. The GHI values under clear sky conditions have minor deviations from the measurements. In contrast, under cloud conditions, there are some visible but minor differences between the proposed forecast and the measurements, resulting in a slight decrease in the R^2 indicator. In the temperature case (figure 3.4), the R^2 value drops to 0.85 because of non-expected changes in temperature, which could be generated by wind or other external factors. For example, the cloudy day in December (fig. 3.4-D) shows an increase in the temperature in the first hours of the day and a decrease in temperature after three hours. Regardless of the rapid temperature changes, the BiLSTM model was able to capture the general behaviour of the temperature and the influence of cloud type and solar irradiance.

3.4.3 Solar and temperature scenarios based on cloud type

Figure 3.5 shows one day's solar and temperature scenarios from the selected months. In the GHI scenarios, the principal difference in the irradiance depends on the cloud conditions at midday.

One key consideration is how cloudy conditions affect solar irradiance. As shown in Figure 3.1, we see distinct patterns in cloud types and their corresponding PDFs, indicating potential differences in irradiance under cloudy skies. A second indicator is the possible relationship between cloudy and clear-sky conditions, where the cloud condition at time t could affect the irradiance values at $t-1, t+2$, etc. An occurrence of this case may be the low irradiance for the scenario clear-cloudy-cloudy in June, with values even lower than a full cloudy day case.

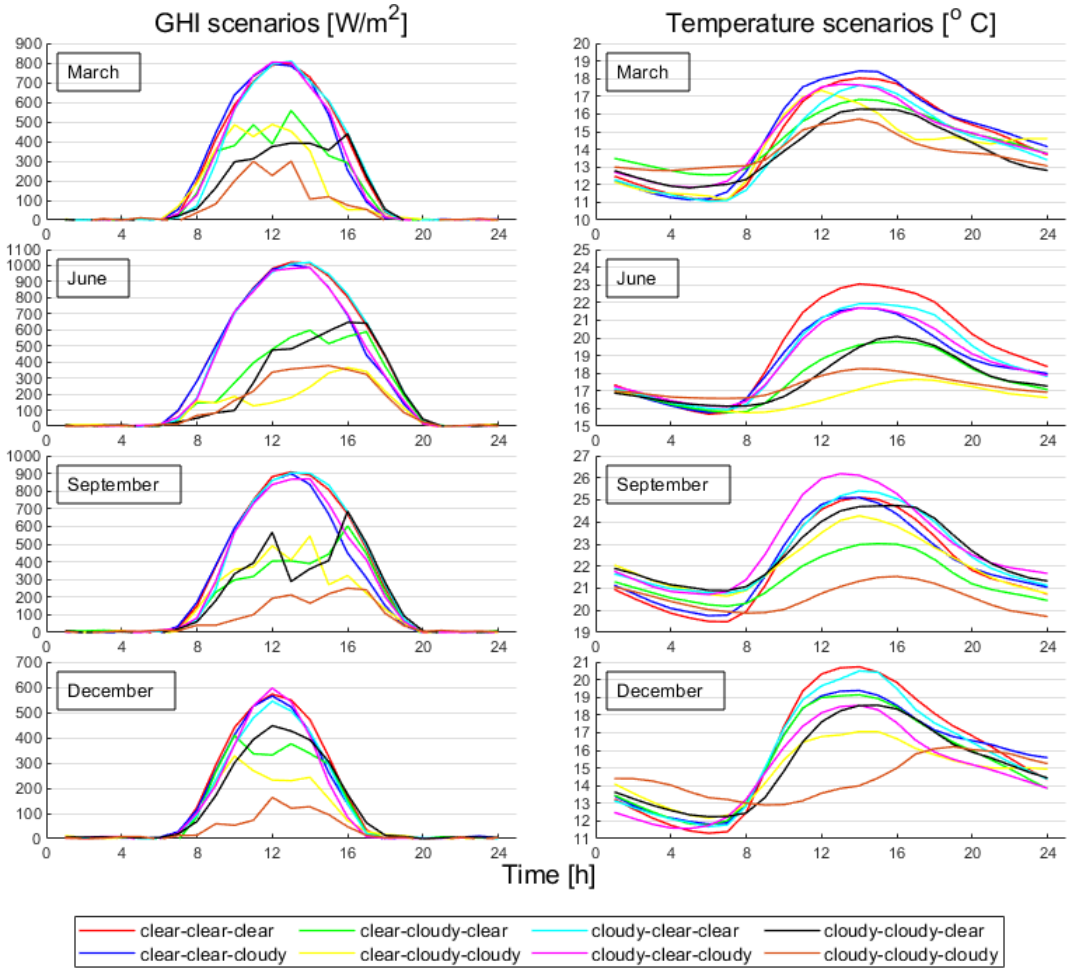

Figure 3.5: Solar and temperature solar scenarios from the selected months for four days. The forecast of solar irradiance was used as input for the temperature scenarios.

From a temperature perspective, our model effectively captures the influence of cloud type and solar irradiance. For instance, in June, the clear-cloudy-cloudy scenario is characterised by both low temperatures and irradiance values. This outcome can be attributed to two factors: the reduced solar input due to cloudy conditions and the emission of infrared radiation from the Earth's surface towards the sky during morning hours when the atmosphere is clearer. Similar effects are observed in the temperature scenarios depicted in Figure 3.5.

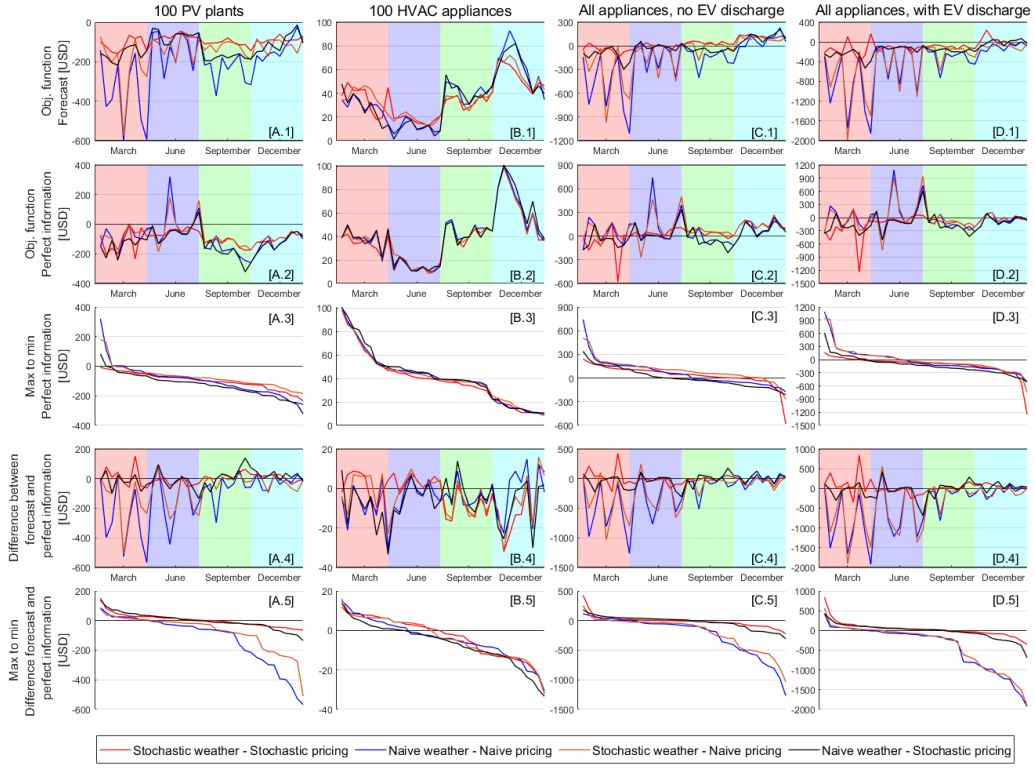

Figure 3.6: Objective function for the 4 sets of appliances and comparison of weather and pricing forecasts against naive forecasts. Subplots with numbers 1, 2, and 4 show the objective function for the forecasted operation, results using perfect forecast information, and the difference between both values, respectively. Subplots 3 and 5 show the objective function using perfect forecast information and differences in the objective function from the maximum to the minimum value.

3.4.4 Forecast evaluation under VPP operation

Various stochastic and naive combinations of pricing and weather scenarios were proposed to evaluate in section 3.3.4, considering four sets of flexible appliances to assess the improvement of the objective function of a stochastic Virtual Power Plant model, section 3.3.1.

Figure 3.6 presents the objective function of the proposed weather and pricing scenarios for each set of appliances, using a letter to differentiate each set (A - PV plants, B - HVAC, C - all appliances without EV discharge and D - all appliances with EV discharge) and a number for the result obtained:

1. VPP obj. function with forecast parameters
2. VPP obj. function with DAM energy bought/sold restricted to the VPP forecast results, using pricing and weather-perfect information
3. Perfect information case shuffled from maximum to minimum
4. Difference between the VPP obj. function of the forecasted and perfect information case

Table 3.5: Objective function for perfect information evaluation with day-ahead energy according to forecast optimisation

		sto. weather sto. pricing [USD]	naive weather naive pricing [USD]	sto. weather naive pricing [USD]	naive weather sto. pricing [USD]
100 PV	sum	-3556.66	-3378.08	-2584.43	-4529.06
	average	-98.80	-93.84	-71.79	-125.81
	stdev	55.23	107.14	75.76	80.30
100 HVAC	sum	1404.83	1473.35	1460.36	1503.33
	average	39.02	40.93	40.57	41.76
	stdev	21.82	22.33	21.11	23.18
All appliances without ev discharge	sum	1251.49	2294.55	3572.87	247.31
	average	34.76	63.74	99.25	6.87
	stdev	134.25	168.49	138.42	122.63
All appliances with ev discharge	sum	-4492.93	-843.92	-249.77	-4453.98
	average	-124.80	-23.44	-6.94	-123.72
	stdev	229.30	290.29	295.38	203.36

5. Difference of both VPP cases shuffled from maximum to minimum

The relevance of the subplots numbered 3 lies in their simplified representation of the operational costs of the different forecast scenarios, where the chronological order is removed, allowing us to compare each forecast against the others, with the lowest value being the expected aim. Similar but not the same, subplots with the number 5 indicate the difference in the objective function of the forecasted and perfect information case, where the ideal case is to have a forecasted objective function as close as possible to the perfect information case, the positive values are the additional cost not considered by the forecast case and the negative values are expected minor cost or additional profits not earned by the perfect information case.

From the total operational cost of the VPP presented in table 3.5, there is no clear better case between the stochastic weather scenarios or the naive weather. However, adding weather scenarios diminishes the impact of high operational costs when naive forecasts fail to capture changes in weather conditions, thereby facilitating the estimation of operational costs in the first stage. First, including the weather scenarios could not represent a decrease in operational cost, as seen in the 100 PV plant case, where the worst-case scenario was the naiveP-stoW; however, the cases including stochastic weather have a lower standard deviation compared to the other cases. Figure 3.6 subplots 3 shows the operational cost from the maximum value to the minimum, where the stoP-stoW case consistently shows the lowest maximum values in the four cases. However, price gradients tend to be smaller than naive approaches. Including multiple scenarios diminishes extreme cases with high operational costs but decreases VPP's capability to exploit some price differences and obtain higher profits.

Including the weather scenarios reduces the difference between the operational cost estimated in the forecast and perfect information cases. Figure 3.6.A.5 shows the difference in the 100 PV plants' operational cost, where the naiveP-stoW forecast reduces the difference near the minimum values compared to the naiveP-naiveW forecast. The inclusion of the stochastic pricing in subplots 3.6.A.5, 3.6.C.5 and 3.6.D.5 shows a significant decrease in the difference compared to the naive pricing scenarios, excepting subplot 3.6.B.5 where the relevance of the weather scenarios for HVAC appliances could be more relevant than the pricing scenarios.

An unexpected observation from the results is the influence of scenario probabilities on the occurrence probability of cloud conditions. Naive weather forecasting (case stoP-naiveW) has an opportunity to replicate last-day conditions and propose energy bids that have a lower cost from the other approaches, as seen in subplots 3.6.C.3 and 3.6.D.3. An option to include their influence is to increase the probability of the most similar case to the naive weather or add it as an additional scenario, requiring modification of scenario probabilities and further research.

Below will be analysed the results per set of appliances:

100 PV plants

In figure 3.6.A.1 is seen a considerable profit in the cases naiveP-naiveW and naiveP-stoW in March, resulting from the price differences that were not confirmed in the perfect information case (3.6.A.2) because of the price changes between days, being these the most significant profit differences shown at the end of 3.6.A.5. On the other hand, the case stoP-stoW have no positive objective function, reducing the energy sold in the DAM when the price is lower than the RTM pricing. This decision was not the most effective in the total 36 days of operation, where the approach stoP-naiveW has a profit of 4529 $USD. The influence of similar weather conditions makes the stoP-naiveW case more profitable, while the stoP-stoW approach is better suited for changing weather conditions. This difference in the operation's profitability can be seen between the naiveP-naiveW and naiveP-stoW cases, with a difference of 793.65 $USD.

100 HVAC appliances

The operational cost of the four forecast approaches was similar to each other, where the approach stoP-stoW has better results at an operational cost of 1404.83 $USD, while the worst case was the stoP-naiveW with a cost operation of 1503.33 $USD (a 6.55% higher, according to table 3.5). The lower cost difference compared to the previous case could be due to two factors: the shift in energy purchase capacity and the thermal inertia of the households. Thermal inertia or storage allows the VPP to displace the need for additional energy for several hours, thereby searching for a lower energy cost. The cases with a stochastic weather

approach could consider worse weather scenarios, making more conservative energy bids in the DAM. Only in December do we have days with a significant difference between expected and actual operational costs (figure 3.6.B.4), which could be due to unexpected weather conditions.

All appliances, without EV discharge

As seen in table 3.5, the operation cost of the stoP-stoW case was 1004 $USD higher than the stoP-naiveW. From the four forecast instances evaluated in figure 3.6.C.3, the stoP-stoW case has the lower value from the four days with a higher and lowest cost per forecast approach, but the stoP-naiveW has a constant lower value in the middle part of the 36 days evaluated. The influence of new appliances, which were unrelated to weather conditions, could reduce the impact of weather scenarios and decrease operational costs.

All appliances, with EV discharge

The introduction of discharge capacity (for electrical storage) enables EVs to actively displace energy in real-time based on DAM and RTM pricing, taking advantage of weather conditions and expected energy to buy or sell from the DAM. The comparison of the subplots 3.6.C.3 and 3.6.D.3 shows a decrease in operational cost in the middle area of the plot, reaching values under zero for a higher number of days. The cost difference between stoP-stoW and stoP-naiveW is minimal (0.87% in favour of stoP-stoW), as seen in table 3.5. This difference could be higher if the EVs were available during midday. The EV used to be unavailable during work hours (8am to 5pm) with some time displacement and occasional EV connected all day. The improvement in the inclusion of electrical storage can be seen in the naiveP-naiveW and naiveP-naiveW cases, reducing the operational cost difference from 1276 $USD to 594 $USD from the case without EV discharge.

3.5 Conclusions

Our study proposes a novel scenario generator for day-ahead weather forecasts based on cloud conditions. This approach considers the cloud type conditions to estimate the transition matrix of the cloud states and capture its seasonal behaviour. By using cloud conditions as input for the LSTM model, our model limits the look-back data to minimise unexpected persistence of day-before conditions in the forecast.

The trained LSTM and BiLSTM models demonstrated excellent performance in capturing the influence of cloud conditions, with low values for MAE and RMSE indicators comparable to other publications that utilise look-back data as input. The significance of the cloud indicators is evident in the temperature and solar scenarios, which show notable differences between

cloudy and clear-sky conditions. For the irradiance model, out trained model accurately captures the effect of the cloud conditions, particularly at midday. In contrast, temperature models capture the effect of clear-sky conditions at night, with a greater decrease in temperature compared to cloudy days.

We applied the proposed weather scenarios to a basic Virtual Power Plant (VPP) model for testing bidding decisions in day-ahead markets, using the scenario occurrence probabilities as scenario probability in the objective function. Using these scenarios, we reduced the difference between the expected and actual operational costs under perfect information, while decreasing high-cost days compared to naive forecast approaches, but slightly increasing mean-case costs.

Future research includes incorporating naive weather conditions as an additional scenario to the model and adjusting the occurrence probability. We can also refine our scenario generation algorithm by introducing new rules that eliminate low-probability scenarios (e.g., those involving two or more cloud transitions). Next, we plan to replace Markov models with Cloud Motion Vector approaches under a dynamic optimisation framework for next-day forecasts. Finally, we aim to extend the proposed approach to include demand forecasting in centralised hubs.

Chapter 4

Price-responsive Demand-side Flexibility Estimation Model with Time-limited Rebound Effect

4.1 Introduction

The presence of renewable generation in recent years, plus its expected increase due to the 2050 net zero plans J. Dixon, Bell, and Brush (2022); Maka, Ghalut, and Elsaye (2024) and the electrification of transport Yuan, Thellufsen, Lund, and Liang (2021) and industrial process Sorknæs et al. (2022) have two expected but hard-to-tackle consequences: The energy required at 2050 will be four times higher than 2020 IRENA (2022) and it is expected that almost 90% of electricity generation in 2050 will come from renewable sources Bouckaert et al. (2021), with solar and wind generation as primary sources.

The vast presence of renewable generation implies a low capacity response from the generation side to changes in demand or transmission contingencies, in addition to the uncertainty and variability produced by solar and wind generation Ringkjøb et al. (2020); Russo et al. (2023); Sharifzadeh, Lubiano-Walochik, and Shah (2017). Under high renewable generation scenarios, the grid needs each available source of flexibility, where demand-side flexibility offers the option to change the scheduled demand from flexible appliances in response to price signals or direct flexibility requirements.

The flexibility estimation problem has been examined following top-down and bottom-up approaches. The top-down approach considers macro elements such as monthly and daily demand or hourly demand profiles from households, buildings, and industries to characterise flexibility as the capacity to modify their demand. Machine learning approaches have been reviewed in Antonopoulos et al. (2020), focused on forecasting, clustering, baseline demand, scheduling and incentives schemes. Data-driven models are used to evaluate EV flexibility according to their changing behaviour Sadeghianpourhamami et al. (2018), and Sajjad, Chicco, and Napoli (2016) evaluates the time-variable demand patterns of aggregate residential customers. The bottom-up approach models the flexible appliance properties to

evaluate its capacity to shift, interrupt and change their demand under an energy management system model, which responds to price signals, CO2 minimisation, demand peak reduction, and other incentives Reynders et al. (2018). Under this approach are studied buildings Junker et al. (2018); H. Li et al. (2023), home energy management systems Munankarmi, Jin, Ding, and Zhao (2020); Srithapon and Månsson (2023) and electric vehicles Gunkel, Bergaentzlé, Græsted Jensen, and Scheller (2020); Taha, Vincent, and Bitar (2024); Zhang et al. (2020), among others. The flexibility offered can be measured using flexibility indicators, where 27 flexibility indicators are evaluated in Marotta et al. (2021) by comparing the energy used in high and low penalty hours. The flexibility power duration curve is presented in Plaum, Rosin, and AhmadiAhangar (2024) as the aggregated response of thermal appliances controlled by HEMS that report their time to reach temperature comfort limits to a demand aggregator.

In contrast to flexibility estimation, the cost of offering flexibility or responding to flexibility prices has been a more challenging problem to tackle. In the literature, estimating the reference curve and the cost of providing flexibility are usually evaluated separately, as seen in Harder et al. (2020a), which runs two optimisation problems. The first estimates the reference demand, while the second receives a flexibility requirement to be followed, being penalised if a deviation occurs. The difference in the operation cost will be the flexibility cost. In De Coninck and Helsen (2016), three optimisation models are proposed to estimate the flexibility cost curve for a building, following the separation between reference demand and flexibility offered in the problem formulation. Similar to Zade et al. (2018), where the HEMS operation is evaluated first, the flexibility price is calculated based on the energy cost in day-ahead and intra-day markets. The main disadvantage of the separation between reference demand and flexibility to offer is the iterative nature of the flexibility cost estimation; whether the amount of flexibility or the hour when required changes, the model needs to re-optimise their operation.

Other approaches include reference demand and flexibility offered under a single optimisation model, as seen in J. P. Iria et al. (2019), which provides upward and downward flexibility according to a tertiary reserve direction binary parameter, thereby limiting flexibility estimation and responsibility among appliances. Under a demand response approach, in Nojavan and Maghouli (2024), the deviation from expected demand is considered in the model formulation, coupling the total daily upward deviation to the total daily downward deviation. Both approaches offer upward or downward flexibility per time-step, and their models do not explicitly consider the rebound effect of flexibility. For only thermal appliance models, the flexibility factor Finck, Li, and Zeiler (2020); Le Dréau and Heiselberg (2016) is introduced to quantify the flexibility cost as the difference between the heating demand in high and low price periods, divided by the sum of both values.

4.1.1 Contributions

This publication develops a day-ahead flexibility estimation model under stochastic conditions and rebound effects, according to the ISO/DSO requirements for load-serving entities (LSE) such as DA and VPP to participate in flexibility markets. The aggregation agent proposes a demand trajectory based on their scheduling decision and offers upward and/or downward flexibility in the day-ahead market (DAM). The model can buy/sell energy in real-time markets (RTM) in each scenario to fulfil the proposed demand trajectory in DAM. The flexibility will be considered as the energy difference between the energy trajectory and the deviation proposed by the LSE, according to the time duration requested by the ISO/DSO. After the requested flexibility duration, the aggregation agent or LSE will have a limited rebound time to return to the appliance's expected 'storage state' defined in each time-step, allowing flexibility to be offered immediately after the rebound time. The 'storage state' is an energy storage indicator for flexible appliances (state of energy on EV, the temperature in HVAC), defined by the appliance operation in each time-step.

The flexibility will be estimated based on the 'alternative flexibility scenario' approach presented in Salgado-Bravo, Negrete-Pincetic, and Kiprakis (2023), which proposes a 'branch' in the evaluated scheduling horizon to estimate maximum positive and negative deviations from expected demand as upward and downward flexibility. The duration of the branch is limited to the duration of the flexibility request, which can be greater than or equal to the time granularity of the time-step. This approach will be extended to consider the rebound effect and associated costs from providing flexibility under stochastic operation, referred to as 'Trajectory-based aggregated flexibility estimation'. In this context, each branch will evaluate upward and downward flexibility and its rebound effect, which depends on the demand trajectory determined by the same model. Including branches makes the flexibility estimation model able to respond to flexibility prices.

The determination of a day-ahead energy bid, demand trajectory, and the inclusion of the rebound effect for various weather and price scenarios simplify the analysis of aggregated demand-side flexibility capabilities, offering a valuable tool for DAM energy and flexibility decisions. The main contributions of this paper are:

- An stochastic flexibility estimation model for Load Serving Entities, able to offer flexibility by continuous time intervals
- The explicit inclusion of the rebound effect in the day-ahead flexibility evaluation
- The offered flexibility responds to price signals and depends on the energy cost, the duration of the rebound time and additional cost from expected EV degradation

4.2 Price-Responsive Flexibility Methodology

4.2.1 Trajectory-based aggregated flexibility estimation

The alternative flexibility scenario was defined as a branch in the evaluation horizon, allowing for the estimation and offer of flexibility from the demand side for the next K timeblocks Salgado-Bravo et al. (2023), where K represents the flexibility duration. This approach will be extended to introduce a stochastic formulation that considers various energy prices and weather conditions, as well as the rebound effect on the offered flexibility by each appliance.

From the VPP on DA scheme, flexibility is the aggregated response of the flexible appliances from the expected demand under regular operation. The same flexibility estimation model needs to determine the demand trajectory for the set of flexible appliances. Under this approach, we defined upward and downward flexibility as the capacity of the aggregator to increase or decrease demand from the reference trajectory in response to price or control signals.

The flexibility estimation will be limited by the aggregator's probability of being called to provide services, similar to a capacity offer. This probability will be referred to as the probability of occurrence (π_{Occ}), enabling the model to estimate the demand trajectory and meet the energy demand without artificially inflating the demand to provide flexibility.

The concept of 'rebound effect' is introduced to describe the condition where the set of flexible appliances needs to return to the expected demand after the flexibility requirement. To meet this condition, the 'storage state' is used as an energy storage variable per appliance. This variable, after the rebound time, must be equal to the expected value without offering flexibility.

The trajectory-based flexibility estimation is formulated to determine an optimal demand trajectory, minimising demand fluctuations for various weather and price scenarios and estimating the flexibility to offer in the DAM. The trajectory-based flexibility estimation model fulfils the following requirements:

- Formulation of a day-ahead demand trajectory for VPP schemes
- Estimation of the maximum flexibility to offer from a set of flexible appliances, without considering rebound effect or energy prices (as a flexibility upper bound)
- Evaluation of the demand deviation from the proposed trajectory in each scenario, limited by the flexibility estimated and flexibility requirement duration.
- Evaluation of the rebound effect, defined by the offered flexibility and the allowed rebound time.

The model is adept at identifying the cost-benefit of flexibility, accomplishing the requirements in a single stage. It employs the alternative flexibility scenario approach, branching from the evaluation horizon. Over the next 24 hours, the model schedules the appliance operation in multiple weather and price scenarios. The first branch estimates the maximum flexibility

to offer, with a duration equal to the flexibility requirement. The second branch evaluates the effect of the flexibility offered and the rebound effect on demand. Both branches are considered at each time-step, to estimate and offer flexibility for the next 24 hours. The model's inclusion of the rebound effect and the valuation of demand deviation in RTM enables it to identify the cost of the flexibility offered, which is always equal to or lower than the benefits obtained from offering flexibility to the grid.

Model considerations

The proposed model can operate under different time intervals according to the flexibility requirements. The constraints expressed have been tested using two approaches: a 30-minute approach (48 time blocks) and a 1-hour approach (24 time blocks). The flexibility estimation uses the notation "1-block" to indicate the number of time blocks the trajectory-based aggregated flexibility response is evaluated. For example, a 30-min approach with a 2-block flexibility estimation evaluates the flexibility for 1 hour in each time block, while a 1-hour approach with a 3-block estimation considers the flexibility response for 3 hours. A 15-min approach (96 time blocks per day) was evaluated but not included due to the high cost of RAM in the model formulation.

The model is capable of estimating flexibility for a variety of appliances, including pool pumps (PP), electric vehicles (EV), air conditioners (HVAC - heating, ventilation and air conditioning), electric water heaters (EWH), and solar panels (PV - Photovoltaics). It will estimate flexibility in continuous time-steps, and the number of time-steps can be modified according to the expected system granularity.

Three different units of time are used:

- t as unit of time, covering the next 24 hours (set T)
- k as unit of flexibility time, limited by the flexibility requirement duration (set K)
- k' as unit of rebound time, limited by the expected rebound time (set K')

In some expressions, two elements in parentheses in the superscript indicate that the constraint needs to be expressed under both elements. An example can be observed in 4.1f, where $[Up, Dn]$ indicates the expression needs to evaluate for upward and downward flexibility separately.

4.2.2 Objective function and operational constraints

The proposed objective function aims to minimise the operation cost of the appliances under various weather and price scenarios, offering one DAM energy bidding and numerous RTM bids (one per scenario). The expression 4.1 considers the energy required/sold to the system in DAM and RTM, penalties for demand trajectory deviations, additional benefits for offering flexibility, and the additional cost of returning to expected operation within the rebound time.

VPP model formulation [eq. 4.1]:

$$\min DA_{cost} + RT_{cost} + B_{pen} - F_{profit} + Dev_{cost} + EV_{pen} \tag{4.1a}$$

$$DA_{cost} = \sum_{dam}^{DAM} \sum_{t}^{T} \pi^{dam} \lambda_t^{dam} \left(E_t^{dam,buy} - E_t^{dam,sell} \right) \tag{4.1b}$$

$$RT_{cost} = \sum_{w}^{W} \sum_{rtm}^{RTM} \sum_{t}^{T} \pi^{rtm} \pi^{w} \lambda_t^{rtm} \left(E_{w,rtm,t}^{rtm,buy} - E_{w,rtm,t}^{rtm,sell} \right) \tag{4.1c}$$

$$B_{pen} = \sum_{w}^{W} \sum_{rtm}^{RTM} \sum_{t}^{T} \pi^{rtm} \pi^{w} Band_{pen} \left(\phi_{w,rtm,t}^{+} + \phi_{w,rtm,t}^{-} \right) \tag{4.1d}$$

$$F_{profit} = \sum_{t}^{T} \pi_{Occ} \left[\lambda_t^{FlexUp} KFup_t + \left(\lambda_t^{FlexDn} + \sum_{rtm}^{RTM} \pi^{rtm} \lambda_t^{rtm} \right) KFdn_t \right] \tag{4.1e}$$

$$Dev_{cost} = \sum_{rtm}^{RTM} \sum_{t}^{T} \sum_{k'}^{K'} \pi_{Occ} \pi^{rtm} \lambda_t^{rtm} \left(D_{w,rtm,t,K+k'}^{alt,[Up,Dn]} - D_{w,rtm,t,K+k'} \right) \tag{4.1f}$$

$$\begin{aligned} EV_{pen} = \sum_{w}^{W} \sum_{rtm}^{RTM} \sum_{t}^{T} \sum_{ev}^{EV} \pi^{rtm} \pi^{w} SoH^{pen} \Big\{ & P_{w,rtm,t}^{ev,dch} \\ & + \pi_{Occ} \sum_{k}^{K+K'} \left(P_{w,rtm,t,k}^{ev,dch,Up} + P_{w,rtm,t,k}^{ev,dch,Dn} \right) \Big\} \end{aligned} \tag{4.1g}$$

The expression 4.1b corresponds to DAM energy bids (only one bid), while expression 4.1c are the bids in RTM in each scenario. The expression 4.1d covers demand deviation from the expected trajectory determined by the model. The expression 4.1e represents the revenues from offering flexibility, according to the flexibility price, plus the sale of energy diminished by downward flexibility requirements. The expression 4.1f estimates the cost or revenue of the rebound effect when flexibility is offered, considering RTM prices. The expression 4.1g added a penalisation for EV discharge in time, upward and downward flexibility cases, related to the state of health (SoH) of the battery, as discussed in section 4.2.7.

Demand balance constraints:

$$\begin{aligned} D_{w,rtm,t} = & \sum^{PP} P_{w,rtm,t}^{pp} + \sum^{EV} \left(P_{w,rtm,t}^{ev,ch} - P_{w,rtm,t}^{ev,dch} \right) - \sum^{PV} P_{w,rtm,t}^{pv} \\ & + \sum^{HVAC} \left(P_{w,rtm,t}^{hvac,heat} + P_{w,rtm,t}^{hvac,cool} \right) + \sum^{EWH} P_{w,rtm,t}^{ewh} \end{aligned} \tag{4.2}$$

$$D_{w,rtm,t} = E_t^{dam,buy} - E_t^{dam,sell} + E_{w,rtm,t}^{rtm,buy} - E_{w,rtm,t}^{rtm,sell} \tag{4.3}$$

$$Tr_t - \eta \frac{E_a}{\Delta t} - \phi_{w,rtm,t}^{-} \leq D_{w,rtm,t} \leq Tr_t + \eta \frac{E_a}{\Delta t} + \phi_{w,rtm,t}^{+} \tag{4.4}$$

The expression 4.2 defines the 'demand' as the sum of the energy requested/provided from the demand-side, while expression 4.3 introduces the energy requested from external sources, being the expressions 4.2 and 4.3 the generation-demand constraints. The expression 4.4 introduces the proposed demand trajectory to follow by the LSE, plus an allowed band for a slight deviation (term $\eta \frac{E_a}{\Delta t}$). The model determines the demand trajectory and must be followed in each weather and price scenario, allowing for non-penalised deviations by a constant parameter η, which is multiplied by the expected total energy requested by the aggregator for the day, divided by Δt, equal to 24 hours.

$$-\sum_{pr}^{Pros} Pmax_{pr}^{cont} \leq D_{w,rtm,t} \leq \sum_{pr}^{Pros} Pmax_{pr}^{cont} \tag{4.5}$$

$$\sum_{t}^{T} E_t^{DAsell} + E_{w,rtm,t}^{RTsell} \leq \sum_{t}^{T} (P_{w,rtm,t}^{ev,dch} + P_{w,rtm,t}^{pv}) \tag{4.6}$$

The expressions 4.5 and 4.6 limit energy flow in two different approaches. First eq. 4.5 limits the energy demand according to the maximum power by contract, while eq. 4.6 forces the model to only sell energy to the EV battery discharge and PV power, thereby avoiding energy bids motivated by price differences between DAM and RTM markets.

Aggregated upwand and downward flexibility constraints:

$$\begin{aligned} Fup_t \leq & \sum_{EWH} Fup_{w,rtm,t,k}^{ewh} + \sum_{PP} Fup_{w,rtm,t,k}^{pp} + \sum_{HVAC} \left(Fup_{w,rtm,t,k}^{heat,hvac} + Fup_{w,rtm,t,k}^{cool,hvac} \right) \\ & + \sum_{EV} (Fup_{w,rtm,t,k}^{ev,ch} + Fup_{w,rtm,t,k}^{ev,dch}) + \sum_{PV} Fup_{w,rtm,t,k}^{pv} \qquad \forall t \in T, k \in K \end{aligned} \tag{4.7}$$

$$\begin{aligned} Fdn_t \leq & \sum_{EWH} Fdn_{w,rtm,t,k}^{ewh} + \sum_{PP} Fdn_{w,rtm,t,k}^{pp} + \sum_{HVAC} \left(Fdn_{w,rtm,t,k}^{heat,hvac} + Fdn_{w,rtm,t,k}^{cool,hvac} \right) \\ & + \sum_{EV} (Fdn_{w,rtm,t,k}^{ev,ch} + Fdn_{w,rtm,t,k}^{ev,dch}) + \sum_{PV} Fdn_{w,rtm,t,k}^{pv} \qquad \forall t \in T, k \in K \end{aligned} \tag{4.8}$$

Expressions 4.7 and 4.8 ensure the flexibility values Fup_t and Fdn_t for the next K time intervals. The flexibility is evaluated in each scenario as the sum of the flexibility provided by the appliances. However, the flexibility offers Fup_t and Fdn_t, which are the maximum values that all scenarios can provide.

The flexibility estimation depends on the appliance conditions, weather and prices. In addition, the flexibility can be influenced by market requirements or their capacity to fulfil the request. Limitations explored in expressions 4.9 to 4.11.

$$Fup_t \leq BigM * Fup_t^{offer} \tag{4.9}$$

$$Fdn_t \leq BigM * Fdn_t^{offer} \tag{4.10}$$

$$\sum_t \left(Fdn_t^{offer} + Fup_t^{offer} \right) \leq N^{Offers} \tag{4.11}$$

Expressions 4.9 and 4.10 were associated with the capacity of the DA to provide flexibility offers at time t. The binary variables Fup_t^{offer} and Fdn_t^{offer} could be changed to parameters according to the aggregator's interest, thereby decreasing the complexity of the problem and facilitating decision-making at time t when only upward or downward flexibility is evaluated. The expression 4.11 limits the number of flexibility offers per day, diminishing the flexibility provided but bidding for the most profitable offers for the LSE. For testing purposes, N^{Offers} do not limit the number of flexibility offers during the day.

Demand balance under flexibility bid and rebound effect:

$$Tr_{t+k} - \eta \frac{E_a}{\Delta t} + Fup_t \leq D_{w,rtm,t,k}^{alt,Up} \leq Tr_{t+k} + Fup_t \qquad \forall k \in K \tag{4.12}$$

$$Tr_{t+k} - \eta \frac{E_a}{\Delta t} - Fdn_t \leq D_{w,rtm,t,k}^{alt,Dn} \leq Tr_{t+k} - Fdn_t \qquad \forall k \in K \tag{4.13}$$

$$\begin{aligned} D_{w,rtm,t,k}^{alt,[Up,Dn]} = & \sum^{PP} P_{w,rtm,t,k}^{pp,[Up,Dn]} + \sum^{EV} \left(P_{w,rtm,t,k}^{ev,ch,[Up,Dn]} - P_{w,rtm,t,k}^{ev,dch,[Up,Dn]} \right) \\ & + \sum^{HVAC} \left(P_{w,rtm,t,k}^{hvac,heat,[Up,Dn]} + P_{w,rtm,t,k}^{hvac,cool,[Up,Dn]} \right) \\ & + \sum^{EWH} P_{w,rtm,t,k}^{ewh,[Up,Dn]} - \sum^{PV} E_{w,rtm,t,k}^{pv,[Up,Dn]} \end{aligned} \tag{4.14}$$

$$-BigMFup_t^{offer} \leq D_{w,rtm,t,K+k'}^{alt,Up} - D_{w,rtm,t+K+k'} \leq BigMFup_t^{offer} \tag{4.15}$$

$$-BigMFdn_t^{offer} \leq D_{w,rtm,t,K+k'}^{alt,Dn} - D_{w,rtm,t,K+k'} \leq BigMFdn_t^{offer} \tag{4.16}$$

The expressions 4.12 to 4.16 focus on estimating the rebound effect after the flexibility is offered. The expressions 4.12 and 4.13 displace the demand trajectory according to the upward or downward flexibility for the following K time steps. The expression 4.14 creates an alternative evaluation of the demand to offer flexibility and evaluate the rebound effect. Expressions 4.15 and 4.16 link the flexibility offered by binary variables Fup_t^{offer} and Fdn_t^{offer} to the quantification of the demand in the alternative path, forcing the same demand in both scenarios when the model does not offer flexibility.

4.2.3 Appliance constraints

The trajectory-based aggregated flexibility estimation requires three units of time for scheduling, flexibility estimation and rebound effect, as explained in section 4.2.1. This approach implies that each modelled appliance requires operational constraints for each time unit, as indicated below:

- Appliance operation for time t.
- Flexibility estimation, as maximum demand deviation according to operational and comfort constraints
- Flexibility and rebound evaluation, as an alternative operation that offers flexibility.

The flexibility and rebound evaluation assumes that the 'storage state' variable per each appliance will have the same value at the end of the rebound effect (time t, alternative time or branch $K+K'$) and the appliance operation at $t+K+K'$. This constraint ensures the model's capacity to return to the proposed trajectory while evaluating the rebound effect.

The appliances evaluated are presented below:

Pool Pump

The pool pump can be considered a basic deferrable appliance because of its capacity to be stopped or shifted with minimal penalties. In comparison with other models in literature Ali, Malik, and Raza (2020); Gomes, Ruano, and Ruano (2023), the model introduced in eq. 4.17 introduces the state of energy of the PP ($SoE^{pp}_{w,rtm,t}$) as the energy delivered to the appliance in a similar approach to EV model. $SoE^{pp}_{w,rtm,t}$ is the 'storage state' for the PP. The expression 4.17a limit the operation of the PP according to their availability (Av^{PP}_t), while expressions 4.17b, 4.17c and 4.17d monitors the PP $SoE^{pp}_{w,rtm,t}$ and encourage to the model to deliver the required energy at the end of the day.

$$0 \leq P^{pp}_{w,rtm,t} \leq P^{pp}_{max} * Av^{PP}_t \qquad \forall t \in T, \forall w \in W, \forall rtm \in RTM \tag{4.17a}$$

$$SoE^{pp}_{w,rtm,0} = P^{pp}_{w,rtm,t} \tag{4.17b}$$

$$SoE^{pp}_{w,rtm,t} = SoE^{pp}_{w,rtm,t-1} + P^{pp}_{w,rtm,t} \tag{4.17c}$$

$$SoE^{pp}_{w,rtm,t_{end}} = E^{pp} \tag{4.17d}$$

$$\tag{4.17e}$$

The flexibility estimation comes from the capacity to increase/limit its demand in the next K time-steps, where 4.18a evaluates the capacity to energy increase at $t+k$ time and 4.18b defines downward flexibility as the possible demand reduction from $t+k$.

$$Fup^{pp}_{w,rtm,t,k} <= P^{pp}_{max} Av^{pp}_{t+k} - P^{pp}_{w,rtm,t+k} \qquad \forall k \in K \tag{4.18a}$$

$$Fdn^{pp}_{w,rtm,t,k} <= P^{pp}_{w,rtm,t+k} \qquad \forall k \in K \tag{4.18b}$$

The flexibility and rebound evaluation is presented in expression 4.19, in a similar approach to 4.17 but considering the alternative flexibility scenario that starts in time t until $t+K+K'$. The constraint 4.19d encourages the PP state of energy to be the same value under regular operation and after offering flexibility.

$$0 \leq P^{pp,[Up,Dn]}_{w,rtm,t,k} \leq P^{pp}_{max} * Av^{PP}_{t+k} \qquad \forall t \in T, \forall w \in W, \forall rtm \in RTM \tag{4.19a}$$

$$SoE^{pp,[Up,Dn]}_{w,rtm,t,0} = SoE^{pp}_{w,rtm,t-1} + P^{pp,[Up,Dn]}_{w,rtm,t,k} \tag{4.19b}$$

$$SoE^{pp,[Up,Dn]}_{w,rtm,t,k} = SoE^{pp,[Up,Dn]}_{w,rtm,t,k-1} + P^{pp,[Up,Dn]}_{w,rtm,t,k} \tag{4.19c}$$

$$SoE^{pp,[Up,Dn]}_{w,rtm,t,K+K'} = SoE^{pp}_{w,rtm,t+K+K'} \tag{4.19d}$$

Electric Vehicles

The EV appliances are the most relevant source of flexibility on the demand-side. Their high energy requirements and internal battery storage are associated with high consumption and the potential to displace demand under certain conditions. The EV model presented in expression 4.20 introduces charge, discharge, expected usage and expected departures, limited by the EV SoE. The EV state of energy (SoE) is the 'storage state' for the EV. The model does not consider a binary representation of the charging/discharging process but includes a state of health (SoH) penalisation associated with EV discharge in the objective function, as explained in section 4.2.7. If no penalisation is considered, the model can charge/discharge without limitations, increasing the EV battery degradation.

$$SoE^{ev}_{min} * Av^{ev}_{t} \leq SoE^{ev}_{w,rtm,t} \leq SoE^{ev}_{max} \tag{4.20a}$$

$$SoE^{ev}_{w,rtm,t} = SoE^{ev,start} + \eta P^{ev,ch}_{w,rtm,t} - \frac{1}{\eta} P^{ev,dch}_{w,rtm,t} + (1 - Av^{ev}_{t}) Dch^{ev}_{usage} \tag{4.20b}$$

$$SoE^{ev}_{w,rtm,t} = SoE^{ev}_{w,rtm,t-1} + \eta P^{ev,ch}_{w,rtm,t} - \frac{1}{\eta} P^{ev,dch}_{w,rtm,t} + (1 - Av^{ev}_{t}) Dch^{ev}_{usage} \tag{4.20c}$$

$$0 \leq P^{ev,ch}_{w,rtm,t} + P^{ev,dch}_{w,rtm,t} \leq P^{ev}_{max} Av^{ev}_{t} \tag{4.20d}$$

$$SoE^{ev,ExDep} \leq SoE^{ev}_{w,rtm,t=dep} \quad \forall t \in T, \forall n \in N, \forall dep \in ExDep \tag{4.20e}$$

$$SoE^{ev,start} Av^{ev}_{t_{end}} \leq SoE^{ev}_{w,rtm,t_{end}} \tag{4.20f}$$

The expression 4.20a limits EV SoE to the expected minimum and maximum, allowing the vehicle to reach $SoE = 0$ if the EV is not available to charge (by Av^{ev}_{t}). Expressions 4.20b and 4.20c evaluate the evolution of the SoE status, and 4.20d limits the maximum energy to charge/discharge. The parameter Dch^{ev}_{usage} represents the expected battery discharge due to usage, which depends on the EV model and the expected daily mileage. Non-common constraints are the expression 4.20e as an additional constraint to encourage the EV departures

to have a minimal charge (as an input parameter), and expression 4.20f wants to maintain the same level of charge from start to the end of the evaluation horizon. If the stored energy from the previous day can be used but not replenished, the operational cost of the model will be artificially reduced.

The flexibility estimation constraints for the EV are shown below:

EV flexibility constraints [eq. 4.21]:

$$Fup^{ev,ch}_{w,rtm,t,k} \leq P^{ev}_{max} - P^{ev,ch}_{w,rtm,t+k} - P^{ev,dch}_{w,rtm,t+k} \tag{4.21a}$$

$$Fup^{ev,dch}_{w,rtm,t,k} \leq P^{ev,dch}_{w,rtm,t+k} \tag{4.21b}$$

$$Fdn^{ev,ch}_{w,rtm,t,k} \leq P^{ev,ch}_{w,rtm,t+k} \tag{4.21c}$$

$$Fdn^{ev,dch}_{w,rtm,t,k} \leq P^{ev}_{max} - P^{ev,ch}_{w,rtm,t+k} - P^{ev,dch}_{w,rtm,t+k} \tag{4.21d}$$

$$SoE^{ev}_{min} * Av^{ev}_{t+k} \leq SoE^{ev,Up\,eval}_{w,rtm,t,k} \leq SoE^{ev}_{max} \tag{4.21e}$$

$$SoE^{ev}_{min} * Av^{ev}_{t+k} \leq SoE^{ev,Dn\,eval}_{w,rtm,t,k} \leq SoE^{ev}_{max} \tag{4.21f}$$

$$SoE^{ev,Up\,eval}_{w,rtm,t,k} = SoE^{ev}_{w,rtm,t-1} + \eta(P^{ev,ch}_{w,rtm,t+k} + Fup^{ev,ch}_{w,rtm,t,k}) - \frac{1}{\eta}(P^{ev,dch}_{w,rtm,t} - Fup^{ev,dch}_{w,rtm,t,k}) + (1 - Av^{ev}_{t})Dch^{ev}_{usage} \qquad if\, k = 0 \tag{4.21g}$$

$$SoE^{ev,Up\,eval}_{w,rtm,t,k} = SoE^{ev,Up\,eval}_{w,rtm,t,k-1} + \eta(P^{ev,ch}_{w,rtm,t+k} + Fup^{ev,ch}_{w,rtm,t,k}) - \frac{1}{\eta}(P^{ev,dch}_{w,rtm,t} - Fup^{ev,dch}_{w,rtm,t,k}) + (1 - Av^{ev}_{t})Dch^{ev}_{usage} \tag{4.21h}$$

$$SoE^{ev,Dn\,eval}_{w,rtm,t,k} = SoE^{ev}_{w,rtm,t-1} + \eta(P^{ev,ch}_{w,rtm,t+k} - Fdn^{ev,ch}_{w,rtm,t,k}) - \frac{1}{\eta}(P^{ev,dch}_{w,rtm,t} + Fdn^{ev,dch}_{w,rtm,t,k}) + (1 - Av^{ev}_{t})Dch^{ev}_{usage} \qquad if\, k = 0 \tag{4.21i}$$

$$SoE^{ev,Dn\,eval}_{w,rtm,t,k} = SoE^{ev,Dn\,eval}_{w,rtm,t,k-1} + \eta(P^{ev,ch}_{w,rtm,t+k} - Fdn^{ev,ch}_{w,rtm,t,k}) - \frac{1}{\eta}(P^{ev,dch}_{w,rtm,t} + Fdn^{ev,dch}_{w,rtm,t,k}) + (1 - Av^{ev}_{t})Dch^{ev}_{usage} \tag{4.21j}$$

(4.21k)

Expressions 4.21a and 4.21b introduce upward and downward flexibility from the charging process, being limited by the maximum power and the expected consumption in time $t+k$, while 4.21c and 4.21d are equivalent constraints for the discharging process. Expressions 4.21e and 4.21f limit the EV SoE under Upward and Downward flexibility estimation, while expressions from 4.21g to 4.21j calculate SoE including upward and downward flexibility in k time.

The flexibility and rebound evaluation necessitate an additional parameter to determine the availability of the EV during rebound time. The parameter $Av^{ev,flex}$ addresses this by indicating whether the EV can meet a flexibility requirement until the end of the rebound time ($Av^{ev,flex}_{t} = 2$), part of the rebound time ($Av^{ev,flex}_{t} = 1$), or if it is not available to offer flexibility ($Av^{ev,flex}_{t} = 0$).

$$Av_t^{ev,flex} = \begin{cases} 2 \text{ if } t+K+K' < dep \\ 1 \text{ if } t+K+K' \geq dep \text{ and } t+K < dep \\ 0 \text{ otherwise} \end{cases}$$

The flexibility and rebound constraints are introduced in expression 4.22, similar to the EV usual operation constraints presented in 4.20. The main difference is the introduction of expressions 4.22e and 4.22f, which depends on the flexibility available array $Av^{ev,flex}$ to couple the EV SoE at the end of the rebound time for upward and downward flexibility with the expected SoE at EV regular operation.

SoE evaluation under flexibility offers [eq. 4.22]:

$$SoE_{min}^{ev} * Av_{t+k}^{ev} \leq SoE_{w,rtm,t,k}^{ev,[Up,Dn]} \leq SoE_{max}^{ev} \tag{4.22a}$$

$$0 \leq P_{w,rtm,t,k}^{ev,ch,[Up,Dn]} + P_{w,rtm,t,k}^{ev,dch,[Up,Dn]} \leq P_{max}^{ev} Av_{t+k}^{ev} \tag{4.22b}$$

$$SoE_{w,rtm,t,k}^{ev,[Up,Dn]} = SoE_{w,rtm,t-1}^{ev} + \eta P_{w,rtm,t,k}^{ev,ch,[Up,Dn]} - \frac{1}{\eta} P_{w,rtm,t,k}^{ev,dch,[Up,Dn]} + (1 - Av_{t+k}^{ev}) Dch_{usage}^{ev} \tag{4.22c}$$

$$SoE_{w,rtm,t,k}^{ev,[Up,Dn]} = SoE_{w,rtm,t,k-1}^{ev,[Up,Dn]} + \eta P_{w,rtm,t,k}^{ev,ch,[Up,Dn]} - \frac{1}{\eta} P_{w,rtm,t,k}^{ev,dch,[Up,Dn]} + (1 - Av_{t+k}^{ev}) Dch_{usage}^{ev} \tag{4.22d}$$

$$SoE_{w,rtm,t,K+K'}^{ev,[Up,Dn]} = SoE_{w,rtm,t+K+K'}^{ev} \qquad if Av_t^{ev,flex} = 2 \tag{4.22e}$$

$$SoE_{w,rtm,t,K+K'+t-dep}^{ev,[Up,Dn]} = SoE_{w,rtm,dep}^{ev} \quad if Av_t^{ev,flex} = 1 \tag{4.22f}$$

HVAC appliances

A linearization of the ISO 13790:2008 hourly method ISO 13790:2008(E) (2008) is used to estimate the air temperature in a building, thereby estimating the flexibility in thermal appliances. The thermal model is presented under the Crank-Nicholson scheme in Annexe .2, using a 5R1C (five resistances, one capacitance) lumped parameter network. The HVAC formulation (eq. 4.23) exploits the capacity of the internal wall temperature to be considered as a thermal storage variable, where its temperature values, the effect of solar irradiance through walls and windows, air flows and the HVAC operation will determine the air temperature.

HVAC model constraints [eq. 4.23]:

$$\theta_{w,rtm,t}^{air,hvac} = \frac{H_{tr,is}^{hvac} R_{5,w,rtm,t} + H_{ve}^{hvac} \theta_{w,t}^{sup,hvac} + \Phi_{w,t}^{ia,hvac}}{H_{tr,is}^{hvac} + H_{ve}^{hvac}} + \frac{\left(1 + H_{tr,is}^{hvac} R_6\right) \eta_{eff}^{hvac} * \left[P_{w,rtm,t}^{hvac,heat} - P_{w,rtm,t}^{hvac,cool}\right]}{H_{tr,is}^{hvac} + H_{ve}^{hvac}} \tag{4.23a}$$

$$\theta_{w,rtm,t}^{mt,hvac} = \frac{R_2}{R_3} \theta_{w,rtm,t-1}^{mt,hvac} + \frac{R_1}{R_3} + \frac{1}{R_3} \frac{H_{tr,3}^{hvac} H_{tr,1}^{hvac}}{H_{tr,2}^{hvac} H_{ve}^{hvac}} \eta_{eff}^{hvac} * \left[P_{w,rtm,t}^{hvac,heat} - P_{w,rtm,t}^{hvac,cool}\right] \tag{4.23b}$$

$$0 \leq P_{w,rtm,t}^{hvac,heat} + P_{w,rtm,t}^{hvac,cool} \leq P_{max}^{hvac} \tag{4.23c}$$

$$\theta_{min}^{air,hvac} \leq \theta_{w,rtm,t}^{air,hvac} \leq \theta_{max}^{air,hvac} \tag{4.23d}$$

The air temperature in eq. 4.23a depends on the surface wall temperature (eq. 1m) associated to R_5 and R_6 plus inner heat gains $\Phi_{w,t}^{ia,hvac}$, ventilation transfer coefficient ($\theta_{w,rtm,t}^{mt,hvac}$) and heating/cooling decisions. The internal wall temperature $\theta_{w,rtm,t}^{mt,hvac}$ is associated with internal wall heat flow (related to R_1), previous wall temperature and HVAC heating/cooling decisions. The expression 4.23c limits HVAC consumption, and 4.23d limits air temperature under comfort requirements. Usual HVAC formulations are associated with binary variables for heating/cooling decisions. However, in this case, a relaxed-restricted heuristic explained in section 4.2.4 is implemented as a binary model replacement.

The HVAC Flexibility estimation begins by limiting the flexibility based on its demand. The expression 4.24a limits upward flexibility as the difference between maximum consumption and demand at $t+k$ time, while downward flexibility is limited in 4.24b and 4.24c as the capacity of the appliance to move from their scheduled demand. Air temperature limitations for upward and downward flexibility are expressed in 4.24d and 4.24e.

$$0 \leq P_{w,rtm,t+k}^{hvac,heat} + Fup_{w,rtm,t,k}^{hvac,heat} + P_{w,rtm,t+k}^{hvac,cool} + Fup_{w,rtm,t,k}^{hvac,cool} \leq P_{max}^{hvac} \tag{4.24a}$$

$$Fdn_{w,rtm,t,k}^{hvac,heat} \leq P_{w,rtm,t+k}^{hvac,heat} \tag{4.24b}$$

$$Fdn_{w,rtm,t,k}^{hvac,cool} \leq P_{w,rtm,t+k}^{hvac,cool} \tag{4.24c}$$

$$\theta_{min}^{air,hvac} \leq \theta_{w,rtm,t,k}^{air,hvac,UpEval} \leq \theta_{max}^{air,hvac} \tag{4.24d}$$

$$\theta_{min}^{air,hvac} \leq \theta_{w,rtm,t,k}^{air,hvac,DnEval} \leq \theta_{max}^{air,hvac} \tag{4.24e}$$

Temperature calculation under flexibility scenarios is shown in expression 4.25. The impact of the offered flexibility is considered in the internal wall and air temperature for upward flexibility (expressions 4.25a, 4.25b and 4.25c) and downward flexibility (expressions 4.25d, 4.25e and 4.25f).

HVAC temperature limits under flexibility [eq. 4.25]:

$$\theta_{w,rtm,t,k}^{air,hvac,UpEval} = \frac{H_{tr,is}^{hvac} R_{5,w,rtm,t+k} + H_{ve}^{hvac} \theta_{w,t+k}^{sup,hvac} + \Phi_{w,t+k}^{ia,hvac}}{H_{tr,is}^{hvac} + H_{ve}^{hvac}} \tag{4.25a}$$

$$+ \frac{\left(1 + H_{tr,is}^{hvac} R_6\right)}{H_{tr,is}^{hvac} + H_{ve}^{hvac}} \eta_{eff}^{hvac} \left[P_{w,rtm,t+k}^{hvac,heat} + Fup_{w,rtm,t,k}^{hvac,heat} - P_{w,rtm,t+k}^{hvac,cool} - Fup_{w,rtm,t,k}^{hvac,cool}\right]$$

$$\theta_{w,rtm,t,k}^{mt,hvac,UpEval} = \frac{R_2}{R_3} \theta_{w,rtm,t-1}^{mt,hvac} + \frac{R_1}{R_3} \tag{4.25b}$$

$$+ \frac{1}{R_3} \frac{H_{tr,3}^{hvac} H_{tr,1}^{hvac}}{H_{tr,2}^{hvac} H_{ve}^{hvac}} \eta_{eff}^{hvac} * \left[P_{w,rtm,t+k}^{hvac,heat} + Fup_{w,rtm,t,k}^{hvac,heat} - P_{w,rtm,t+k}^{hvac,cool} - Fup_{w,rtm,t,k}^{hvac,cool}\right]$$

$$\theta_{w,rtm,t,k}^{mt,hvac,UpEval} = \frac{R_2}{R_3} \theta_{w,rtm,t,k-1}^{mt,hvac,UpEval} + \frac{R_1}{R_3} \tag{4.25c}$$

$$+\frac{1}{R_3}\frac{H_{tr,3}^{hvac}H_{tr,1}^{hvac}}{H_{tr,2}^{hvac}H_{ve}^{hvac}}\eta_{eff}^{hvac}*\left[P_{w,rtm,t+k}^{hvac,heat}+Fup_{w,rtm,t,k}^{hvac,heat}-P_{w,rtm,t+k}^{hvac,cool}-Fup_{w,rtm,t,k}^{hvac,cool}\right]$$

$$\theta_{w,rtm,t,k}^{air,hvac,DnEval}=\frac{H_{tr,is}^{hvac}R_{5,w,rtm,t+k}+H_{ve}^{hvac}\theta_{w,t+k}^{sup,hvac}+\Phi_{w,t+k}^{ia,hvac}}{H_{tr,is}^{hvac}+H_{ve}^{hvac}} \tag{4.25d}$$

$$+\frac{\left(1+H_{tr,is}^{hvac}R_6\right)}{H_{tr,is}^{hvac}+H_{ve}^{hvac}}\eta_{eff}^{hvac}\left[P_{w,rtm,t+k}^{hvac,heat}-Fdn_{w,rtm,t,k}^{hvac,heat}-P_{w,rtm,t+k}^{hvac,cool}+Fdn_{w,rtm,t,k}^{hvac,cool}\right]$$

$$\theta_{w,rtm,t,k}^{mt,hvac,DnEval}=\frac{R_2}{R_3}\theta_{w,rtm,t-1}^{mt,hvac}+\frac{R_1}{R_3} \tag{4.25e}$$

$$+\frac{1}{R_3}\frac{H_{tr,3}^{hvac}H_{tr,1}^{hvac}}{H_{tr,2}^{hvac}H_{ve}^{hvac}}\eta_{eff}^{hvac}*\left[P_{w,rtm,t+k}^{hvac,heat}-Fdn_{w,rtm,t,k}^{hvac,heat}-P_{w,rtm,t+k}^{hvac,cool}+Fdn_{w,rtm,t,k}^{hvac,cool}\right]$$

$$\theta_{w,rtm,t,k}^{mt,hvac,DnEval}=\frac{R_2}{R_3}\theta_{w,rtm,t,k-1}^{mt,hvac,DnEval}+\frac{R_1}{R_3} \tag{4.25f}$$

$$+\frac{1}{R_3}\frac{H_{tr,3}^{hvac}H_{tr,1}^{hvac}}{H_{tr,2}^{hvac}H_{ve}^{hvac}}\eta_{eff}^{hvac}*\left[P_{w,rtm,t+k}^{hvac,heat}-Fdn_{w,rtm,t,k}^{hvac,heat}-P_{w,rtm,t+k}^{hvac,cool}+Fdn_{w,rtm,t,k}^{hvac,cool}\right]$$

The flexibility and rebound evaluation for HVAC appliances is presented in expression 4.26, in a similar approach to 4.23 for the alternative flexibility scenario that starts in time t until $t+K+K'$. The constraint 4.26f associates the internal wall temperature to have the same value under regular operation and after offering flexibility.

HVAC model under flexibility and rebound effect [eq. 4.26]:

$$0\leq P_{w,rtm,t,k}^{hvac,heat,[Up,Dn]}+P_{w,rtm,t,k}^{hvac,cool,[Up,Dn]}\leq P_{max}^{hvac} \tag{4.26a}$$

$$\theta_{min}^{air,hvac}\leq\theta_{w,rtm,t,k}^{air,hvac,[Up,Dn]}\leq\theta_{max}^{air,hvac} \tag{4.26b}$$

$$\theta_{w,rtm,t,k}^{air,hvac,[Up,Dn]}=\frac{H_{tr,is}^{hvac}R_{5,w,rtm,t}+H_{ve}^{hvac}\theta_{w,t}^{sup,hvac}+\Phi_{w,t}^{ia,hvac}}{H_{tr,is}^{hvac}+H_{ve}^{hvac}} \tag{4.26c}$$

$$+\frac{\left(1+H_{tr,is}^{hvac}R_6\right)}{H_{tr,is}^{hvac}+H_{ve}^{hvac}}\eta_{eff}^{hvac}\left[P_{w,rtm,t,k}^{hvac,heat}-P_{w,rtm,t,k}^{hvac,cool}\right]$$

$$\theta_{w,rtm,t,k}^{mt,hvac,[Up,Dn]}=\frac{R_2}{R_3}\theta_{w,rtm,t-1}^{mt,hvac}+\frac{R_1}{R_3} \tag{4.26d}$$

$$+\frac{1}{R_3}\frac{H_{tr,3}^{hvac}H_{tr,1}^{hvac}}{H_{tr,2}^{hvac}H_{ve}^{hvac}}\eta_{eff}^{hvac}\left[P_{w,rtm,t,k}^{hvac,heat,[Up,Dn]}-P_{w,rtm,t,k}^{hvac,cool,[Up,Dn]}\right]$$

$$\theta_{w,rtm,t,k}^{mt,hvac,[Up,Dn]}=\frac{R_2}{R_3}\theta_{w,rtm,t,k-1}^{mt,hvac,[Up,Dn]}+\frac{R_1}{R_3} \tag{4.26e}$$

$$+\frac{1}{R_3}\frac{H_{tr,3}^{hvac}H_{tr,1}^{hvac}}{H_{tr,2}^{hvac}H_{ve}^{hvac}}\eta_{eff}^{hvac}\left[P_{w,rtm,t,k}^{hvac,heat,[Up,Dn]}-P_{w,rtm,t,k}^{hvac,cool,[Up,Dn]}\right]$$

$$\theta_{w,rtm,t,K+K'}^{mt,hvac,[Up,Dn]}=\theta_{w,rtm,t+K+K'}^{mt,hvac} \tag{4.26f}$$

Electric Water Heater

The presence of EWH in households Lakshmanan, Sæle, and Degefa (2021) and their capacity to store heat with minimal losses shows its importance for demand shifting and flexibility services. The EWH model used in this work (expression (4.27)) is based on the one-node approach, where the water temperature is assumed to be homogeneous throughout the tank. The expression 4.27a introduces the temperature evolution per time-step, including the user's water usage ($Wuse_t$) and thermal losses with the room (W_{tank}). Expression (4.27b) limits the water temperature, while expression 4.27c limits EWH power. Water temperature ($\theta^{ewh}_{w,rtm,t}$) is the 'storage state' for EWH.

$$\theta^{ewh}_{w,rtm,t} = \theta^{ewh}_{w,rtm,t-1}\frac{V_{tank}-Wuse_t}{V_{tank}} + \theta^{input}_{water}\frac{Wuse_t}{V_{tank}} + \frac{P^{ewh}_{w,rtm,t} - W_{tank}(\theta^{ewh}_{w,rtm,t-1}-\theta_{room})}{V_{tank}\rho_{water}\frac{Cp_{water}}{3600}} \quad if\, t \neq 0 \tag{4.27a}$$

$$\theta^{ewh}_{min} \leq \theta^{ewh}_{w,rtm,t} \leq \theta^{ewh}_{max} \quad \forall t \in T \tag{4.27b}$$

$$0 \leq P^{ewh}_{w,rtm,t} \leq P^{ewh}_{max} \quad \forall t \in T \tag{4.27c}$$

The flexibility evaluation follows the approach presented in previous appliances. The expression 4.28a limits upward flexibility by maximum demand, while 4.28b associate downward flexibility to EWH demand that can be reduced. The upward flexibility is evaluated in expressions 4.28d and 4.28e as the increase in water temperature under upward flexibility, while expressions 4.28f and 4.28g are the analogous constraints for downward flexibility. The water temperature is limited by 4.28c.

EWH operation under flexibility bid [eq. 4.28]:

$$0 \leq P^{ewh}_{w,rtm,t+k} + Fup^{ewh}_{w,rtm,t,k} \leq P^{ewh}_{max} \quad \forall t \in T \tag{4.28a}$$

$$Fdn^{ewh}_{w,rtm,t,k} \leq P^{ewh}_{w,rtm,t+k} \tag{4.28b}$$

$$\theta^{ewh}_{min} \leq \theta^{ewh,[UpEval,DnEval]}_{w,rtm,t,k} \leq \theta^{ewh}_{max} \quad \forall t \in T \tag{4.28c}$$

$$\theta^{ewh,UpEval}_{w,rtm,t,k} = \theta^{ewh}_{w,rtm,t-1}\frac{V_{tank}-Wuse_{t+k}}{V_{tank}} + \theta^{input}_{water}\frac{Wuse_{t+k}}{V_{tank}} + \frac{P^{ewh}_{w,rtm,t+k} + Fup^{ewh}_{w,rtm,t,k} - W_{tank}(\theta^{ewh}_{w,rtm,t-1}-\theta_{room})}{V_{tank}\rho_{water}\frac{Cp_{water}}{3600}} \quad if\, k = 0 \tag{4.28d}$$

$$\theta^{ewh,UpEval}_{w,rtm,t,k} = \theta^{ewh,UpEval}_{w,rtm,t,k-1}\frac{V_{tank}-Wuse_{t+k}}{V_{tank}} + \theta^{input}_{water}\frac{Wuse_{t+k}}{V_{tank}} + \frac{P^{ewh}_{w,rtm,t+k} + Fup^{ewh}_{w,rtm,t,k} - W_{tank}(\theta^{ewh,UpEval}_{w,rtm,t,k-1}-\theta_{room})}{V_{tank}\rho_{water}\frac{Cp_{water}}{3600}} \quad if\, k \neq 0 \tag{4.28e}$$

$$\theta^{ewh,DnEval}_{w,rtm,t,k} = \theta^{ewh}_{w,rtm,t-1}\frac{V_{tank}-Wuse_{t+k}}{V_{tank}} + \theta^{input}_{water}\frac{Wuse_{t+k}}{V_{tank}} + \frac{P^{ewh}_{w,rtm,t+k} - Fdn^{ewh}_{w,rtm,t,k} - W_{tank}(\theta^{ewh}_{w,rtm,t-1}-\theta_{room})}{V_{tank}\rho_{water}\frac{Cp_{water}}{3600}} \quad if\, k = 0 \tag{4.28f}$$

$$\theta^{ewh,DnEval}_{w,rtm,t,k} = \theta^{ewh,DnEval}_{w,rtm,t,k-1}\frac{V_{tank}-Wuse_{t+k}}{V_{tank}} + \theta^{input}_{water}\frac{Wuse_{t+k}}{V_{tank}} + \frac{P^{ewh}_{w,rtm,t+k} - +Fdn^{ewh}_{w,rtm,t,k} - W_{tank}(\theta^{ewh,DnEval}_{w,rtm,t,k-1} - \theta_{room})}{V_{tank}\rho_{water}\frac{Cp_{water}}{3600}} \quad if\ k \neq 0 \tag{4.28g}$$

The flexibility and rebound evaluation for EWH is presented in expression 4.29 for the alternative flexibility scenario between time t and $t+K+K'$. The constraint 4.29e couples the water temperature at the end of the rebound time with temperature under regular operation.

$$\theta^{ewh}_{min} \leq \theta^{ewh,[Up,Dn]}_{w,rtm,t,k} \leq \theta^{ewh}_{max} \quad \forall t \in T \tag{4.29a}$$

$$0 \leq P^{ewh,[Up,Dn]}_{w,rtm,t,k} \leq P^{ewh}_{max} \quad \forall t \in T \tag{4.29b}$$

$$\theta^{ewh,[Up,Dn]}_{w,rtm,t,k} = \theta^{ewh}_{w,rtm,t-1}\frac{V_{tank}-Wuse_{t+k}}{V_{tank}} + \theta^{input}_{water}\frac{Wuse_{t+k}}{V_{tank}} + \frac{P^{ewh,[Up,Dn]}_{w,rtm,t,k} - W_{tank}(\theta^{ewh}_{w,rtm,t-1} - \theta_{room})}{V_{tank}\rho_{water}\frac{Cp_{water}}{3600}} \quad if\ k = 0 \tag{4.29c}$$

$$\theta^{ewh,[Up,Dn]}_{w,rtm,t,k} = \theta^{ewh,[Up,Dn]}_{w,rtm,t,k-1}\frac{V_{tank}-Wuse_{t+k}}{V_{tank}} + \theta^{input}_{water}\frac{Wuse_{t+k}}{V_{tank}} + \frac{P^{ewh,[Up,Dn]}_{w,rtm,t,k} - W_{tank}(\theta^{ewh,[Up,Dn]}_{w,rtm,t,k-1} - \theta_{room})}{V_{tank}\rho_{water}\frac{Cp_{water}}{3600}} \quad if\ k \geq 0 \tag{4.29d}$$

$$\theta^{ewh,[Up,Dn]}_{w,rtm,t,K+K'} = \theta^{ewh}_{w,rtm,t+K+K'} \tag{4.29e}$$

Photovoltaic Panels

The expected PV generation was precalculated and not included in the optimisation model, based on the forecasted solar irradiance, outdoor temperature, PV cell properties, zenith, and azimuth, as presented in expression 4.30. The PVlib library was used to calculate hourly solar of direct horizontal irradiance (DHI) and diffuse normal irradiance (DNI) using the Boland approximation Boland et al. (2001) to estimate the irradiance in the plane of array (PoA) of the solar panels.

$$\theta^{cell,PV}_{w,t} = \theta^{e}_{w,t} + \left[\frac{NOCT-20}{800}\right] * G^{PoA}_{w,t} \tag{4.30a}$$

$$\eta^{elec,PV}_{w,t} = \eta^{ref,pv}\left(1 - N^{T,pv}(\theta^{cell,PV}_{w,t} - \theta^{ref})\right) \tag{4.30b}$$

$$E^{pv}_{w,t} = n^{pv} * A^{pv} * G^{PoA}_{w,t} * \eta^{elec,PV}_{w,t} \tag{4.30c}$$

The PV operation differs from previous appliances. The solar panels do not have a 'storage state' because they depend on instantaneous solar irradiance, offering flexibility by curtailing their generation. The PV generation and curtailment under regular operation are presented in expression 4.31a. The upward flexibility is related to the capacity to reduce its generation from the expected value in 4.31b. In contrast, downward flexibility depends on energy curtailed (expression 4.31c). The flexibility and rebound operation is described in expression 4.31d.

$$P^{pv}_{w,rtm,t} + PC^{pv}_{w,rtm,t} = E^{pv}_{w,t} \tag{4.31a}$$

$$Fup^{pv}_{w,rtm,t,k} <= P^{pv}_{w,rtm,t+k} \qquad \forall k \in K \tag{4.31b}$$

$$Fdn^{pv}_{w,rtm,t,k} <= PC^{pv}_{w,rtm,t+k} \qquad \forall k \in K \tag{4.31c}$$

$$P^{pv,[Up,Dn]}_{w,rtm,t,k} + PC^{pv,[Up,Dn]}_{w,rtm,t,k} = E^{pv}_{w,t+k} \qquad \forall k \in K + K' \tag{4.31d}$$

4.2.4 Relaxed-restricted HVAC model operation

In the formulation of HVAC appliances, a good practice is to associate a binary variable with a bigM number to limit the heating and cooling operations of the appliance, where only one binary variable can be active in each time block. This practice added to the model 2 * timeblock * scenario * 'number of appliances' binary variables, increasing the model complexity until it cannot be resolved quickly.

A relaxed-restricted approach is proposed to avoid the increase in the computational complexity of the model. In this approach, a first iteration of the HVAC scheduling and operation is calculated, allowing heating and cooling at the same timeblock. In the second iteration, only the process that requires more energy in the first iteration is available, forcing the other to be equal to zero. This approach reduces the time required to solve the problem while maintaining the quality of the results when the different appliances are calculated in the VPP model. In section 4.3.1, both formulations for the HVAC appliances are tested.

4.2.5 Price and weather scenarios

The weather scenario generation follows the approach presented in Salgado-Bravo, Kirli, Negrete-Pincetic, and Kiprakis (2025), which proposes the cloud index indicator as input to an LSTM model trained to forecast solar irradiance and temperature. The Markov transition probability defines possible transitions in cloud conditions, generating eight temperature and solar irradiance scenarios with different cloud conditions and indicating the probability of each scenario. The model was trained using weather data from San Diego, California.

The scenarios for DAM and RTM prices have been considered independent of the weather scenario generator. The Deep-VAR model Salinas et al. (2019, 2020) was trained using energy prices data from 2017 to 2019, using PyTorch Forecasting libraries. The multivariate Gaussian copula process allows the forecast model to be run multiple times to estimate the percentiles used as pricing scenarios. A total of 100 iterations were run to calculate five levels of percentile: 10th, 25th, 50th, 75th and 90th percentiles. By default, only the 10th and 90th percentiles in case studies were evaluated unless otherwise stated.

4.2.6 Case studies

To validate the model's capacity to capture flexibility under a day-ahead predefined trajectory, the operational cost and flexibility offered under different scenario conditions will be evaluated:

Test 1 - Comparison between HVAC binary operational model and relaxed-constrained operation.

Test 2 - Flexibility evaluation under fixed DAM and RTM prices.

Test 3 - Flexibility estimation under DAM, RTM and weather scenarios per season.

Test 4 - Differences between stochastic and naive forecast for weather and pricing.

Test 5 - Variations in the rebound duration for a flexibility requirement

Test 6 - Evaluation of the flexibility offered using primary frequency response pricing.

The HVAC formulation presented in section 4.2.3 does not consider the capacity to limit its operation to heat or cooling in a timeblock. Because of this limitation, Test 1 estimates the difference between the binary operation (chooses between heating and cooling using binary variables) and a double operation of the model as indicated in section 4.2.4. The validated relaxed-restricted HVAC operation will be used on the other tests.

Tests 2 to 4 evaluate the VPP flexibility under different market conditions. Starting with a basic fixed tariff to understand the flexibility available in demand, adding DAM and RTM forecasting schemes, plus seasonal effects in weather as elements that can modify flexibility in the system.

Test 5 will evaluate the changes in flexibility based on the rebound duration. The aim is to observe how the VPP restoration capacity allows the appliances to increase or reduce the flexibility offered.

Finally, test 6 uses the regulation-down prices from CAISO as flexibility prices to evaluate differences in flexibility during the day under realistic conditions. The stochastic and naive prices will be considered in the test.

For the presented set of test cases, two sets of appliances were used to evaluate the effectiveness of the model:

- 50 appliances - 10 HVAC, 10 PP, 10 EWH, 10 PV and 10 EV (Test 1)
- 500 appliances - 100 HVAC, 100 PP, 100 EWH, 100 PV and 100 EV (Test 2 to 6)

4.2.7 Data sources

The house properties for the HVAC model are extracted from the TABULA and EPISCOPE projects database Loga et al. (2016); *Website of the TABULA and EPISCOPE projects, section Publications/Download* (n.d.). Houses from Spain, Italy, and France were selected because of their similarities in climate and household characteristics in the southwestern part of the USA. Each EWH evaluated has a 120L tank and a maximum power consumption of 2200W. The hot water consumption profiles were generated with the software *Load Profile Generator* Pflugradt (2016). The Pool Pumps were selected from 46 commercial pool pump models, assuming their requested energy demand as the energy required to filter the total amount of water at least twice daily. PV panel properties come from the module JASolar JAM66S30 500/MR, with peak power randomised between 2 kW to 10 kW, orientation true south $\pm 15^{\circ}$. Angle is $32^{\circ} \pm 5^{\circ}$.

The EV properties were extracted from the 30 most viewed vehicles in the *EV Database Electric Vehicle Database* (n.d.), while the expected penalty from battery usage is based on the battery degradation estimation from mileage presented in Canals Casals, Etxandi-Santolaya, Bibiloni-Mulet, Corchero, and Trilla (2022). According to the battery size per EV, the total energy required by the EV to get a 25% Depth of Discharge is calculated, which is the recommended battery degradation for replacing EV batteries. The replacement cost is calculated assuming a $ 120 USD per kW from the battery size plus $ 500 USD in labour. When the battery is discharged, the expected degradation cost is reached by dividing the replacement cost by the total energy required to replace the batteries.

The cloud type information and solar irradiance for the weather scenario generator were obtained from the National Solar Radiation Database (NSRDB) Sengupta et al. (2018), location San Diego International Airport (KSAN), California (32° 43' 48", -117° 10' 48"). The cloud type and solar irradiance data from 2013 to 2020 were used for HMM, while data from 2017 to 2019 were employed to train LSTM models. Temperature data was obtained from NOAA National Weather Service for the exact location between 2017 and 2019. The case studies were developed in Python 3.9 van Rossum (1995) using additional libraries provided by Tensorflow Abadi et al. (2016) for the weather generator. For optimisation, the DAM and RTM prices were downloaded from the CAISO OASIS platform *California Independent System Operator. Open access same time information system* (2022), and the Deep-Var model Salinas et al. (2019, 2020) was used to forecast DAM and RTM prices. The case studies were coded in Python using Pyomo libraries Hart et al. (2017, 2011). The Boland approximation and estimation of the plane of array (PoA) in the PV panels utilised the PVlib library Anderson et al. (2023). The solver GUROBI Gurobi Optimization, LLC (2024) with a 0.02 MIP GAP is chosen to solve the proposed problems, with a time limit of 3600 seconds if the GAP is not reached.

4.3 Results

Before discussing the six tests proposed in the section 4.2.6, the results from September 19 will be presented to explain the trajectories and flexibility estimation obtained from the model.

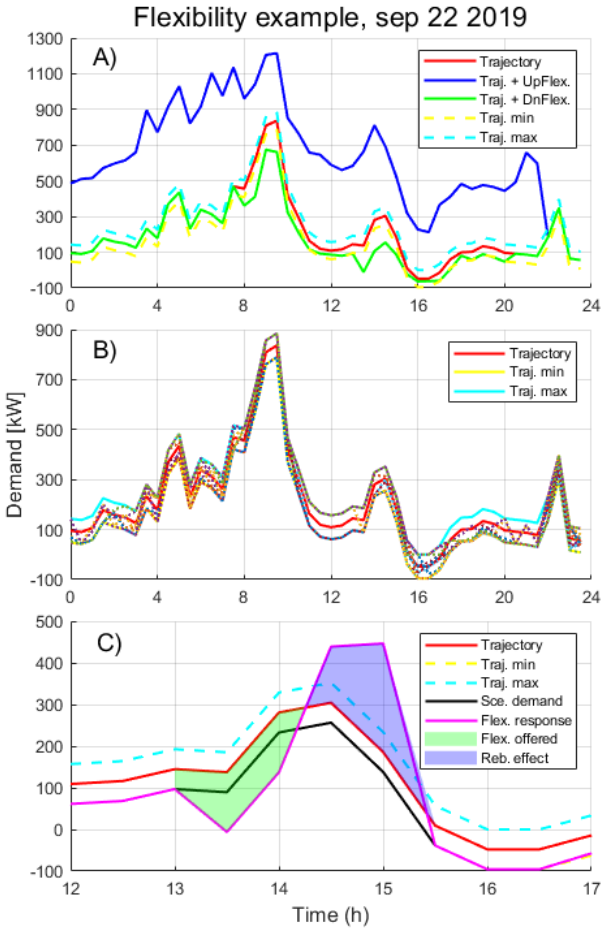

Figure 4.1: Demand trajectory and flexibility obtained from the 500 appliances. Figure A shows the trajectory, band limitations, and upward and downward flexibility obtained. Figure B shows the trajectory, band limits and demand obtained in each stochastic scenario (dotted lines). Figure C shows a downward flexibility requirement being served by the model. The green area is the downward flexibility offered from the proposed trajectory, and the blue area is the rebound effect of the flexibility offered.

Figure 4.1 shows the day-ahead proposed trajectory, upward and downward flexibility, and the effect of offering flexibility in the demand for one day as a demonstrative case. The flexibility price for upward and downward was $10 USD/MW, with the upward flexibility significantly higher than the offered downward flexibility at the same price. In figure 4.1.A the minimum and maximum trajectories are added as the allowed deviation without penalisation from the proposed demand trajectory. Figure 4.1.B adds the demand per stochastic scenario (2 price and eight weather scenarios, 16 cases) as dotted lines, where each demand scenario does

not surpass the trajectory limits (under a $1000 USD/MW penalisation). Figure 4.1.C considers the effect of the downward flexibility at 13.30 hrs, maintains the flexibility requirement for two timeblocks (1 hour) and has a rebound time of 2 timeblocks. The model estimates the flexibility offered as one offer per timeblock but evaluates the capacity to comply with the flexibility offered in each scenario, returning to the expected demand after each rebound time per each flexibility offer.

4.3.1 Comparison between HVAC binary operational model and relaxed-constrained operation.

As indicated in section 4.2.4, a first appliance scheduling is performed assuming the HVAC appliances can heat and cool the building simultaneously. The second scheduling run extracts the HVAC operation results from the first scheduling to limit their operation to the higher demand in each time-step.

The relaxed-restricted HVAC model has been compared with the binary HVAC scheduling model, using the objective function as the comparison parameter. Table 4.1 shows the objective function for the relaxed HVAC operation and the percentage of difference from the lowest objective function obtained, limited to 15 minutes in the calculation. The limitation stems from the low number of appliances tested (10 HVAC loads). Considering a higher number of loads or more scenarios would increase the computational time required for the binary model to hours or even days, making it impractical for a fast and daily/hourly operation model.

Table 4.1: Comparison between the objective function for the relaxed HVAC operation and its difference with the relaxed-constrained method (forced) and the HVAC binary operation, considering only 10 HVAC appliances in the first case and 10 HVAC, PP, EV, EWH and PV in the second case.

	10 HVAC appliances			Each appliance x10		
Case	objFun relaxed	Diff. forced	Diff. binary	objFun relaxed	Diff. forced	Diff. binany
march 20	4.46	0.25%	0.27%	9.27	0.03%	0.03%
march 21	4.54	5.40%	5.46%	9.45	2.57%	2.56%
march 22	3.39	1.94%	1.93%	6.11	0.54%	0.87%
june 20	2.20	0.52%	0.64%	6.40	0.02%	0.01%
june 21	1.81	1.04%	1.16%	5.32	0.02%	0.01%
june 22	1.64	1.94%	1.85%	4.54	0.04%	0.02%
sep 20	1.89	1.75%	2.45%	8.48	0.05%	0.05%
sep 21	2.05	1.33%	1.78%	9.62	0.02%	0.02%
sep 22	1.63	11.58%	18.95%	6.86	0.04%	0.05%
dec 20	6.52	1.45%	1.64%	18.20	0.01%	0.01%
dec 21	5.78	24.47%	18.03%	18.13	0.01%	0.01%
dec 22	4.84	0.39%	0.45%	16.11	0.01%	0.01%

The difference in the objective function between the relaxed-restricted and binary models from the 10 HVAC case is higher than the values obtained in the all-appliances case. Including additional flexible loads in the problem reduced the difficulty of operating within the proposed trajectory band, as well as the PV, which can inject energy into the grid, thereby reducing operational costs at midday. The average and standard deviation from the presented results are introduced in table 4.2.

Table 4.2: Average and standard deviation values of the difference from the relaxed-restricted and binary approach from the relaxed objective function. The values labelled 'without extreme cases' exclude values from Sep 22 and Dec 21 in table 4.1.

	10 HVAC			
	Average forced	Stdev forced	Average binary	Stdev binary
Diff. percentage	4.34%	7.09%	4.55%	6.65%
Diff. objFun	0.180	0.396	0.163	0.293
Diff. percentage without extreme cases	1.60%	1.47%	1.76%	1.48%
Diff. objFun without extreme cases	0.056	0.072	0.060	0.072

	each appliance X10			
	Average forced	Stdev forced	Average binary	Stdev binary
Diff. percentage	0.28%	0.74%	0.30%	0.75%
Diff. objFun	0.025	0.069	0.026	0.070

The average difference between the 10 HVAC loads and each appliance by 10 for the relaxed-restricted and binary approach presents similar values. The difference in the percentage obtained from the 10 HVAC loads comes from the increased cost in the relaxed-restricted case (24.47% against 18.03% from the binary case) in one of the days with higher operational costs. Whether the two days with higher differences are removed from the analysis, the average and difference are practically the same value for both approaches. Meanwhile, the results obtained with each appliance by 10 are identical (table 4.2). The values obtained show no significant difference in the results from both approaches, validating the use of the relaxed-restricted approach in the presented model for evaluating a higher number of appliances across more scenarios in a shorter time than a binary heating/cooling approach.

4.3.2 Flexibility estimation under fixed prices

The flexibility response assuming a fixed DAM and RTM price of $20 [USD/MW] was evaluated, where the offered flexibility price varies between $1 [USD/MW] to $200 [USD/MW]. Four days were evaluated (March 22, June 22, September 22 and December 22), evaluating eight weather scenarios adapted to each month. Figure 4.2 shows the hourly flexibility offered under a two timeblock flexibility and rebound time, where each timeblock corresponds to 30 minutes. The upward and downward flexibility were estimated individually, and the flexibility values in figure 4.2 were normalised using the average demand trajectory with a flexibility price of $1 [USD/MW] as reference.

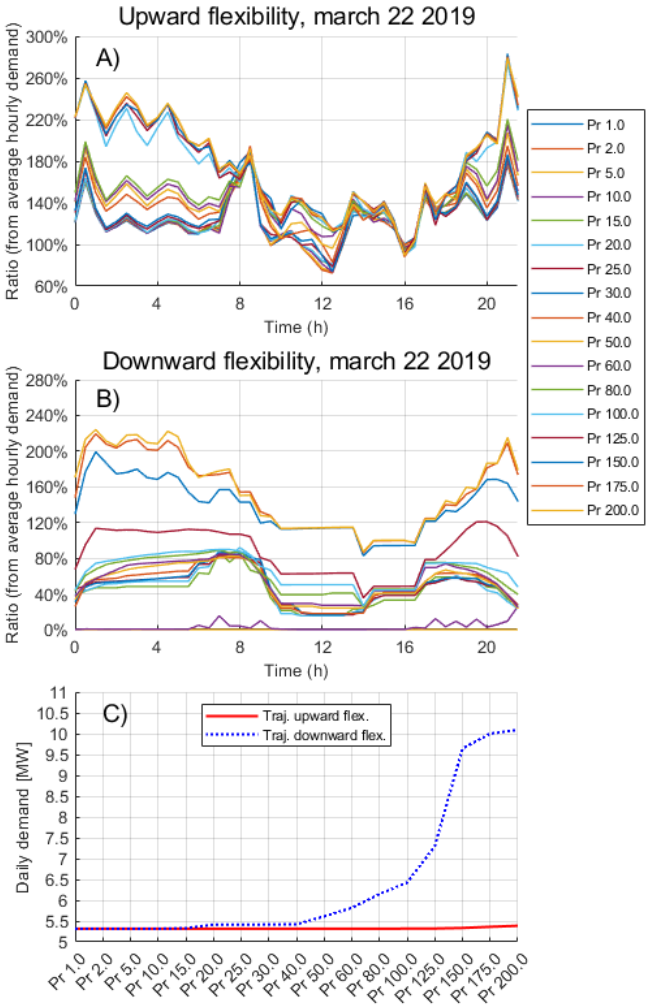

Figure 4.2: Upward and downward flexibility for March 22, 2019. The flexibility price rises from $1 [USD/MW] to $200 [USD/MW], demonstrating the model response to price signals. The increase in the average demand trajectory (figure C) comes from the solar generation curtailed to increase negative flexibility at higher prices.

Figure 4.2.A shows the upward flexibility response to the flexibility price. The offered upward flexibility used to be high at low prices due to the nature of the offered flexibility, where the system is paid to increase its demand, while simultaneously decreasing its consumption in the rebound period. This behaviour can be considered a double benefit, offering both flexibility in payment and savings from reduced energy requirements during the rebound time. Under this approach, it could be possible for the aggregator to respond to negative upward flexibility prices.

On the other side, figure 4.2.B shows the downward flexibility response to the prices, being nearly zero unless the flexibility price provided surpasses $10 [USD/MW]. The jump in flexibility between $10 and $15 [USD/MW] is done by the pool pumps, as the element with minimal cost to offer flexibility rather than energy costs in rebound time. The differences in flexibility between $15 to $100 [USD/MW] can be associated with the efficiency in the flexibility offered, plus weather conditions. An example is the variation in flexibility between 9:00 and 14:00 hrs, associated exclusively with the energy curtailed from solar generation. The second jump in flexibility is a mixture between the solar panel curtailment and the EV discharge associated with the penalisation cost introduced by battery discharge. From figure 4.2.C is observed the 'increase' in the average demand trajectory is mainly responsible for the curtailment decision of the PV panels, with minor adjustments from the HVAC and EWH operations.

The total downward flexibility offered divided by 24 hours from the appliances is shown in figure 4.3, where fig. 4.3.A sustain the idea of a first deployment of flexibility from pool pumps, a lower flexibility increase between $15 to $100 [USD/MW] and a second jump after $125 [USD/MW], a valid observation from the four days evaluated. Some differences in the flexibility response curve between March and the rest of the months are attributed to weather conditions.

The increase in flexibility, as represented by the pricing divided by the price difference, is presented in figure 4.3.B for March 22. The observed increase was fitted using normal distributions, allowing for the separation of four different effects on flexibility. For the total flexibility offered, the normal cumulative density function (normCDF) is proposed, as shown in expression 4.32, where 'erf' is the Gauss error function.

$$Flex^{fit}(p) = \sum_{i=1}^{4} A_i \Phi\left(\frac{p-\mu_i}{\sigma_i}\right) \tag{4.32a}$$

$$= \sum_{i=1}^{4} \frac{A_i}{2}\left[1 + erf\left(\frac{p-\mu_i}{\sqrt{2}\sigma_i}\right)\right] \tag{4.32b}$$

The effectiveness of using normCDF to fit the offered downward flexibility is seen in figure 4.3.C. The RMSE and R-square values for the four cases are presented in table 4.3, with RMSE values lower than 2000 W, indicating a maximum flexibility of nearly 0.6 MW. The R-square values are higher than 0.999 in the four cases. The most relevant information from the

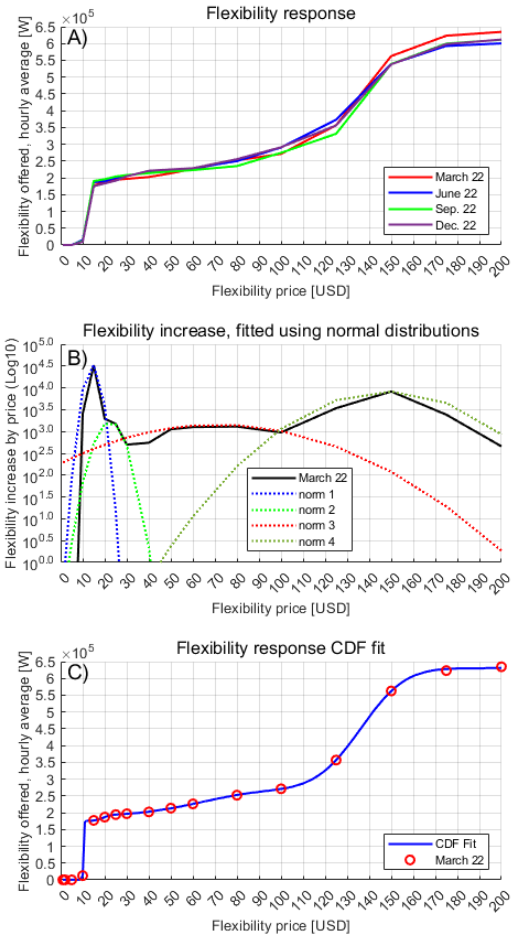

Figure 4.3: Figure A illustrates the downward flexibility response curve to flexibility prices. The increase in the flexibility offered was plotted in Figure B, as the sum of four normal distributions. Figure C presents the downward flexibility response curve fitted with four normal cumulative distribution functions. The focus is to show that at specific price barriers, the flexibility changes drastically.

CDF fit is the μ and σ values, which indicate the location of the flexibility increase and the weight on the price axis. A first peak is localised by μ_1 between \$10 to \$12.5 [USD/MW], associated with the pool pump flexibility. The value of μ_2 moves between \$19 to \$29 [USD/MW], associated with the first appliances that can offer flexibility with high efficiency (do not charge EV, minimal changes in HVAC and EWH operation). A second localised peak is detected by μ_3 and σ_3, which are the combined effects of the discharge process in EV and an aggressive curtailment in solar plants. The σ_3 value near 15 is explained by the EV penalisation, which differs in each model, as well as the variability of the aggregated demand in each scenario.

Finally, the values of μ_4 and σ_4 are not precisely localised and have a relevant presence but can be associated with the lower increase in flexibility between \$25 to \$100 [USD/MW] seen in 4.3.A, being not as efficient flexibility and weather dependent. The exception to the rule is the μ_3 and μ_4 values for September, where the normal function overlaps.

In conclusion, using the normCDF to moderate flexibility enables us to identify flexibility peaks in price and distribution, and to limit flexibility at higher prices. Even if the flexibility price is \$ 5000 [USD/MW], the aggregator cannot offer more than the available flexibility, being normCDF an appropriate fitting function.

Table 4.3: A, μ and σ values from expression 4.32 plus evaluation metrics RMSE and R-square, obtained from the fit of the flexibility offered with four normal cumulative density functions for the 4 cases evaluated. The energy price in DAM and RTM was fixed at \$20 [USD/MW].

	March 22	June 22	Sept. 22	Dec. 22
μ_1	10.43	10.83	11.89	12.22
σ_1	0.29	0.56	1.17	1.38
A_1	174869.63	180959.72	185730.05	176961.39
μ_2	19.26	26.72	22.94	28.74
σ_2	2.79	10.83	8.92	7.78
A_2	16391.02	40039.30	28186.09	48020.91
μ_3	136.16	137.76	143.65	138.03
σ_3	15.81	15.42	7.30	15.68
A_3	359481.44	275074.92	196640.46	313738.87
μ_4	63.53	91.53	118.15	81.45
σ_4	22.50	20.83	33.17	12.60
A_4	79829.98	101812.80	200000.00	68136.57
RMSE [W]	1561	1222	1417	1901
R-square	0.99994	0.99996	0.99994	0.99990

4.3.3 Flexibility estimation under stochastic DAM and RTM prices

In the previous section, the flexibility was evaluated under a fixed price. Because the energy prices during the flexibility request and rebound time change over time, the 10th and 90th percentiles obtained from the Deep-Var model, as explained in section 4.2.5, have been used as energy forecasts for the DAM and RTM markets.

The total flexibility offered for days 20, 21 and 22 of March, June, September and December is shown in figure 4.4. The upward and downward flexibility was estimated together (4.4.A and 4.4.C) and individually (4.4.B for upward flexibility and 4.4.D for downward flexibility)

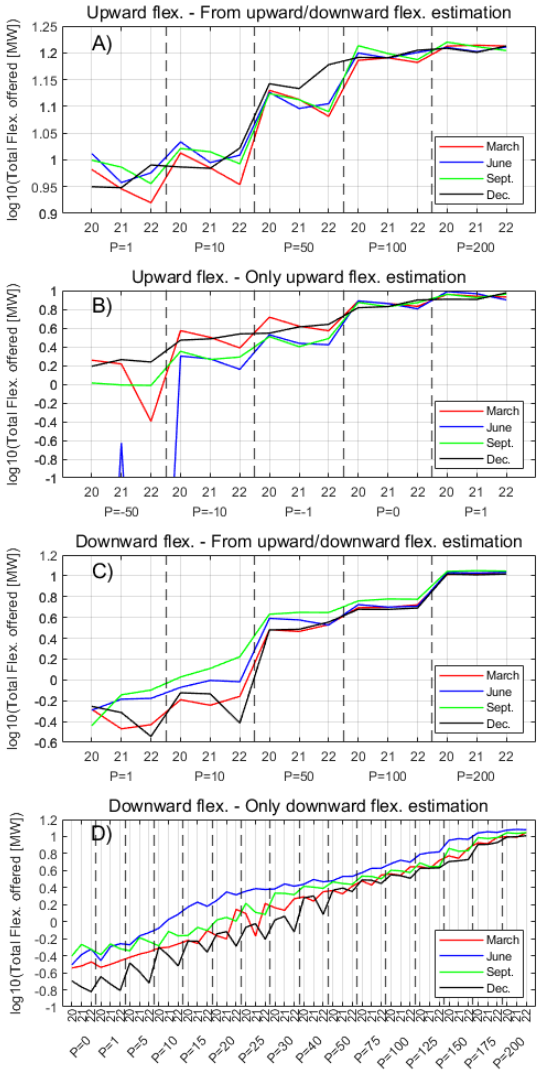

Figure 4.4: Flexibility response curve for upward and downward flexibility under stochastic prices for three days in March, June, September and December. The upward and downward flexibility in Figures A and C were estimated together, while flexibility in Figures B and D was evaluated individually. For upward flexibility, the model was interested in offering flexibility even at $-50 USD/MW, focused on future savings from selling surplus energy or not buying in RTM. For downward flexibility, the number of flexibility prices evaluated was extended to identify normal distributions associated with changes in flexibility.

From the upward flexibility in figure 4.4.A confirms the tendency to offer its flexibility without limitation under a double-benefit logic. Where the model increases its demand and is paid, plus the savings from the energy not required during the rebound time, consequently, upward flexibility can be offered even at negative prices, where the aggregator is willing to pay % 50 USD/MW in some months to provide flexibility (figure 4.4.B). Consequently, there are no active incentives to provide upward flexibility from demand because the model is always available, even with penalties. We must note that this behaviour is possible because there is no limitation on the rebound effect in demand, which increases the flexibility available.

The downward flexibility has changed from the results in section 4.3.2. The total flexibility offered at $ 200 USD/MW decreases considerably from the case with fixed prices. However, the higher variation is associated with the flexibility offered at lower prices. As seen in figure 4.4.C, the flexibility offered at $ -1 and $10 USD/MW differs each month and day, but the influence of the upward flexibility distorts the results. In response, the downward flexibility is shown in figure 4.4.D does not consider the upward flexibility.

The offered flexibility in June 2019 shows a localised increase between % 10 and % 40 USD/MW, which could be explained by the lower energy cost in RTM and higher demand from HVAC loads because of higher temperatures. Demonstrating the weather influence can be difficult, but the price influence can be easier explained, following the fitting procedure using expression 4.32, by extracting the μ values and fitting them with the average daily energy price.

Similar to the results obtained in table 4.3, two μ values can be associated with specific flexibility activation, presented in figure 4.5. A linear fitting shows the relationship between the 10th and 90th percentile average prices for the RTM market and the μ_1 and μ_3 values, which are compared with RTM prices due to their lower cost compared to DAM prices. A lower energy price explains the increase in downward flexibility observed in June in figure 4.4.D, shifting the Gaussian mean (μ_1) to the left while a higher price moves the Gaussian mean to the right, as seen in December. The same happens for μ_3, where the price difference between the flexibility duration time and the rebound time plus the penalisation cost by discharging EVs is represented in 4.5.B, being the intercept value near to the expected penalisation cost of the EV discharge.

4.3.4 Differences by naive and stochastic forecast

The flexibility analysis in previous test cases depends on the weather and price scenarios generated, as indicated in section 4.2.5. For comparison purposes, the day before price and weather conditions (naive scenario) will offer a second flexibility estimation. The objective function of the model using perfect price and weather data will be calculated, following the demand trajectory and flexibility determined by the stochastic and naive scenarios.

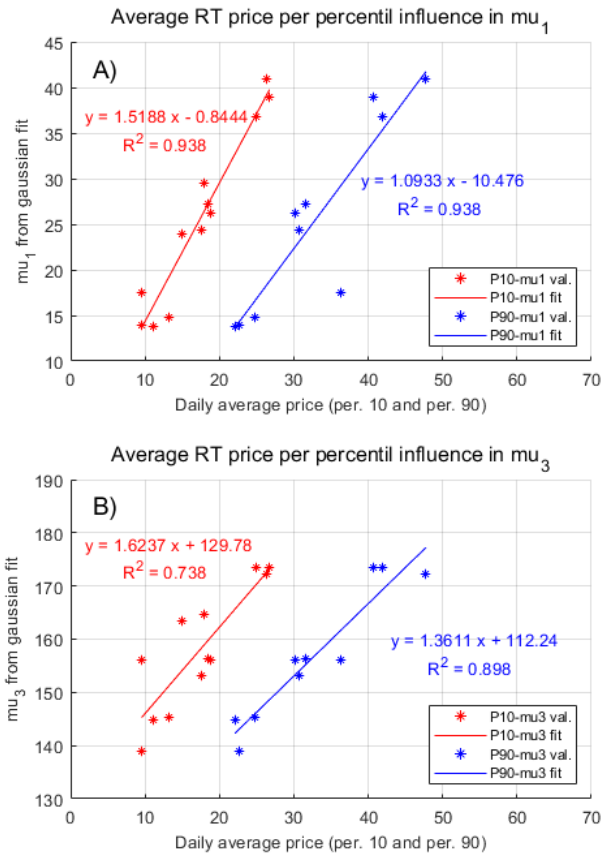

Figure 4.5: Linear fitting between average RTM prices from 10th and 90th percentile scenarios with μ_1 and μ_3 values from the normal CDF fits. The normal mean μ_1 is associated with high-efficiency flexibility sources, while μ_3 is associated with EV discharge penalties and directly depends on the energy prices for rebound purposes. This 'intuitive' conclusion must consider self-consumption from PV generation and price differences between DAM and RTM.

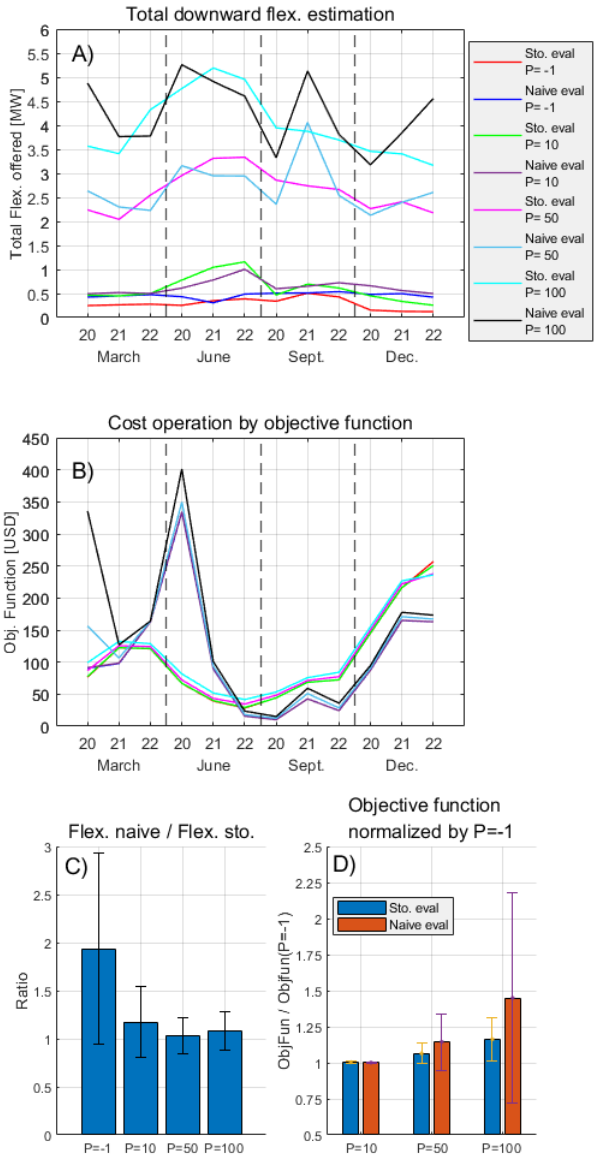

Figure 4.6: Flexibility estimation differences using naive and stochastic weather and price scenarios. Figure A illustrates the difference in total downward flexibility offered at four different flexibility prices. Figure B shows the objective function of both approaches. The naive scenario estimates a hard-to-reach and expensive flexibility offer on March 20, while on June 20, it proposes a trajectory that produces deviations in demand. Figures C and D compare the flexibility and objective function of stochastic and naive scenarios..

Figure 4.6 presents the differences in flexibility and objective function between naive and stochastic scenarios. The naive forecast offers more flexibility than the stochastic forecast, as seen in figure 4.6.A, the naive approach as a unique scenario searches for the time-steps with a lower cost for the flexibility offered. In contrast, the stochastic scenario does not reveal those differences due to the two price options having unrelated values and the variability of

weather scenarios. The exception is the flexibility offered in June for $10 USD/MW, where the stochastic approach presents a better flexibility offer, which coincides with the results exposed in section 4.3.3, where the lower energy prices move the flexibility curve to the left. Although the difference is inversely proportional to the flexibility price, with a lower difference in flexibility as the price increases, as seen in figure 4.6.C.

The objective function using perfect weather and price information with the trajectory and flexibility offered by the stochastic and naive cases is presented in figure 4.6.B. First, the naive forecast shows lower prices and higher flexibility during September and December. However, under high-variability conditions (prices and weather), the naive approach yields high-cost demand trajectories and flexibility conditions that are impossible to follow. A high-cost demand trajectory occurs on June 20, where an incorrect price forecast artificially increases the operational cost, as seen in the four flexibility prices. The increased objective function in March stems from a hard-to-reach and expensive flexibility offer proposed by the model. Conversely, as the model offers more flexibility, the penalisation will have a higher impact on the objective function. Finally, in figure 4.6.D shows the average increase in the objective function in comparison with their values at a flexibility price of $ -1 USD/MW. The flexibility offered by the naive forecast increases their operative cost near 50% at $ 100 USD/MW because the day-before forecast is blind to anomalies or non-expected conditions. In contrast, the stochastic forecast increases its cost but less than the naive forecast.

4.3.5 Limited rebound time effect in flexibility

One of the model's main benefits is introducing the demand trajectory to quantify flexibility and ensure that after the rebound time, the aggregator can return to their expected demand and flexibility offers for the following hours. In contrast, the model forces the flexible appliances to return to the expected 'storage state' value at the end of the rebound time, limiting the available flexibility.

As an exercise to understand how the rebound time modifies the flexibility, the downward flexibility offered will be evaluated by modifying the flexibility duration and rebound time between 1 to 4 time-steps, normalising the results by the flexibility available at equal flexibility duration and rebound time. The flexibility price was $ 10, % 50 and %100 USD/MW, evaluating one day for March, June, September and December.

Two opposite behaviours in flexibility were observed. First, there is a direct dependence between the flexibility offered and the rebound time, as seen in table 4.4. Duplicating the rebound time can increase the flexibility offered by nearly 30%, while reducing the rebound time to half of the flexibility duration reduces its capacity response by 21% to 25%. Both the increase and decrease in flexibility are lower than the increase/decrease in rebound time,

Table 4.4: Flexibility difference for various flexible and rebound timeblocks. Cases with equal flexibility-rebound duration have been used to normalise the flexibility values. The average ratio and deviation come from the cases with flexibility prices of $ 50 and $ 100 USD/MW.

	Reb 1 ± stdev	Reb 2 ± stdev	Reb 3 ± stdev	Reb 4 ± stdev
Flex 1	1	1.29±0.15	1.49±0.27	1.69±0.34
Flex 2	0.79±0.06	1	1.18±0.06	1.33±0.12
Flex 3	0.68±0.05	0.85±0.04	1	1.12±0.05
Flex 4	0.60±0.05	0.76±0.05	0.89±0.03	1

showing how the limitations in the demand and the capacity of the appliances to restore to their expected operation affect the flexibility, respectively. This behaviour was observed in cases with flexibility prices of $50 and $100 USD/MW and in June with a price of $ 10 USD/MW.

Table 4.5: Unexpected behaviour from the rebound influence in flexibility. The flexibility price needed to be increased to observe changes related to the rebound effect, except in some specific hours. The values presented come from the months of September and December 2019, with a flexibility price of $ 10 USD/MW

Sept.

	Reb 1	Reb2	Reb3	Reb4
Flex 1	1	0.95	1.00	1.00
Flex 2	1.05	1	1.04	1.07
Flex 3	1.05	0.91	1	1.11
Flex 4	1.00	0.76	0.86	1

Dec.

	Reb 1	Reb2	Reb3	Reb4
Flex 1	1	0.66	0.52	0.50
Flex 2	1.18	1	1.09	1.06
Flex 3	1.10	1.07	1	1.11
Flex 4	1.29	1.01	0.97	1

The second and unexpected behaviour in flexibility is introduced in table 4.5. The flexibility variations are not directly related to the rebound effect. In some cases, the flexibility offered with a lower rebound time will be greater than the downward flexibility in the symmetrical flexibility-rebound case. The explanation for this phenomenon comes from the impact of energy prices on flexibility. The reward of providing flexibility does not surpass the additional cost of the rebound, so the model is reluctant to offer flexibility except during specific hours. Whether the model is forced to extend their rebound to hours with a higher energy cost, even less flexibility will be provided. This effect becomes more visible as the flexibility price is lower.

4.3.6 Flexibility provided under primary frequency pricing

In previous sections, the flexibility price was considered as a fixed value to evaluate the response in time and prices for the flexibility offered. Given that this is an unrealistic assumption, the regulation down prices from the CAISO system will be used as the flexibility price, as seen in figure 4.7.A. One day will be evaluated for March, June, September, and December under stochastic and naive forecasts for weather and energy prices.

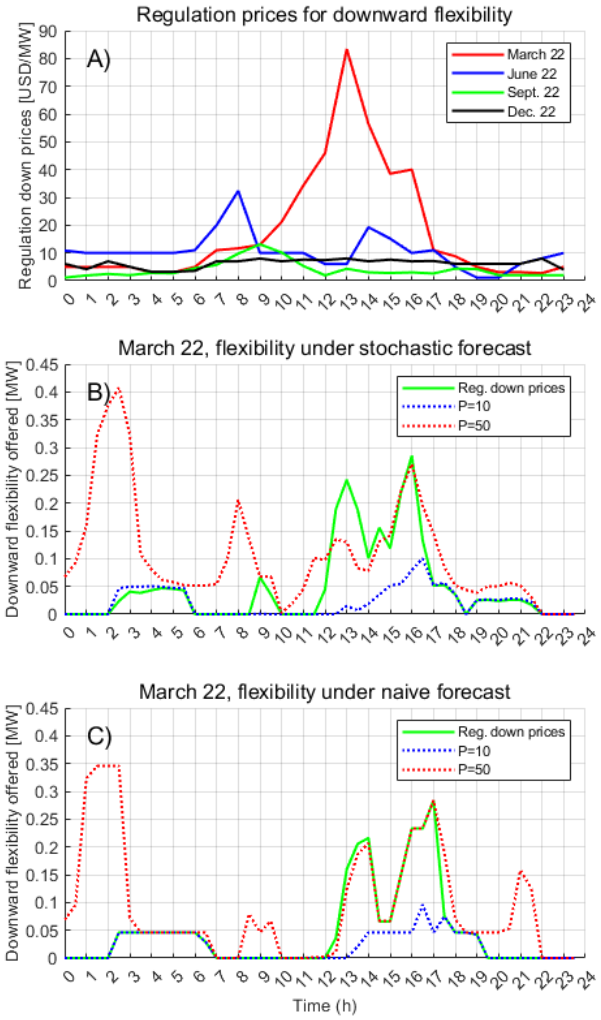

Figure 4.7: Flexibility estimation using the regulation down prices from CAISO. Figure A shows the regulation prices for one day in March, June, September and December. Figure B compares the flexibility estimated under a stochastic mode with the flexibility estimated at $ 10 USD and $50 USD/MW, while the comparison with a naive forecast and the same flexibility prices is shown in Figure C.

The flexibility obtained in June, September and December was similar to the results using a flexibility price of $ 10 USD/MW, showing insufficient differences to be exposed. On the other hand, the flexibility offered in March is responsive to the flexibility price and the forecasting approach. Figure 4.7.B introduces the flexibility response under the stochastic approach, getting similar values to the flexibility estimated at $ 10 USD/MW between 2:00 to 6:00 hrs and between 17:00 to 22:00 hrs., while between 14:00 to 16:00 hrs., the flexibility has similar values to the estimations under $ 50 USD/MW. The higher flexibility values between 12:00 to 14:00 hrs. come from the influence of price and weather scenarios, where the flexibility needs to be capable of being delivered in each scenario, reducing the flexibility available but showing a positive response to higher prices.

The flexibility response differs in the naive forecast approach (figure 4.7.C), where the flexibility values are similar to the flexibility at $ 50 USD/MW, showing no higher responsiveness of the flexibility in the price unless some specific prices are surpassed, even if the flexibility price reaches values over $ 80 USD/MW. This behaviour could be explained by the cost of the model to provide flexibility; in a case with a unique price and weather, the flexibility cost can be considered as a ladder with near-zero σ values (following the normCDF fitting approach introduced in section 4.3.2).

4.4 Conclusions

A day-ahead flexibility estimation model is proposed to study the demand-side response using various flexible appliances available in buildings. The proposed approach operates under the concept of a demand trajectory plus a trajectory band, serving as a slack demand for each scenario, where the flexibility capabilities are measured by the demand deviation from the demand trajectory. The model follows the 'alternative flexibility estimation' idea, which uses branches from the evaluation horizon to estimate flexibility for continuous time intervals. Integrating the rebound effect, along with the 'storage state' variable per appliance, enables the fulfilment of continuous flexibility requirements throughout the day.

The integration of the rebound effect in the flexibility offered enables the model to estimate the flexibility response curve to the flexibility price, allowing it to fit its response as the sum of normal cumulative distribution functions. Under a fixed energy price in day-ahead and real-time markets, two normal distributions identify specific increases in flexibility associated with the pool pump and electric vehicle flexibility. The first peak is associated with efficient flexibility with minimal disadvantages, while the second peak is related to the penalisation cost of discharging the battery. Both normal distribution peaks are confirmed under stochastic weather and pricing, where the σ could be associated with the energy price intra-day variations, and the average energy price can shift the μ values.

The flexibility response curve exhibits a smoother response, considering both weather and price scenarios. Under the normal distribution fitting, the σ value increases due to the variation in energy prices, as well as the effect of weather conditions on the appliance's operation. The flexibility offered under the stochastic approach tends to be lower than naive forecasting. Still, the additional resilience of the stochastic evaluation diminishes the possibility of being penalised if the demand trajectory deviates from the expected values or when the operator cannot provide the offered flexibility. In addition, the operational cost may be higher in the stochastic approach; however, the cost variations when the flexibility price increases are lower.

The restoration capacity of the appliances was observed under modifications to the duration of the rebound time. Whether the rebound time is reduced to half of the flexibility requirement, the total flexibility offered is reduced between 21% to 25%. The opposite effect was similar, with a 30% increase in flexibility when the rebound time is doubled. The introduction and definition of the rebound time enable the model to adapt its flexibility response according to the ISO/DSO requirements for ancillary services, or can be used as a market design tool to understand and value how an extended or shorter rebound time modifies the flexibility offer and its cost to providers.

The proposed model creates multiple opportunities for future work. First, the capacity to model the day-ahead flexibility response curve can simplify the participation of multiple aggregators in a flexibility market, where each participant knows their flexibility response and can evaluate the response from other participants in the market. The agents in the flexibility market could focus more on the market strategies and grid constraints than on the flexibility estimation. Second, the aggregator could extend the alternative flexibility scenario to include multiple flexibility prices simultaneously, offering a responsive flexibility bidding curve with different prices according to the quantity of flexibility required. The mean values from the normal cumulative density function used to fit the response curve can determine some relevant price levels for flexibility offers. Third, the influence of the market rules on the cost of flexibility. The rebound cost, primary, secondary or tertiary regulation market participation, and the capacity to buy energy in day-ahead, real-time, power-purchase agreements, or other energy markets influence the flexibility cost and the aggregator's response to market signals. Finally, the effect of the flexibility market definitions on the flexibility offered. The participation of a demand aggregator can be defined by the requirements to offer flexibility. For example, the response time of the appliances in providing flexibility could change the product offered by the aggregator, where the model estimates the flexibility services for primary, secondary, and tertiary frequency control using the same set of appliances. Fast-response appliances such as electric vehicles, solar panels, and pool pumps, could be part of the primary to tertiary frequency markets, leaving thermal appliances to offer services in tertiary frequency markets.

Chapter 5

Conclusions and future work

This thesis explores the demand-side flexibility estimation problem as a bottom-up approach, starting from basic operational models for flexible appliances as the initial step in the chain, and culminating in the formulation of a stochastic virtual power plant that schedules distributed energy resources to offer their flexibility in the day-ahead market. To address the proposed challenge, the demand deviation capacities of a single appliance and the aggregated response of multiple appliances were studied, including how external elements, external agents, and the coordinator's interest can modify their scheduling and the estimated flexibility, as highlighted below.

In chapter 2, a deterministic approach to estimating demand-side flexibility was proposed, focusing on the 'alternative flexibility scenario' approach to define the reference demand and the flexibility available as the demand deviation for a defined number of time steps. The model estimates the appliances' aggregated deviation capacity and capability to maintain the offered flexibility over time in various weather conditions and energy prices from the day-ahead market.

In chapter 3, a scenario generator for next-day weather conditions was developed to integrate variable weather conditions into the flexible appliance operation. Using a neural network model, the cloud index parameter was utilised as an indicator of cloud conditions to associate with weather patterns. The scenario generator employs the hidden Markov model to analyse cloud transitions during the day, and LSTM models to forecast solar irradiance and temperature for the next 24 hours. The cloud transition probabilities were used to define a set of eight weather scenarios for evaluation under a basic virtual power plant model, resulting in a lower VPP operational cost during exceptional weather conditions compared to naive forecasting.

Finally, in chapter 4 a stochastic virtual power plant model was developed, incorporating the 'alternative flexibility scenario' approach and the weather scenario in the case evaluation. The model employs the 'alternative flexibility scenario' to estimate demand-side flexibility and extends this concept to include a rebound effect within a limited time window, thereby making the proposed approach price-sensitive to flexibility prices. The stochastic VPP can adjust

its operation based on DAM and RTM prices, weather conditions, flexibility conditions, user comfort, and usage behaviour. The model determines the appliance scheduling and aggregated flexibility, being computationally efficient due to the relaxed-restricted implementation for binary variables in thermal models.

The main conclusions of the presented thesis are summarised below:

- The duration of a flexibility requirement impacts flexibility estimation, where the same set of flexible appliances shows different scheduling strategies and flexibility responses according to the duration requirement. The introduction of the 'alternative flexibility scenario' to evaluate the flexibility effect on demand at different time intervals in optimisation models facilitates the test of various flexibility requirements during the day in one iteration, allowing to appraise of flexibility under variable duration with additional iterations or increasing the number of flexibility scenarios, adding computational complexity to the problem.
- Multiple elements influence the flexibility available from a set of appliances, such as energy prices, user comfort and ISO/DSO operational requirements, among others. The flexibility estimation approaches must be easily adaptable to different conditions in various regions/markets, thereby reducing the number of iterations and the computational complexity of the proposed models for evaluating flexibility.
- The representation of various weather patterns in the scenario generation diminishes the effect of unexpected weather changes during the day, which artificially increases the VPP operational cost. The inclusion of cloud condition information facilitates pattern recognition on solar irradiance and temperature scenarios, improving the scheduling of thermal appliances and their flexibility response capacity.
- The incorporation of the rebound effect with a limited duration changes the flexibility estimation model capabilities as a price-sensitive model, allowing it to respond to energy and flexibility prices to schedule appliances and available flexibility. The rebound duration appears as a new element that directly influences the flexibility available, allowing the aggregator agent to offer flexibility immediately after the rebound time.

5.1 Thesis contributions

The main contributions of this thesis can be summarised as follows:

- The development of operational models for flexible appliances with flexibility variables in their formulation, for future integration into aggregated optimisation models. The coordination of flexible appliances permits extended flexibility services that cannot be delivered by the appliances individually.

- The introduction of the 'alternative flexibility scenario' for flexibility estimation diminished the number of iterations required by including both reference demand and flexibility evaluation in the model. Consequently, the model's computational complexity increases, allowing flexibility to be evaluated in each time interval in one iteration rather than iterating over the selected time granularity to obtain the flexibility available during the evaluated time window.
- The use of cloud condition indicators as a cloud index improves the model's capacity to capture temperature and solar irradiance patterns and variations during the day, resulting from changes in cloud conditions. Thermal models benefit most from the cloud changes between scenarios, offering robust appliance scheduling to unexpected changes in weather conditions.
- The rebound effect can be used as a limitation to the appliances to offer flexibility, where the appliances must recover from the demand deviation in a limited time. Under this approach, the flexibility estimation model serves as a sensitive model for flexibility prices, where the additional energy cost during the rebound time in each 'alternative flexibility scenario' is directly related to the flexibility offered.
- The flexibility response can be recognised as the sum of normal cumulative density functions. The mean value from two normal CDFs was associated with low-cost flexibility from pool pumps and electric vehicle flexibility after the activation of battery penalties. The standard deviation may depend on the weather conditions in the evaluated scenarios and the energy price differences between the flexibility and rebound times, requiring further research to correlate their influence on the flexibility response curve.

5.2 Thesis Validation

The central hypothesis of this thesis is that a bottom-up modeling framework, incorporating appliance-level physical constraints (rebound effects), stochastic weather variables, and market price uncertainty, can accurately characterize and provide superior economic management of demand-side flexibility within a Virtual Power Plant context. Based on the results and analysis presented in Chapters 2, 3 and 4; this hypothesis is validated as follows:

- **Verification of physical model and the rebound effect**: The hypothesis suggested that specific appliance limitations are primary drivers of flexibility availability. In Chapter 2, the validation demonstrated that the "alternative flexibility scenario" approach, which accounts for the energy recovery phase (rebound effect), is crucial for grid reliability and accurate flexibility estimation. By contrasting with flexibility models that do not impose time-limited constraints, it was demonstrated that ignoring physical constraints leads to an overestimation of available flexibility.

- **Weather influence and uncertainty**: The hypothesis claimed that integrating weather and price uncertainty would allow for more effective flexibility management. Chapter 3 validated this through the implementation of an LSTM-based scenario generator. The results showed that by mapping temporal dependencies in weather data and defining a set of weather scenarios, the VPP could mitigate the risks of high-cost operational days. The validation of the LSTM architecture (achieving a MAPE below 8% for critical variables) confirms that stochastic modeling is necessary for managing the variability cited in the hypothesis.
- **Economic improvement and market integration**: The hypothesis anticipated that an integrated model would improve the response capacity and economic standing of a VPP. The economic evaluation in Chapter 4 provided the quantitative proof: the integrated framework resulted in a 15% revenue increase over a one-year simulation compared to "naive" baseline models, confirming how the bottom-up flexibility estimation approach translates into measurable economic value and improved market competitiveness for demand-side aggregators.

In summary, the alignment between the obtained results from flexibility estimation and the initial research claims suggests that the proposed models are not only a theoretical idea, but also a practical necessity. The integration of the physical, meteorological, and economic layers successfully addressed the research gaps identified in the introduction, fulfilling the general objective of this doctoral work.

5.3 Research Limitations

The proposed flexibility estimation framework demonstrates improvements in flexibility management, but, several technical and systemic limitations must be acknowledged:

- **Spatial and Thermal Granularity**: The 5R1C thermal model utilized in Chapter 2 is a lumped-parameter approach. This approach is computationally efficient for large-scale simulations because it assumes a uniform internal temperature in each room. Larger buildings exhibit spatial temperature gradients and variations in each time interval, which may lead to user dissatisfaction if the temperature limits are surpassed.
- **Data Dependency**: The forecasting performance detailed in Chapter 3 dependent on the quality and resolution of historical data. The LSTM models were trained on datasets from CAISO and local weather stations from San Diego, US. For places with lower-quality data, the model's effectiveness in associating cloud conditions with weather forecasting will be diminished.

- **Behavioural Uncertainty**: While the thesis accounts for the physical rebound effect, it assumes that users will strictly adhere to the optimised schedules provided by the aggregation agent. The impact of human actions, which could change setpoints or require EVs outside of the expected time window, represents a stochastic behaviour that was outside the scope of this thesis.

5.4 Future research

From the research presented in this thesis, the ideas presented below can be explored in next years:

- The development of a heuristic to optimise the flexibility duration to offer in energy markets based on the scheduled demand, appliance properties, energy prices and historical flexibility duration requirements. Each flexible appliance can participate in multiple flexibility markets, such as non-spin and primary and secondary reserve markets. The heuristic or optimisation model can decide which market will be offered the flexibility, following additional constraints such as flexibility response time, duration, ramp capability or curtailability, to maximise profitability from offering various flexibility services. One approach to achieving these goals is to extend the alternative flexibility scenario to simultaneously include multiple flexibility prices, thereby providing a responsive flexibility bidding curve with different prices for each evaluated market. For example, the model can schedule fast-response appliances, such as electric vehicles, solar panels, and pool pumps, to participate in primary and secondary frequency markets, while leaving thermal appliances to offer services in tertiary frequency markets. An increase in the computational complexity of the problem can limit the effectiveness of this approach.
- The weather scenario generator depends on Markov models to define the probability of each scenario, which could be replaced by a numerical weather prediction or cloud motion vector model to predict future cloud conditions and improve temperature and solar irradiance forecasts, taking advantage of the trained LSTM model, which characterises weather patterns from cloud conditions.
- The characterisation of the flexibility response curve, based on the set of available flexible appliances, weather conditions and pricing scenarios, could reduce or remove the use of optimisation models to evaluate future flexibility by following statistical and data-driven models.
- The influence of the market rules on the cost of flexibility and the flexibility offered. The rebound cost, primary, secondary, or tertiary regulation market participation, and the capacity to buy energy in day-ahead, real-time, or power-purchase agreements, as well as other market requirements or constraints, influence the flexibility cost and the aggregator's response to market signals using the same set of flexible appliances.

- The capacity to model the flexibility response curve per each aggregator can simplify the participation of numerous aggregation agents, such as VPP or DA, in a flexibility market, where each agent knows their flexibility curve and can evaluate the response curve of other agents. Under this approach, the aggregation agents can focus on the market strategies and grid constraints rather than on flexibility estimation.
- Evaluation of behavioural uncertainty from users in the flexibility estimation model. For electric vehicles, the model needs to evaluate unexpected departure scenarios, where users override or stop EV charging schedules. For thermal appliances, explore the trade-off between flexibility provision and user dissatisfaction. This research would benefit from incorporating Reward-based approaches that quantify the economic incentives to prevent users from not following the scheduled operation during critical grid events.

5.5 Final Remarks

This thesis provides a bridge between the physical limits of flexible appliances and the complex signals of the energy market. This work proposes a scalable framework for estimating demand-side flexibility from distributed resources, enabling ISO/DSO operators and aggregation agents to integrate unused appliances and offer flexibility services, thereby facilitating the transition to a reliable and decarbonised energy system.

Bibliography

Abadi, M., Agarwal, A., Barham, P., Brevdo, E., Chen, Z., Citro, C., ... others (2016). Tensorflow: Large-scale machine learning on heterogeneous distributed systems. *arXiv preprint arXiv:1603.04467*.

Aduda, K., Labeodan, T., Zeiler, W., Boxem, G., & Zhao, Y. (2016). Demand side flexibility: Potentials and building performance implications. *Sustainable cities and society*, *22*, 146–163.

Afram, A., & Janabi-Sharifi, F. (2015). Black-box modeling of residential hvac system and comparison of gray-box and black-box modeling methods. *Energy and Buildings*, *94*, 121-149. Retrieved from https://www.sciencedirect.com/science/article/pii/S0378778815001504 doi: https://doi.org/10.1016/j.enbuild.2015.02.045

Alfadda, A., Rahman, S., & Pipattanasomporn, M. (2018). Solar irradiance forecast using aerosols measurements: A data driven approach. *Solar Energy*, *170*, 924-939. Retrieved from https://www.sciencedirect.com/science/article/pii/S0038092X18305309 doi: https://doi.org/10.1016/j.solener.2018.05.089

Ali, S., Malik, T. N., & Raza, A. (2020). Risk-averse home energy management system. *IEEE Access*, *8*, 91779-91798. doi: 10.1109/ACCESS.2020.2994462

Alipour, M., Mohammadi-Ivatloo, B., Moradi-Dalvand, M., & Zare, K. (2017). Stochastic scheduling of aggregators of plug-in electric vehicles for participation in energy and ancillary service markets. *Energy*, *118*, 1168-1179. Retrieved from https://www.sciencedirect.com/science/article/pii/S0360544216315870 doi: https://doi.org/10.1016/j.energy.2016.10.141

Amara, F., Agbossou, K., Cardenas, A., Dubé, Y., & Kelouwani, S. (2015). Comparison and simulation of building thermal models for effective energy management. *Smart Grid and renewable energy*, *6*(04), 95-112.

Anderson, K. S., Hansen, C. W., Holmgren, W. F., Jensen, A. R., Mikofski, M. A., & Driesse, A. (2023). pvlib python: 2023 project update. *Journal of Open Source Software*, *8*(92), 5994. Retrieved from https://doi.org/10.21105/joss.05994 doi: 10.21105/joss.05994

Andrews, A., & Jain, R. K. (2022). Beyond energy efficiency: A clustering approach to embed demand flexibility into building energy benchmarking. *Applied Energy*, *327*, 119989. Retrieved from https://www.sciencedirect.com/science/article/pii/S0306261922012466 doi: https://doi.org/10.1016/j.apenergy.2022.119989

Antonopoulos, I., Robu, V., Couraud, B., Kirli, D., Norbu, S., Kiprakis, A., ... Wattam, S. (2020). Artificial intelligence and machine learning approaches to energy demand-side response: A systematic review. *Renewable and Sustainable Energy Reviews*, *130*, 109899. Retrieved from https://www.sciencedirect.com/science/article/pii/S136403212030191X doi: https://doi.org/10.1016/j.rser.2020.109899

Arendt, K., Jradi, M., Shaker, H. R., & Veje, C. (2018). Comparative analysis of white-, gray- and black-box models for thermal simulation of indoor environment: Teaching building case study. In *Proceedings of the 2018 building performance modeling conference and simbuild co-organized by ashrae and ibpsa-usa, chicago, il, usa* (pp. 26–28).

Arguez, A., Durre, I., Applequist, S., Squires, M., Vose, R., Yin, X., & Bilotta, R. (2010). [NOAA's U.S. Climate Normals (1981-2010). *NOAA National Centers for Environmental Information.*. doi: 10.7289/V5PN93JP

Bampoulas, A., Saffari, M., Pallonetto, F., Mangina, E., & Finn, D. P. (2021). A fundamental unified framework to quantify and characterise energy flexibility of residential buildings with multiple electrical and thermal energy systems. *Applied Energy*, *282*, 116096. Retrieved from https://www.sciencedirect.com/science/article/pii/S0306261920315191 doi: https://doi.org/10.1016/j.apenergy.2020.116096

Barooah, P., Buic, A., & Meyn, S. (2015). Spectral decomposition of demand-side flexibility for reliable ancillary services in a smart grid. In *2015 48th hawaii international conference on system sciences* (p. 2700-2709). doi: 10.1109/HICSS.2015.325

Belmahdi, B., Louzazni, M., & Bouardi, A. E. (2020). A hybrid arima–ann method to forecast daily global solar radiation in three different cities in morocco. *The European Physical Journal Plus*, *135*, 1–23.

Bessa, R., Moreira, C., Silva, B., & Matos, M. (2014). Handling renewable energy variability and uncertainty in power systems operation. *WIREs Energy and Environment*, *3*(2), 156-178. Retrieved from https://wires.onlinelibrary.wiley.com/doi/abs/10.1002/wene.76 doi: https://doi.org/10.1002/wene.76

Bloomberg. (2025). *New energy Outlook 2025.* http://https://about.bnef.com/insights/clean-energy/new-energy-outlook/#overview. (Accessed: 2026-01-03)

Boland, J., Scott, L., & Luther, M. (2001). Modelling the diffuse fraction of global solar radiation on a horizontal surface. *Environmetrics*, *12*(2), 103-116. Retrieved from https://onlinelibrary.wiley.com/doi/abs/10.1002/1099-095X%28200103%2912%3A2%3C103%3A%3AAID-ENV447%3E3.0.CO%3B2-2 doi: https://doi.org/10.1002/1099-095X(200103)12:2<103::AID-ENV447>3.0.CO;2-2

Bothwell, C., & Hobbs, B. F. (2017). Crediting wind and solar renewables in electricity capacity markets: The effects of alternative definitions upon market efficiency. *The Energy Journal*, *38*(1_suppl), 173-188. Retrieved from https://doi.org/10.5547/01956574.38.SI1.cbot doi: 10.5547/01956574.38.SI1.cbot

Boualit, S. B., & Mellit, A. (2016). Sarima-svm hybrid model for the prediction of daily global solar radiation time series. In *2016 international renewable and sustainable energy conference (irsec)* (p. 712-717). doi: 10.1109/IRSEC.2016.7983867

Bouckaert, S., Pales, A. F., McGlade, C., Remme, U., Wanner, B., Varro, L., ... Spencer, T. (2021). *Net zero by 2050: A roadmap for the global energy sector.* (https://iea.blob.core.windows.net/assets/063ae08a-7114-4b58-a34e-39db2112d0a2/NetZeroby2050-ARoadmapfortheGlobalEnergySector.pdf, accessed: 12-12-2024)

Bouzerdoum, M., Mellit, A., & Massi Pavan, A. (2013). A hybrid model (sarima–svm) for short-term power forecasting of a small-scale grid-connected photovoltaic plant. *Solar Energy*, *98*, 226-235. Retrieved from https://www.sciencedirect.com/science/article/pii/S0038092X13004039 doi: https://doi.org/10.1016/j.solener.2013.10.002

Brusokas, J., Pedersen, T. B., Šikšnys, L., Zhang, D., & Chen, K. (2021). Heatflex: Machine learning based data-driven flexibility prediction for individual heat pumps. In *Proceedings of the twelfth acm international conference on future energy systems* (p. 160–170). New York, NY, USA: Association for Computing Machinery. Retrieved from https://doi.org/10.1145/3447555.3464866 doi: 10.1145/3447555.3464866

California Independent System Operator. Open access same time information system. (2022). http://oasis.caiso.com/mrioasis/logon.do. (Accessed: 2022-06-14)

Canals Casals, L., Etxandi-Santolaya, M., Bibiloni-Mulet, P. A., Corchero, C., & Trilla, L. (2022). Electric vehicle battery health expected at end of life in the upcoming years based on uk data. *Batteries*, *8*(10). Retrieved from https://www.mdpi.com/2313-0105/8/10/164 doi: 10.3390/batteries8100164

Center, E. M. (2003). *The gfs atmospheric model.* Retrieved from https://cir.nii.ac.jp/crid/1370848661487497601

Chen, Y., Xu, P., Gu, J., Schmidt, F., & Li, W. (2018). Measures to improve energy demand flexibility in buildings for demand response (dr): A review. *Energy and Buildings*, *177*, 125-139. Retrieved from https://www.sciencedirect.com/science/article/pii/S0378778818310387 doi: https://doi.org/10.1016/j.enbuild.2018.08.003

Chodakowska, E., Nazarko, J., Nazarko, L., Rabayah, H. S., Abendeh, R. M., & Alawneh, R. (2023). Arima models in solar radiation forecasting in different geographic locations. *Energies*, *16*(13). Retrieved from https://www.mdpi.com/1996-1073/16/13/5029 doi: 10.3390/en16135029

Chyong, C. K., Pollitt, M., Reiner, D., & Li, C. (2024). Modelling flexibility requirements in deep decarbonisation scenarios: The role of conventional flexibility and sector coupling options in the european 2050 energy system. *Energy Strategy Reviews*, *52*, 101322. Retrieved from https://www.sciencedirect.com/science/article/pii/S2211467X24000294 doi: https://doi.org/10.1016/j.esr.2024.101322

Clairand, J.-M. (2020). Participation of electric vehicle aggregators in ancillary services considering users' preferences. *Sustainability*, *12*(1). Retrieved from https://www.mdpi.com/2071-1050/12/1/8 doi: 10.3390/su12010008

Colbert, C. (2016). *Issue paper: Frequency response phase 2.* (https://www.caiso.com/Documents/IssuePaper_FrequencyResponsePhase2.pdf, accessed: 3-10-2022)

Corporation, C. I. S. O. (2013). *Caiso iso tariff, appendix b.2, participating generator agreement.* Retrieved from https://www.caiso.com/documents/appendixb4_participatingloadagreement_asof_jun12_2013.pdf (Accessed: 23-12-2024)

Couraud, B., Andoni, M., Robu, V., Norbu, S., Chen, S., & Flynn, D. (2023). Responsive flexibility: A smart local energy system. *Renewable and Sustainable Energy Reviews*, *182*, 113343. Retrieved from https://www.sciencedirect.com/science/article/pii/S1364032123002009 doi: https://doi.org/10.1016/j.rser.2023.113343

Cruz, M. R. M., Fitiwi, D. Z., Santos, S. F., & Catalão, J. P. S. (2018). A comprehensive survey of flexibility options for supporting the low-carbon energy future. *Renewable and Sustainable Energy Reviews*, *97*(August), 338–353. Retrieved from https://doi.org/10.1016/j.rser.2018.08.028 doi: 10.1016/j.rser.2018.08.028

Cui, B., Fan, C., Munk, J., Mao, N., Xiao, F., Dong, J., & Kuruganti, T. (2019). A hybrid building thermal modeling approach for predicting temperatures in typical, detached, two-story houses. *Applied Energy*, *236*, 101-116. Retrieved from https://www.sciencedirect.com/science/article/pii/S0306261918317938 doi: https://doi.org/10.1016/j.apenergy.2018.11.077

De Coninck, R., & Helsen, L. (2016). Quantification of flexibility in buildings by cost curves – methodology and application. *Applied Energy*, *162*, 653-665. Retrieved from https://www.sciencedirect.com/science/article/pii/S0306261915013501 doi: https://doi.org/10.1016/j.apenergy.2015.10.114

De Coninck, R., & Helsen, L. (2016). Quantification of flexibility in buildings by cost curves–methodology and application. *Applied Energy*, *162*, 653–665.

De Rosa, M., Brennenstuhl, M., Andrade Cabrera, C., Eicker, U., & Finn, D. P. (2019). An iterative methodology for model complexity reduction in residential building simulation. *Energies*, *12*(12). Retrieved from https://www.mdpi.com/1996-1073/12/12/2448 doi: 10.3390/en12122448

Diao, R., Lu, S., Elizondo, M., Mayhorn, E., Zhang, Y., & Samaan, N. (2012). Electric water heater modeling and control strategies for demand response. In *2012 ieee power and energy society general meeting* (p. 1-8). doi: 10.1109/PESGM.2012.6345632

Diaz-Londono, C., Colangelo, L., Ruiz, F., Patino, D., Novara, C., & Chicco, G. (2019). Optimal strategy to exploit the flexibility of an electric vehicle charging station. *Energies*, *12*(20). Retrieved from https://www.mdpi.com/1996-1073/12/20/3834 doi: 10.3390/en12203834

Dixon, A. (2019). Chapter 2 - what can provide frequency control? In A. Dixon (Ed.), *Modern aspects of power system frequency stability and control* (p. 23-37). Academic Press. Retrieved from https://www.sciencedirect.com/science/article/pii/B9780128161395000023 doi: https://doi.org/10.1016/B978-0-12-816139-5.00002-3

Dixon, J., Bell, K., & Brush, S. (2022). Which way to net zero? a comparative analysis of seven uk 2050 decarbonisation pathways. *Renewable and Sustainable Energy Transition*, *2*, 100016. Retrieved from https://www.sciencedirect.com/science/article/pii/S2667095X21000167 doi: https://doi.org/10.1016/j.rset.2021.100016

DoE, U. (2010). Energyplus, input output reference: The encyclopedic reference to energyplus input and output. *USA, Department of Energy*.

Dong, B., Cao, C., & Lee, S. E. (2005). Applying support vector machines to predict building energy consumption in tropical region. *Energy and Buildings*, *37*(5), 545-553. Retrieved from https://www.sciencedirect.com/science/article/pii/S0378778804002981 doi: https://doi.org/10.1016/j.enbuild.2004.09.009

Dyson, M. E., Borgeson, S. D., Tabone, M. D., & Callaway, D. S. (2014). Using smart meter data to estimate demand response potential, with application to solar energy integration. *Energy Policy*, *73*, 607-619. Retrieved from https://www.sciencedirect.com/science/article/pii/S0301421514003681 doi: https://doi.org/10.1016/j.enpol.2014.05.053

D'hulst, R., Labeeuw, W., Beusen, B., Claessens, S., Deconinck, G., & Vanthournout, K. (2015). Demand response flexibility and flexibility potential of residential smart appliances: Experiences from large pilot test in belgium. *Applied Energy*, *155*, 79-90. Retrieved from https://www.sciencedirect.com/science/article/pii/S0306261915007345 doi: https://doi.org/10.1016/j.apenergy.2015.05.101

Earl, J., & Fell, M. J. (2019). Electric vehicle manufacturers' perceptions of the market potential for demand-side flexibility using electric vehicles in the united kingdom. *Energy policy*, *129*, 646–652.

Ela, E., Diakov, V., Ibanez, E., & Heaney, M. (2013). *Impacts of variability and uncertainty in solar photovoltaic generation at multiple timescales* (Tech. Rep.). National Renewable Energy Lab.(NREL), Golden, CO (United States).

Electric Vehicle Database. (n.d.). `https://ev-database.org/`. (Accessed: 2023-09-12)

Ember. (2023). *Yearly electricity data.* (`https://ember-energy.org/data/yearly-electricity-data/`, accessed: 10-12-2024)

Enerdata. (2025). *Energy & emissions projections 2050 – EnerOutlook.* `https://eneroutlook.enerdata.net/total-electricity-generation-projections.html`. (Accessed: 2026-01-08)

Energy performance of buildings — Calculation of energy use for space heating and cooling (Vol. 2008; Standard). (2008, March). Geneva, CH: International Organization for Standardization.

ERCOT. (2021). *Ercot methodologies for determining minimum as requirements.* (`https://www.ercot.com/files/docs/2021/12/02/18_2022_ERCOT_Methodologies_for_Determining_Minimum_AS_Requirements.pdf`, accessed: 3-10-2022)

Erdinç, O., Taşcikaraoğlu, A., Paterakis, N. G., Eren, Y., & Catalão, J. P. (2017). End-User Comfort Oriented Day-Ahead Planning for Responsive Residential HVAC Demand Aggregation Considering Weather Forecasts. *IEEE Transactions on Smart Grid*, *8*(1), 362–372. doi: 10.1109/TSG.2016.2556619

Evans, M.-A., Bono, C., & Wang, Y. (2022). Toward net-zero electricity in europe: What are the challenges for the power system? *IEEE Power and Energy Magazine*, *20*(4), 44-54. doi: 10.1109/MPE.2022.3167575

Fam, A., & Fam, S. (2024). Review of the us 2050 long term strategy to reach net zero carbon emissions. *Energy Reports*, *12*, 845-860. Retrieved from `https://www.sciencedirect.com/science/article/pii/S2352484724003883` doi: https://doi.org/10.1016/j.egyr.2024.06.031

Fan, C., Xiao, F., & Wang, S. (2014). Development of prediction models for next-day building energy consumption and peak power demand using data mining techniques. *Applied Energy*, *127*, 1-10. Retrieved from `https://www.sciencedirect.com/science/article/pii/S0306261914003596` doi: https://doi.org/10.1016/j.apenergy.2014.04.016

Faqiry, M. N., Wang, L., & Wu, H. (2019). Hems-enabled transactive flexibility in real-time operation of three-phase unbalanced distribution systems. *Journal of Modern Power Systems and Clean Energy*, *7*(6), 1434-1449. doi: 10.1007/s40565-019-0553-2

Feng, C., Cui, M., Hodge, B.-M., Lu, S., Hamann, H. F., & Zhang, J. (2018). Unsupervised clustering-based short-term solar forecasting. *IEEE Transactions on Sustainable Energy*, *10*(4), 2174–2185.

Finck, C., Li, R., & Zeiler, W. (2020). Optimal control of demand flexibility under real-time pricing for heating systems in buildings: A real-life demonstration. *Applied Energy*, *263*, 114671. Retrieved from https://www.sciencedirect.com/science/article/pii/S0306261920301835 doi: https://doi.org/10.1016/j.apenergy.2020.114671

Flachsland, C., & Levi, S. (2021). Germany's federal climate change act. *Environmental Politics*, *30*(sup1), 118–140. Retrieved from https://doi.org/10.1080/09644016.2021.1980288 doi: 10.1080/09644016.2021.1980288

Fraisse, G., Viardot, C., Lafabrie, O., & Achard, G. (2002). Development of a simplified and accurate building model based on electrical analogy. *Energy and Buildings*, *34*(10), 1017-1031. Retrieved from https://www.sciencedirect.com/science/article/pii/S0378778802000191 doi: https://doi.org/10.1016/S0378-7788(02)00019-1

Fritzson, P., & Engelson, V. (1998). Modelica—a unified object-oriented language for system modeling and simulation. In *European conference on object-oriented programming* (pp. 67–90).

Gaeta, M., Nsangwe Businge, C., & Gelmini, A. (2022). Achieving net zero emissions in italy by 2050: Challenges and opportunities. *Energies*, *15*(1). Retrieved from https://www.mdpi.com/1996-1073/15/1/46 doi: 10.3390/en15010046

Gao, B., Huang, X., Shi, J., Tai, Y., & Zhang, J. (2020). Hourly forecasting of solar irradiance based on ceemdan and multi-strategy cnn-lstm neural networks. *Renewable Energy*, *162*, 1665-1683. Retrieved from https://www.sciencedirect.com/science/article/pii/S0960148120315652 doi: https://doi.org/10.1016/j.renene.2020.09.141

Gazafroudi, A. S., Pinto, T., Prieto-Castrillo, F., Corchado, J. M., Abrishambaf, O., Jozi, A., & Vale, Z. (2017). Energy flexibility assessment of a multi agent-based smart home energy system. In *2017 ieee 17th international conference on ubiquitous wireless broadband (icuwb)* (p. 1-7). doi: 10.1109/ICUWB.2017.8251008

Ghasvarian Jahromi, K., Gharavian, D., & Mahdiani, H. (2020). A novel method for day-ahead solar power prediction based on hidden markov model and cosine similarity. *Soft computing*, *24*, 4991–5004.

Gomes, I., Ruano, M., & Ruano, A. (2023). Milp-based model predictive control for home energy management systems: A real case study in algarve, portugal. *Energy and Buildings*, *281*, 112774. Retrieved from https://www.sciencedirect.com/science/article/pii/S037877882300004X doi: https://doi.org/10.1016/j.enbuild.2023.112774

Gottwalt, S., Gärttner, J., Schmeck, H., & Weinhardt, C. (2016). Modeling and valuation of residential demand flexibility for renewable energy integration. *IEEE Transactions on Smart Grid*, *8*(6), 2565–2574.

Gunkel, P. A., Bergaentzlé, C., Græsted Jensen, I., & Scheller, F. (2020). From passive to active: Flexibility from electric vehicles in the context of transmission system development. *Applied Energy*, *277*, 115526. Retrieved from https://www.sciencedirect.com/science/article/pii/S0306261920310382 doi: https://doi.org/10.1016/j.apenergy.2020.115526

Gurobi Optimization, LLC. (2024). *Gurobi Optimizer Reference Manual.* Retrieved from https://www.gurobi.com

Hao, H., & Chen, W. (2014). Characterizing flexibility of an aggregation of deferrable loads. In *53rd ieee conference on decision and control* (p. 4059-4064). doi: 10.1109/CDC.2014.7040020

Haque, E., Tabassum, S., & Hossain, E. (2021). A comparative analysis of deep neural networks for hourly temperature forecasting. *IEEE Access*, *9*, 160646-160660. doi: 10.1109/ACCESS.2021.3131533

Harder, N., Qussous, R., & Weidlich, A. (2020a). The cost of providing operational flexibility from distributed energy resources. *Applied Energy*, *279*, 115784.

Harder, N., Qussous, R., & Weidlich, A. (2020b). The cost of providing operational flexibility from distributed energy resources. *Applied Energy*, *279*, 115784.

Hart, W. E., Laird, C. D., Watson, J.-P., Woodruff, D. L., Hackebeil, G. A., Nicholson, B. L., & Siirola, J. D. (2017). *Pyomo optimization modeling in python* (2nd ed.). Springer Publishing Company, Incorporated.

Hart, W. E., Watson, J.-P., & Woodruff, D. L. (2011). Pyomo: modeling and solving mathematical programs in python. *Mathematical Programming Computation*, *3*(3), 219–260.

Heffron, R., Körner, M.-F., Wagner, J., Weibelzahl, M., & Fridgen, G. (2020). Industrial demand-side flexibility: A key element of a just energy transition and industrial development. *Applied Energy*, *269*, 115026.

Heidinger, A. K., Foster, M. J., Walther, A., & Zhao, X. T. (2014). The pathfinder atmospheres–extended avhrr climate dataset. *Bulletin of the American Meteorological Society*, *95*(6), 909–922.

Hekmat, N., Cai, H., Zufferey, T., Hug, G., & Heer, P. (2023). Data-driven demand-side flexibility quantification: Prediction and approximation of flexibility envelopes. In *2023 ieee belgrade powertech* (p. 1-6). doi: 10.1109/PowerTech55446.2023.10202703

Henych, M., Mamula, O., Sovka, P., & Šůcha, P. (2023). Machine learning-based forecasting of the automatic frequency restoration reserve demand. In *2023 ieee pes innovative smart grid technologies europe (isgt europe)* (p. 1-5). doi: 10.1109/ISGTEUROPE56780.2023.10407977

Hochreiter, S., & Schmidhuber, J. (1997). Long short-term memory. *Neural computation*, *9*(8), 1735–1780.

IRENA, F. (2022). *World energy transitions outlook 2022: 1.5 °c pathway.*

Irena renewable power generation costs in 2022. (2023). *International Renewable Energy Agency: Abu Dhabi, UAE*. Retrieved from `https://www.irena.org/-/media/Files/IRENA/Agency/Publication/2023/Aug/IRENA_Renewable_power_generation_costs_in_2022.pdf`

Iria, J., Scott, P., Attarha, A., Gordon, D., & Franklin, E. (2022). Mv-lv network-secure bidding optimisation of an aggregator of prosumers in real-time energy and reserve markets. *Energy*, *242*, 122962. Retrieved from `https://www.sciencedirect.com/science/article/pii/S0360544221032114` doi: https://doi.org/10.1016/j.energy.2021.122962

Iria, J., Soares, F., & Matos, M. (2019). Optimal bidding strategy for an aggregator of prosumers in energy and secondary reserve markets. *Applied Energy*, *238*, 1361–1372.

Iria, J. P., Soares, F. J., & Matos, M. A. (2018). Trading small prosumers flexibility in the energy and tertiary reserve markets. *IEEE transactions on smart grid*, *10*(3), 2371–2382.

Iria, J. P., Soares, F. J., & Matos, M. A. (2019). Trading small prosumers flexibility in the energy and tertiary reserve markets. *IEEE Transactions on Smart Grid*, *10*(3), 2371-2382. doi: 10.1109/TSG.2018.2797001

Jiao, Z., & Emura, K. (2022). Joint probability distribution of air temperature and global solar radiation for outdoor design conditions based on copula approach. *Building Services Engineering Research and Technology*, *43*(6), 669–683.

Jin, X., Wu, Q., & Jia, H. (2020). Local flexibility markets: Literature review on concepts, models and clearing methods. *Applied Energy*, *261*, 114387. Retrieved from https://www.sciencedirect.com/science/article/pii/S0306261919320744 doi: https://doi.org/10.1016/j.apenergy.2019.114387

Jingwei Hou, J. Z., Yanjuan Wang, & Tian, Q. (2022). Prediction of hourly air temperature based on cnn–lstm. *Geomatics, Natural Hazards and Risk*, *13*(1), 1962-1986. Retrieved from https://doi.org/10.1080/19475705.2022.2102942 doi: 10.1080/19475705.2022.2102942

Junker, R. G., Azar, A. G., Lopes, R. A., Lindberg, K. B., Reynders, G., Relan, R., & Madsen, H. (2018). Characterizing the energy flexibility of buildings and districts. *Applied Energy*, *225*, 175-182. Retrieved from https://www.sciencedirect.com/science/article/pii/S030626191830730X doi: https://doi.org/10.1016/j.apenergy.2018.05.037

Just, S., & Weber, C. (2008). Pricing of reserves: Valuing system reserve capacity against spot prices in electricity markets. *Energy Economics*, *30*(6), 3198-3221. Retrieved from https://www.sciencedirect.com/science/article/pii/S0140988308000789 (Technological Change and the Environment) doi: https://doi.org/10.1016/j.eneco.2008.05.004

Kara, E. C., Tabone, M. D., MacDonald, J. S., Callaway, D. S., & Kiliccote, S. (2014). Quantifying flexibility of residential thermostatically controlled loads for demand response: A data-driven approach. In *Proceedings of the 1st acm conference on embedded systems for energy-efficient buildings* (p. 140–147). New York, NY, USA: Association for Computing Machinery. Retrieved from https://doi.org/10.1145/2674061.2674082 doi: 10.1145/2674061.2674082

Kathirgamanathan, A., De Rosa, M., Mangina, E., & Finn, D. P. (2021). Data-driven predictive control for unlocking building energy flexibility: A review. *Renewable and Sustainable Energy Reviews*, *135*, 110120. Retrieved from https://www.sciencedirect.com/science/article/pii/S1364032120304111 doi: https://doi.org/10.1016/j.rser.2020.110120

Kathirgamanathan, A., De Rosa, M., Mangina, E., & Finn, D. P. (2021). Data-driven predictive control for unlocking building energy flexibility: A review. *Renewable and Sustainable Energy Reviews*, *135*, 110120.

Kathirgamanathan, A., Péan, T., Zhang, K., De Rosa, M., Salom, J., Kummert, M., & Finn, D. P. (2020). Towards standardising market-independent indicators for quantifying energy flexibility in buildings. *Energy and Buildings*, *220*, 110027. Retrieved from https://www.sciencedirect.com/science/article/pii/S0378778820301456 doi: https://doi.org/10.1016/j.enbuild.2020.110027

Klein, K., Herkel, S., Henning, H.-M., & Felsmann, C. (2017). Load shifting using the heating and cooling system of an office building: Quantitative potential evaluation for different flexibility and storage options. *Applied Energy*, *203*, 917-937. Retrieved from https://www.sciencedirect.com/science/article/pii/S0306261917308231 doi: https://doi.org/10.1016/j.apenergy.2017.06.073

Klein, K., Langner, R., Kalz, D., Herkel, S., & Henning, H.-M. (2016). Grid support coefficients for electricity-based heating and cooling and field data analysis of present-day installations in germany. *Applied Energy*, *162*, 853-867. Retrieved from https://www.sciencedirect.com/science/article/pii/S0306261915013434 doi: https://doi.org/10.1016/j.apenergy.2015.10.107

Klein, S. e. a. (2017). *Trnsys 18: A transient system simulation program, solar energy laboratory, university of wisconsin, madison, usa.* Retrieved from http://sel.me.wisc.edu/trnsys

Kohlhepp, P., Gröll, L., & Hagenmeyer, V. (2021). Characterization of aggregated building heating, ventilation, and air conditioning load as a flexibility service using gray-box modeling. *Energy Technology*, *9*(9), 2100251.

Kreuzer, D., Munz, M., & Schlüter, S. (2020). Short-term temperature forecasts using a convolutional neural network — an application to different weather stations in germany. *Machine Learning with Applications*, *2*, 100007. Retrieved from https://www.sciencedirect.com/science/article/pii/S2666827020300074 doi: https://doi.org/10.1016/j.mlwa.2020.100007

Kumar Dubey, A., Kumar, A., García-Díaz, V., Kumar Sharma, A., & Kanhaiya, K. (2021). Study and analysis of sarima and lstm in forecasting time series data. *Sustainable Energy Technologies and Assessments*, *47*, 101474. Retrieved from https://www.sciencedirect.com/science/article/pii/S2213138821004847 doi: https://doi.org/10.1016/j.seta.2021.101474

Lakshmanan, V., Sæle, H., & Degefa, M. Z. (2021). Electric water heater flexibility potential and activation impact in system operator perspective – norwegian scenario case study. *Energy*, *236*, 121490. Retrieved from https://www.sciencedirect.com/science/article/pii/S0360544221017382 doi: https://doi.org/10.1016/j.energy.2021.121490

Lazoglou, G., & Anagnostopoulou, C. (2019). Joint distribution of temperature and precipitation in the mediterranean, using the copula method. *Theoretical and applied climatology*, *135*, 1399–1411.

Le Dréau, J., & Heiselberg, P. (2016). Energy flexibility of residential buildings using short term heat storage in the thermal mass. *Energy*, *111*, 991-1002. Retrieved from https://www.sciencedirect.com/science/article/pii/S0360544216306934 doi: https://doi.org/10.1016/j.energy.2016.05.076

Le réseau de transport d'électricité. (2022). *Manual frequency restoration reserve and replacement reserve terms and conditions.* (https://www.services-rte.com/files/live/sites/services-rte/files/documentsLibrary/2022-01-01_REGLES_RRRC_3597_en, accessed: 3-10-2022)

Lei, X., Yu, H., Zhong, J., Jia, Y., Shao, Z., & Jian, L. (2024). Exploring electric vehicle's potential as capacity reservation through v2g operation to compensate load deviation in distribution systems. *Journal of Cleaner Production*, *451*, 141997. Retrieved from https://www.sciencedirect.com/science/article/pii/S0959652624014458 doi: https://doi.org/10.1016/j.jclepro.2024.141997

Li, G., & Yang, N. (2023). A hybrid sarima-lstm model for air temperature forecasting. *Advanced Theory and Simulations*, *6*(2), 2200502.

Li, H., Johra, H., de Andrade Pereira, F., Hong, T., Le Dréau, J., Maturo, A., ... Dong, B. (2023). Data-driven key performance indicators and datasets for building energy flexibility: A review and perspectives. *Applied Energy*, *343*, 121217. Retrieved from https://www.sciencedirect.com/science/article/pii/S0306261923005810 doi: https://doi.org/10.1016/j.apenergy.2023.121217

Li, H., Wang, Z., Hong, T., & Piette, M. A. (2021). Energy flexibility of residential buildings: A systematic review of characterization and quantification methods and applications. *Advances in Applied Energy*, *3*, 100054. Retrieved from https://www.sciencedirect.com/science/article/pii/S2666792421000469 doi: https://doi.org/10.1016/j.adapen.2021.100054

Loga, T., Stein, B., & Diefenbach, N. (2016). Tabula building typologies in 20 european countries—making energy-related features of residential building stocks comparable. *Energy and Buildings*, *132*, 4–12.

Lu, F., Lv, J., Zhang, Y., Liu, H., Zheng, S., Li, Y., & Hong, M. (2021). Ultra-short-term prediction of ev aggregator's demond response flexibility using arima, gaussian-arima, lstm and gaussian-lstm. In *2021 3rd international academic exchange conference on science and technology innovation (iaecst)* (p. 1775-1781). doi: 10.1109/IAECST54258.2021.9695933

Luo, N., Langevin, J., Chandra-Putra, H., & Lee, S. H. (2022). Quantifying the effect of multiple load flexibility strategies on commercial building electricity demand and services via surrogate modeling. *Applied Energy*, *309*, 118372. Retrieved from https://www.sciencedirect.com/science/article/pii/S0306261921016147 doi: https://doi.org/10.1016/j.apenergy.2021.118372

Luo, Z., Peng, J., Cao, J., Yin, R., Zou, B., Tan, Y., & Yan, J. (2022). Demand flexibility of residential buildings: Definitions, flexible loads, and quantification methods. *Engineering*, *16*, 123-140. Retrieved from https://www.sciencedirect.com/science/article/pii/S2095809922001436 doi: https://doi.org/10.1016/j.eng.2022.01.010

Luoma, J., Mathiesen, P., & Kleissl, J. (2014). Forecast value considering energy pricing in california. *Applied Energy*, *125*, 230-237. Retrieved from https://www.sciencedirect.com/science/article/pii/S0306261914003018 doi: https://doi.org/10.1016/j.apenergy.2014.03.061

Maka, A. O., Ghalut, T., & Elsaye, E. (2024). The pathway towards decarbonisation and net-zero emissions by 2050: The role of solar energy technology. *Green Technologies and Sustainability*, *2*(3), 100107. Retrieved from https://www.sciencedirect.com/science/article/pii/S2949736124000344 doi: https://doi.org/10.1016/j.grets.2024.100107

Mao, M., Jin, P., Hatziargyriou, N. D., & Chang, L. (2014). Multiagent-based hybrid energy management system for microgrids. *IEEE Transactions on Sustainable Energy*, *5*(3), 938–946.

Marotta, I., Guarino, F., Cellura, M., & Longo, S. (2021). Investigation of design strategies and quantification of energy flexibility in buildings: A case-study in southern italy. *Journal of Building Engineering*, *41*, 102392. Retrieved from https://www.sciencedirect.com/science/article/pii/S2352710221002503 doi: https://doi.org/10.1016/j.jobe.2021.102392

Mazhar, A. R., Zou, Y., Zeng, C., Shen, Y., & Liu, S. (2022). An algorithm to assess the heating strategy of buildings in cold climates: a case study of germany. *International Journal of Low-Carbon Technologies*, *17*, 662–677.

Mengelkamp, E., Gärttner, J., Rock, K., Kessler, S., Orsini, L., & Weinhardt, C. (2018). Designing microgrid energy markets: A case study: The brooklyn microgrid. *Applied Energy*, *210*, 870-880. Retrieved from https://www.sciencedirect.com/science/article/pii/S030626191730805X doi: https://doi.org/10.1016/j.apenergy.2017.06.054

Miller, S. D., Rogers, M. A., Haynes, J. M., Sengupta, M., & Heidinger, A. K. (2018). Short-term solar irradiance forecasting via satellite/model coupling. *Solar Energy*, *168*, 102-117. Retrieved from https://www.sciencedirect.com/science/article/pii/S0038092X17310435 (Advances in Solar Resource Assessment and Forecasting) doi: https://doi.org/10.1016/j.solener.2017.11.049

Ministerio del medio ambient, C. (2021). *Estrategia climática de largo plazo 2050.* Retrieved from https://cambioclimatico.mma.gob.cl/wp-content/uploads/2021/11/ECLP-LIVIANO.pdf (Accessed: 16-12-2024)

Moura, P., Yu, G. K., & Mohammadi, J. (2020). Management of electric vehicles as flexibility resource for optimized integration of renewable energy with large buildings. In *2020 ieee pes innovative smart grid technologies europe (isgt-europe)* (p. 474-478). doi: 10.1109/ISGT-Europe47291.2020.9248808

Mukherjee, M., Bhattarai, B., Hanif, S., & Pratt, R. (2022). Electric water heaters for transactive systems: Model evaluations and performance quantification. *IEEE Transactions on Industrial Informatics*, *18*(9), 5783-5794. doi: 10.1109/TII.2021.3128212

Munankarmi, P., Jin, X., Ding, F., & Zhao, C. (2020). Quantification of load flexibility in residential buildings using home energy management systems. In *2020 american control conference (acc)* (p. 1311-1316). doi: 10.23919/ACC45564.2020.9147459

Murat, M., Malinowska, I., Gos, M., & Krzyszczak, J. (2018). Forecasting daily meteorological time series using arima and regression models. *International agrophysics*, *32*(2).

Nel, P. J. C., Booysen, M. J., & van der Merwe, B. (2018). A computationally inexpensive energy model for horizontal electric water heaters with scheduling. *IEEE Transactions on Smart Grid*, *9*(1), 48-56. doi: 10.1109/TSG.2016.2544882

Nojavan, M., & Maghouli, P. (2024). A novel dynamic pricing time-based demand response program for net-load flexibility of microgrids. *International Journal of Energy Research*, *2024*(1), 2104716. Retrieved from https://onlinelibrary.wiley.com/doi/abs/10.1155/2024/2104716 doi: https://doi.org/10.1155/2024/2104716

O'Connell, N., Pinson, P., Madsen, H., & O'Malley, M. (2014). Benefits and challenges of electrical demand response: A critical review. *Renewable and Sustainable Energy Reviews*, *39*, 686-699. Retrieved from https://www.sciencedirect.com/science/article/pii/S1364032114005504 doi: https://doi.org/10.1016/j.rser.2014.07.098

Oldewurtel, F., Sturzenegger, D., Andersson, G., Morari, M., & Smith, R. S. (2013). Towards a standardized building assessment for demand response. In *52nd ieee conference on decision and control* (p. 7083-7088). doi: 10.1109/CDC.2013.6761012

on Climate Change), U. U. N. F. C. (2023). *Outcome of the first global stocktake, draft decision -/cma.5.* (https://unfccc.int/sites/default/files/resource/cma2023_L17_adv.pdf, accessed: 11-12-2024)

Ozbek, A., Sekertekin, A., Bilgili, M., & Arslan, N. (2021). Prediction of 10-min, hourly, and daily atmospheric air temperature: comparison of lstm, anfis-fcm, and arma. *Arabian Journal of Geosciences*, *14*, 1–16.

Pflugradt, N. (2016). *Modellierung von wasser-und energieverbräuchen in haushalten "* (Unpublished doctoral dissertation). Technical University of Chemnitz.

Plaum, F., Rosin, A., & AhmadiAhangar, R. (2024). Novel quantification method of aggregated energy flexibility based on power-duration curves. *IEEE Access*, *12*, 132825-132837. doi: 10.1109/ACCESS.2024.3461151

Qi, N., Cheng, L., Xu, H., Wu, K., Li, X., Wang, Y., & Liu, R. (2020). Smart meter data-driven evaluation of operational demand response potential of residential air conditioning loads. *Applied Energy*, *279*, 115708. Retrieved from https://www.sciencedirect.com/science/article/pii/S0306261920312022 doi: https://doi.org/10.1016/j.apenergy.2020.115708

Qureshi, F. A., & Jones, C. N. (2018). Hierarchical control of building hvac system for ancillary services provision. *Energy and Buildings*, *169*, 216-227. Retrieved from https://www.sciencedirect.com/science/article/pii/S0378778817315190 doi: https://doi.org/10.1016/j.enbuild.2018.03.004

Reynders, G., Amaral Lopes, R., Marszal-Pomianowska, A., Aelenei, D., Martins, J., & Saelens, D. (2018). Energy flexible buildings: An evaluation of definitions and quantification methodologies applied to thermal storage. *Energy and Buildings*, *166*, 372-390. Retrieved from https://www.sciencedirect.com/science/article/pii/S037877881732947X doi: https://doi.org/10.1016/j.enbuild.2018.02.040

Rinaldi, A., Yilmaz, S., Patel, M. K., & Parra, D. (2022). What adds more flexibility? an energy system analysis of storage, demand-side response, heating electrification, and distribution reinforcement. *Renewable and Sustainable Energy Reviews*, *167*, 112696. Retrieved from https://www.sciencedirect.com/science/article/pii/S1364032122005858 doi: https://doi.org/10.1016/j.rser.2022.112696

Ringkjøb, H.-K., Haugan, P. M., Seljom, P., Lind, A., Wagner, F., & Mesfun, S. (2020). Short-term solar and wind variability in long-term energy system models - a european case study. *Energy*, *209*, 118377. Retrieved from https://www.sciencedirect.com/science/article/pii/S0360544220314845 doi: https://doi.org/10.1016/j.energy.2020.118377

Russo, M., Carvalho, D., Martins, N., & Monteiro, A. (2023). Future perspectives for wind and solar electricity production under high-resolution climate change scenarios. *Journal of Cleaner Production*, *404*, 136997. Retrieved from https://www.sciencedirect.com/science/article/pii/S0959652623011551 doi: https://doi.org/10.1016/j.jclepro.2023.136997

Ryan, D., Long, R., Lauf, D., Ledbetter, M., & Reeves, A. (2013). *Water heater market profile 2010.* Retrieved from https://nepis.epa.gov/Exe/ZyPURL.cgi?Dockey=P100SMSL.txt

Sadeghianpourhamami, N., Refa, N., Strobbe, M., & Develder, C. (2018). Quantitive analysis of electric vehicle flexibility: A data-driven approach. *International Journal of Electrical Power & Energy Systems*, *95*, 451-462. Retrieved from https://www.sciencedirect.com/science/article/pii/S0142061516323687 doi: https://doi.org/10.1016/j.ijepes.2017.09.007

Sajjad, I. A., Chicco, G., & Napoli, R. (2016). Definitions of demand flexibility for aggregate residential loads. *IEEE Transactions on Smart Grid*, *7*(6), 2633-2643. doi: 10.1109/TSG.2016.2522961

Salgado-Bravo, M., Kirli, D., Negrete-Pincetic, M., & Kiprakis, A. E. (2025). *Day-ahead solar irradiance and temperature scenario generator based on cloud states using hidden markov models and lstm networks.* (Unpublished work)

Salgado-Bravo, M., Negrete-Pincetic, M., & Kiprakis, A. (2023). Demand-side energy flexibility estimation for day-ahead models. *Applied Energy*, *347*, 121502. Retrieved from https://www.sciencedirect.com/science/article/pii/S0306261923008668 doi: https://doi.org/10.1016/j.apenergy.2023.121502

Salinas, D., Bohlke-Schneider, M., Callot, L., Medico, R., & Gasthaus, J. (2019). High-dimensional multivariate forecasting with low-rank gaussian copula processes. In H. Wallach, H. Larochelle, A. Beygelzimer, F. d'Alché-Buc, E. Fox, & R. Garnett (Eds.), *Advances in neural information processing systems* (Vol. 32). Curran Associates, Inc. Retrieved from https://proceedings.neurips.cc/paper_files/paper/2019/file/0b105cf1504c4e241fcc6d519ea962fb-Paper.pdf

Salinas, D., Flunkert, V., Gasthaus, J., & Januschowski, T. (2020). Deepar: Probabilistic forecasting with autoregressive recurrent networks. *International Journal of Forecasting*, *36*(3), 1181-1191. Retrieved from https://www.sciencedirect.com/science/article/pii/S0169207019301888 doi: https://doi.org/10.1016/j.ijforecast.2019.07.001

Sanhudo, L., Rodrigues, J., & Ênio Vasconcelos Filho. (2021). Multivariate time series clustering and forecasting for building energy analysis: Application to weather data quality control. *Journal of Building Engineering*, *35*, 101996. Retrieved from https://www.sciencedirect.com/science/article/pii/S2352710220336287 doi: https://doi.org/10.1016/j.jobe.2020.101996

Sarmiento-Vintimilla, J. C., Marene Larruskain, D., Torres, E., & Abarrategi, O. (2024). Assessment of the operational flexibility of virtual power plants to facilitate the integration of distributed energy resources and decision-making under uncertainty. *International Journal of Electrical Power & Energy Systems*, *155*, 109611. Retrieved from https://www.sciencedirect.com/science/article/pii/S0142061523006683 doi: https://doi.org/10.1016/j.ijepes.2023.109611

Schütz, T., Schiffer, L., Harb, H., Fuchs, M., & Müller, D. (2017). Optimal design of energy conversion units and envelopes for residential building retrofits using a comprehensive milp model. *Applied Energy*, *185*, 1–15.

Sekertekin, A., Bilgili, M., Arslan, N., Yildirim, A., Celebi, K., & Ozbek, A. (2021). Short-term air temperature prediction by adaptive neuro-fuzzy inference system (anfis) and long short-term memory (lstm) network. *Meteorology and Atmospheric Physics*, *133*, 943–959.

Sengupta, M., Xie, Y., Lopez, A., Habte, A., Maclaurin, G., & Shelby, J. (2018). The national solar radiation data base (nsrdb). *Renewable and Sustainable Energy Reviews*, *89*, 51-60. Retrieved from https://www.sciencedirect.com/science/article/pii/S136403211830087X doi: https://doi.org/10.1016/j.rser.2018.03.003

Shadab, A., Ahmad, S., & Said, S. (2020). Spatial forecasting of solar radiation using arima model. *Remote Sensing Applications: Society and Environment*, *20*, 100427. Retrieved from https://www.sciencedirect.com/science/article/pii/S2352938520302731 doi: https://doi.org/10.1016/j.rsase.2020.100427

Sharifzadeh, M., Lubiano-Walochik, H., & Shah, N. (2017). Integrated renewable electricity generation considering uncertainties: The uk roadmap to 50% power generation from wind and solar energies. *Renewable and Sustainable Energy Reviews*, *72*, 385-398. Retrieved from https://www.sciencedirect.com/science/article/pii/S1364032117300795 doi: https://doi.org/10.1016/j.rser.2017.01.069

Shaughnessy, E. O., Shah, M., Parra, D., & Ardani, K. (2022). The demand-side resource opportunity for deep grid decarbonization. *Joule*, *6*(5), 972–983. Retrieved from https://doi.org/10.1016/j.joule.2022.04.010 doi: 10.1016/j.joule.2022.04.010

Si, Z., Yang, M., Yu, Y., & Ding, T. (2021). Photovoltaic power forecast based on satellite images considering effects of solar position. *Applied Energy*, *302*, 117514. Retrieved from https://www.sciencedirect.com/science/article/pii/S0306261921008965 doi: https://doi.org/10.1016/j.apenergy.2021.117514

Six, D., Desmedt, J., Vanhoudt, D., & Van Bael, J. (2011). Exploring the flexibility potential of residential heat pumps combined with thermal energy storage for smart grids. In *21th international conference on electricity distribution, paper* (Vol. 442, p. 1-4).

Skamarock, W., Klemp, J., Dudhia, J., Gill, D., Liu, Z., Berner, J., ... others (2021). A description of the advanced research wrf model version 4.3; no. *NCAR/TN556+ STR*.

Sorknæs, P., Johannsen, R. M., Korberg, A. D., Nielsen, T. B., Petersen, U. R., & Mathiesen, B. V. (2022). Electrification of the industrial sector in 100% renewable energy scenarios. *Energy*, *254*, 124339. Retrieved from https://www.sciencedirect.com/science/article/pii/S0360544222012427 doi: https://doi.org/10.1016/j.energy.2022.124339

Srilakshmi, E., & Singh, S. P. (2022). Energy regulation of ev using milp for optimal operation of incentive based prosumer microgrid with uncertainty modelling. *International Journal of Electrical Power & Energy Systems*, *134*, 107353. Retrieved from https://www.sciencedirect.com/science/article/pii/S0142061521005925 doi: https://doi.org/10.1016/j.ijepes.2021.107353

Srithapon, C., & Månsson, D. (2023). Predictive control and coordination for energy community flexibility with electric vehicles, heat pumps and thermal energy storage. *Applied Energy*, *347*, 121500. Retrieved from https://www.sciencedirect.com/science/article/pii/S0306261923008644 doi: https://doi.org/10.1016/j.apenergy.2023.121500

Srivastava, A., Van Passel, S., & Laes, E. (2019). Dissecting demand response: A quantile analysis of flexibility, household attitudes, and demographics. *Energy Research & Social Science*, *52*, 169-180. Retrieved from https://www.sciencedirect.com/science/article/pii/S2214629618311034 doi: https://doi.org/10.1016/j.erss.2019.02.011

Srivastava, S., & Lessmann, S. (2018). A comparative study of lstm neural networks in forecasting day-ahead global horizontal irradiance with satellite data. *Solar Energy*, *162*, 232-247. Retrieved from https://www.sciencedirect.com/science/article/pii/S0038092X18300173 doi: https://doi.org/10.1016/j.solener.2018.01.005

Stinner, S., Huchtemann, K., & Müller, D. (2016). Quantifying the operational flexibility of building energy systems with thermal energy storages. *Applied Energy*, *181*, 140–154.

Strbac, G., Pudjianto, D., Aunedi, M., Papadaskalopoulos, D., Djapic, P., Ye, Y., ... Fan, Y. (2019). Cost-effective decarbonization in a decentralized market: The benefits of using flexible technologies and resources. *IEEE Power and Energy Magazine*, *17*(2), 25-36. doi: 10.1109/MPE.2018.2885390

Sun, M., Feng, C., & Zhang, J. (2020). Probabilistic solar power forecasting based on weather scenario generation. *Applied Energy*, *266*, 114823. Retrieved from `https://www.sciencedirect.com/science/article/pii/S0306261920303354` doi: https://doi.org/10.1016/j.apenergy.2020.114823

Taha, F. A., Vincent, T., & Bitar, E. (2024). An efficient method for quantifying the aggregate flexibility of plug-in electric vehicle populations. *IEEE Transactions on Smart Grid*, 1-1. doi: 10.1109/TSG.2024.3384871

Tina, G. M., Aneli, S., & Gagliano, A. (2022). Technical and economic analysis of the provision of ancillary services through the flexibility of hvac system in shopping centers. *Energy*, *258*, 124860. Retrieved from `https://www.sciencedirect.com/science/article/pii/S0360544222017637` doi: https://doi.org/10.1016/j.energy.2022.124860

Ueckerdt, F., Brecha, R., & Luderer, G. (2015). Analyzing major challenges of wind and solar variability in power systems. *Renewable Energy*, *81*, 1-10. Retrieved from `https://www.sciencedirect.com/science/article/pii/S0960148115001846` doi: https://doi.org/10.1016/j.renene.2015.03.002

Vagropoulos, S. I., Chouliaras, G. I., Kardakos, E. G., Simoglou, C. K., & Bakirtzis, A. G. (2016). Comparison of sarimax, sarima, modified sarima and ann-based models for short-term pv generation forecasting. In *2016 ieee international energy conference (energycon)* (p. 1-6). doi: 10.1109/ENERGYCON.2016.7514029

van Rossum, G. (1995, May). *Python tutorial* (Tech. Rep. No. CS-R9526). Amsterdam: Centrum voor Wiskunde en Informatica (CWI).

Verastegui, F., Lorca, A., Olivares, D., & Negrete-pincetic, M. (2021). Optimization-based analysis of decarbonization pathways and flexibility requirements in highly renewable power systems. *Energy*, *234*, 13. doi: 10.1016/j.energy.2021.121242

Villar, J., Bessa, R., & Matos, M. (2018). Flexibility products and markets: Literature review. *Electric Power Systems Research*, *154*, 329-340. Retrieved from `https://www.sciencedirect.com/science/article/pii/S0378779617303723` doi: https://doi.org/10.1016/j.epsr.2017.09.005

Wang, A., Li, R., & You, S. (2018). Development of a data driven approach to explore the energy flexibility potential of building clusters. *Applied Energy*, *232*, 89-100. Retrieved from https://www.sciencedirect.com/science/article/pii/S0306261918315083 doi: https://doi.org/10.1016/j.apenergy.2018.09.187

Wang, H., Wang, S., & Tang, R. (2019). Development of grid-responsive buildings: Opportunities, challenges, capabilities and applications of hvac systems in non-residential buildings in providing ancillary services by fast demand responses to smart grids. *Applied Energy*, *250*, 697-712. Retrieved from https://www.sciencedirect.com/science/article/pii/S0306261919308190 doi: https://doi.org/10.1016/j.apenergy.2019.04.159

Wang, S., & Wu, W. (2021). Aggregate flexibility of virtual power plants with temporal coupling constraints. *IEEE Transactions on Smart Grid*, *12*(6), 5043-5051. doi: 10.1109/TSG.2021.3106646

Website of the TABULA and EPISCOPE projects, section Publications/Download. (n.d.). https://episcope.eu/communication/download/. (Accessed: 2023-06-30)

Wen, Y., Hu, Z., You, S., & Duan, X. (2022). Aggregate feasible region of ders: Exact formulation and approximate models. *IEEE Transactions on Smart Grid*, 1-1. doi: 10.1109/TSG.2022.3179998

Wenzel, G., Negrete-Pincetic, M., Olivares, D. E., MacDonald, J., & Callaway, D. S. (2018). Real-time charging strategies for an electric vehicle aggregator to provide ancillary services. *IEEE Transactions on Smart Grid*, *9*(5), 5141-5151. doi: 10.1109/TSG.2017.2681961

Yagli, G. M., Yang, D., & Srinivasan, D. (2022). Ensemble solar forecasting and post-processing using dropout neural network and information from neighboring satellite pixels. *Renewable and Sustainable Energy Reviews*, *155*, 111909. Retrieved from https://www.sciencedirect.com/science/article/pii/S1364032121011734 doi: https://doi.org/10.1016/j.rser.2021.111909

Yu, Y., Cao, J., & Zhu, J. (2019). An lstm short-term solar irradiance forecasting under complicated weather conditions. *IEEE Access*, *7*, 145651-145666. doi: 10.1109/ACCESS.2019.2946057

Yuan, M., Thellufsen, J. Z., Lund, H., & Liang, Y. (2021). The electrification of transportation in energy transition. *Energy*, *236*, 121564. Retrieved from https://www.sciencedirect.com/science/article/pii/S0360544221018120 doi: https://doi.org/10.1016/j.energy.2021.121564

Zade, M., Incedag, Y., El-Baz, W., Tzscheutschler, P., & Wagner, U. (2018). Prosumer integration in flexibility markets: A bid development and pricing model. In *2018 2nd ieee conference on energy internet and energy system integration (ei2)* (p. 1-9). doi: 10.1109/EI2.2018.8582022

Zang, H., Liu, L., Sun, L., Cheng, L., Wei, Z., & Sun, G. (2020). Short-term global horizontal irradiance forecasting based on a hybrid cnn-lstm model with spatiotemporal correlations. *Renewable Energy*, *160*, 26-41. Retrieved from `https://www.sciencedirect.com/science/article/pii/S0960148120308557` doi: https://doi.org/10.1016/j.renene.2020.05.150

Zargar, R. H. M., & Yaghmaee Moghaddam, M. H. (2020). Development of a markov-chain-based solar generation model for smart microgrid energy management system. *IEEE Transactions on Sustainable Energy*, *11*(2), 736-745. doi: 10.1109/TSTE.2019.2904436

Zarrella, A., Prataviera, E., Romano, P., Carnieletto, L., & Vivian, J. (2020). Analysis and application of a lumped-capacitance model for urban building energy modelling. *Sustainable Cities and Society*, *63*, 102450.

Zhang, X., Hu, J., Wang, H., Wang, G., Chan, K. W., & Qiu, J. (2020). Electric vehicle participated electricity market model considering flexible ramping product provisions. *IEEE Transactions on Industry Applications*, *56*(5), 5868-5879. doi: 10.1109/TIA.2020.2995560

Zuo, H.-M., Qiu, J., Jia, Y.-H., Wang, Q., & Li, F.-F. (2022). Ten-minute prediction of solar irradiance based on cloud detection and a long short-term memory (lstm) model. *Energy Reports*, *8*, 5146-5157. Retrieved from `https://www.sciencedirect.com/science/article/pii/S2352484722007375` doi: https://doi.org/10.1016/j.egyr.2022.03.182

.1 Thermal models state-of-art

The literature on thermal building modeling can be divided into three categories based on the approach used:

- White-box models: The mathematical formulations known for each one of their expressions, constants, and variables can be considered white-box models, usually based on physical and first-principle models Kathirgamanathan, De Rosa, Mangina, and Finn (2021). Various formulations can be considered white-box models, starting with the static linear approach, and progressing to complex dynamic formulations that evaluate the heat balance between thermal zones. This approach requires detailed physical knowledge to build a proper model (building geometry, material properties) to reduce discrepancies between the simulated building and temperature measurements. The software EnergyPlus De Rosa, Brennenstuhl, Andrade Cabrera, Eicker, and Finn (2019); DoE (2010), TRNSYS S. e. a. Klein (2017), and Modelica Fritzson and Engelson (1998); K. Klein et al. (2017) are used models to simulate the building's thermal behavior, which can be considered a white-box model.
- Black-box models: Formulations that ignore the physics related to the problem and rely on on-site measurements to train data-driven models Amara, Agbossou, Cardenas, Dubé, and Kelouwani (2015). The model training requires measurements of HVAC consumption, operational points, and internal and outdoor temperatures to cover all possible relevant variables to the model, but the predictions provided outperform other thermal approaches Arendt, Jradi, Shaker, and Veje (2018). The dataset must be as comprehensive and extensive as possible, covering all seasons and spanning at least one year to enhance the accuracy of the training process. Artificial Neural Networks Afram and Janabi-Sharifi (2015), Emsemble Learning models Fan, Xiao, and Wang (2014), and Support Vector Machines Dong, Cao, and Lee (2005) are used formulations for black-box models.
- Gray-Box models: A mixed formulation that considers both empirical and physical aspects in the model can be viewed as a gray-box model. It depends on on-site measurements to adjust the parameters introduced in the physical model Cui et al. (2019). Compared to a black-box model, the required training dataset is smaller, consisting of a few weeks of measurements rather than years of data. The resistive-capacitive thermal network model Fraisse, Viardot, Lafabrie, and Achard (2002) is the most used approach that can be considered a gray-box model.

In the proposed approach, it can be challenging to use black-box models because the high number of variables affects the computational power required by the model formulation Arendt et al. (2018). Consequently, the white-box and gray-box approaches are preferred to formulate building optimization models. The white-box approach is usually used in multiple household formulations with minimal information Erdinç, Taşcikaraoğlu, Paterakis, Eren, and Catalão

(2017). Its simplicity in defining household properties in a static linear formulation allows it to include hundreds or thousands of households in demand aggregation or virtual power plant models. In addition, more complex models, such as first-principles approaches presented in EnergyPlus and TRNSYS, offer highly detailed thermal modeling but are computationally expensive for an optimization approach. It is possible to use high-level white-box models in conjunction with a gray-box model, utilizing the data generated by the white-box model as measurements to calibrate the gray-box model De Rosa et al. (2019), thereby simplifying the white-box model for use in an optimization model.

Independent of the white-box or gray-box approach, it is possible to present the parameters in the thermal linear model as constant values (in this work, α and β are used for the parameters) associated with the thermal losses, energy efficiency, and thermal storage in the model. The thermal model presented in this work uses this notation as a generalization, independently of a white-box or gray-box approach.

.2 ISO 13790:2008 thermal model rewriting

The thermal dynamics of the building are modeled following the hourly method described in Annex C of ISO 13790:2008 ISO 13790:2008(E) (2008). This approach utilizes a 5R1C lumped-capacitance model, which represents the building's thermal behavior through five resistances and a single capacitance. To determine the internal wall temperature, the Crank-Nicolson scheme is applied, calculating the temperature as the mean value between time steps t and $t-1$. An advantage of the Crank-Nicolson scheme is the possibility to reformulate the thermal model into a linear expression. This linearization facilitates the isolation of the air conditioner's specific thermal impact from external variables such as solar irradiance, outdoor ambient temperature, and black-body radiation. A detailed explanation of each parameter within this framework is provided in ISO 13790:2008(E) (2008). The rewriting of the thermal model is shown below:

$$R_0 = \Phi_{w,t}^{st,hvac} + H_{tr,w}^{hvac} * \theta_{w,t}^{e,hvac} + H_{tr,1}^{hvac} * \theta_{w,t}^{sup,hvac} + \frac{H_{tr,1}^{hvac}}{H_{ve}^{hvac}} \Phi_{w,t}^{ia,hvac} \tag{1a}$$

$$R_1 = \Phi_{w,t}^{m,hvac} + H_{tr,em}^{hvac} * \theta_{w,t}^{e,hvac} + \frac{H_{tr,3}^{hvac}}{H_{tr,2}^{hvac}} R_0 \tag{1b}$$

$$\Phi_{w,rtm,t}^{mtot,hvac} = R1 + \frac{H_{tr,3}^{hvac} H_{tr,1}^{hvac}}{H_{tr,2}^{hvac} H_{ve}^{hvac}} \eta_{eff}^{hvac} * \left[P_{w,rtm,t}^{hvac,heat} - P_{w,rtm,t}^{hvac,cool} \right] \tag{1c}$$

$$R_2 = \frac{C_m^{hvac}}{3600} - 0.5(H_{tr,3}^{hvac} + H_{tr,em}^{hvac}) \tag{1d}$$

$$R_3 = \frac{C_m^{hvac}}{3600} + 0.5(H_{tr,3}^{hvac} + H_{tr,em}^{hvac}) \tag{1e}$$

$$\theta_{w,rtm,t}^{mt,hvac} = \frac{R_2}{R_3} \theta_{w,rtm,t-1}^{mt,hvac} + \frac{R_1}{R_3} + \frac{1}{R_3} \frac{H_{tr,3}^{hvac} H_{tr,1}^{hvac}}{H_{tr,2}^{hvac} H_{ve}^{hvac}} \eta_{eff}^{hvac} * \left[P_{w,rtm,t}^{hvac,heat} - P_{w,rtm,t}^{hvac,cool} \right] \tag{1f}$$

$$\theta_{w,rtm,t}^{m,hvac} = (\theta_{w,rtm,t}^{mt,hvac} + \theta_{w,rtm,t-1}^{mt,hvac})/2 \tag{1g}$$

$$\theta_{w,rtm,t}^{m,hvac} = \left(1 + \frac{R_2}{R_3}\right) \frac{\theta_{w,rtm,t-1}^{mt,hvac}}{2} + \frac{R_1}{2R_3} + \frac{1}{2R_3} \frac{H_{tr,3}^{hvac} H_{tr,1}^{hvac}}{H_{tr,2}^{hvac} H_{ve}^{hvac}} \eta_{eff}^{hvac} * \left[P_{w,rtm,t}^{hvac,heat} - P_{w,rtm,t}^{hvac,cool} \right] \tag{1h}$$

$$R_4 = H_{tr,ms}^{hvac} + H_{tr,w}^{hvac} + H_{tr,1}^{hvac} \tag{1i}$$

$$\theta_{w,rtm,t}^{s,hvac} = \frac{R_0}{R_4} + \frac{H_{tr,ms}^{hvac} \theta_{w,rtm,t}^{m,hvac}}{R_4} + \frac{H_{tr,1}^{hvac}}{H_{ve}^{hvac} R_4} \eta_{eff}^{hvac} * \left[P_{w,rtm,t}^{hvac,heat} - P_{w,rtm,t}^{hvac,cool} \right] \tag{1j}$$

$$R_{5,w,rtm,t} = \frac{R_0}{R_4} + \frac{H_{tr,ms}^{hvac}}{R4} \left(\frac{\theta_{w,rtm,t-1}^{m,hvac}}{2} \left[1 + \frac{R_2}{R_3} \right] + \frac{R_1}{2R_3} \right) \tag{1k}$$

$$R_6 = \frac{H_{tr,1}^{hvac}}{H_{ve}^{hvac} R_4} \left(1 + \frac{H_{tr,ms}^{hvac}}{2R_3} \frac{H_{tr,3}^{hvac}}{H_{tr,2}^{hvac}} \right) \tag{1l}$$

$$\theta_{w,rtm,t}^{s,hvac} = R_5 + R_6 \eta_{eff}^{hvac} * \left[P_{w,rtm,t}^{hvac,heat} - P_{w,rtm,t}^{hvac,cool} \right] \tag{1m}$$

$$\theta_{w,rtm,t}^{air,hvac} = \frac{H_{tr,is}^{hvac} R_{5,w,rtm,t} + H_{ve}^{hvac} \theta_{w,t}^{sup,hvac} + \Phi_{w,t}^{ia,hvac}}{H_{tr,is}^{hvac} + H_{ve}^{hvac}} + \frac{\left(1 + H_{tr,is}^{hvac} R_6\right) \eta_{eff}^{hvac} * \left[P_{w,rtm,t}^{hvac,heat} - P_{w,rtm,t}^{hvac,cool} \right]}{H_{tr,is}^{hvac} + H_{ve}^{hvac}} \tag{1n}$$

The variables R_0 to R_6 are partial rewriting of the expressions in the ISO 13790:2008 thermal model. In expression 1c, $\Phi_{w,rtm,t}^{mtot,hvac}$ are the energy flows in the internal wall (from solar heat, air renovation, heat from internal sources, and air conditioner). $\theta_{w,rtm,t}^{mt,hvac}$ in expression 1f is the internal wall temperature, which depends on the wall temperature in $t-1$, the energy flow in the internal wall at time t, and the air conditioner operation. The Crank-Nicholson scheme assumes that the instantaneous internal wall temperature at time t is equal to the temperature in time t plus the value at $t-1$ divided by two, as shown in expression 1g, being the instantaneous internal wall temperature the expression 1h. The internal wall temperature allows us to estimate the wall surface temperature in 1m and finally introduce the air temperature in expression 1n. The internal wall temperature is considered the energy storage variable for the thermal model, while the air temperature is the variable of interest for user comfort.